The evolution of condition-dependent self-fertilisation

Thomas Lesaffre*, John R. Pannell and Charles Mullon

Department of Ecology and Evolution, University of Lausanne, 1015 Lausanne, Switzerland

*Corresponding author: thomas.lesaffre@unil.ch

Abstract. Self-fertilisation is common in hermaphrodites, but selfing rates vary among species and populations and among individuals within populations. Most evolutionary theory seeking to explain this variation assumes genetically determined selfing rates. Here we study the evolution and consequences of condition-dependent selfing, where individuals adjust selfing in response to their deleterious mutation load. We analyse a two-locus population-genetic model in which one locus determines condition and the other is a modifier locus that determines condition-dependent selfing rates, and we extend the analysis to a polygenic background in which condition is determined by many loci. Our results show that selection favours positive condition dependence: high-condition individuals self-fertilise whereas low-condition individuals outcross. The resulting reaction norm generates stable within-population variation in realised selfing rates at evolutionary equilibrium and reduces the mutation load. We further show that it persists under environmental heterogeneity, and that pollen discounting favours a gradual increase in selfing with condition, leading to a continuum of selfing phenotypes. Altogether, our results indicate that condition-dependent selfing can generate substantial within-population variation in selfing rates. It may therefore contribute to mating-system diversity, and in particular to the maintenance of mixed mating.

1 Introduction

Most plants and many animals are hermaphroditic. In those with an ability to self-fertilise, the selfing rate varies widely, from predominantly selfing species to strictly outcrossing ones, with many showing mixed mating in which individuals self-fertilise at an intermediate rate [1–5]. This variation occurs not only among but also within species, where different populations often exhibit different selfing rates [5], and within population, where individual plants can differ substantially in their realised selfing rates owing to environmental and morphological differences [6–9]. Because these patterns determine how genes are transmitted across generations, explaining the evolutionary mechanisms that shape selfing-rate diversity within and between populations has been a longstanding problem in evolutionary biology [10–12].

Self-fertilisation comes with major ecological benefits, as it assures reproduction when mates or pollinators are scarce and avoids the costs and risks associated with mate searching (Chap. 1 in [10]; [13–16]). It also carries an inherent transmission advantage: a selfing parent acts as both mother and father and so transmits more gene copies per descendant [17]. Against these advantages stands the cost of inbreeding depression, the reduction in fitness of selfed relative to outcrossed offspring caused by the expression of recessive deleterious mutations segregating in populations (the 'mutation load' [18–20]). According to classical theory, the interaction between inbreeding depression and the advantages of selfing leads to a threshold effect in mating-system evolution [21]. In outcrossing populations, recessive deleterious mutations are held at low frequencies and so are almost always found in the heterozygous state. Selfing increases homozygosity and exposes their effects, which reduces the fitness of selfed offspring [18], but also makes the purging of mutations more effective. This generates a positive feedback for the evolution of selfing, because purging reduces inbreeding depression and therefore strengthens selection for increased selfing. As a result, theory predicts that complete outcrossing should be maintained when inbreeding depression is above a threshold (strong enough to overcome the benefits of selfing), and complete selfing should evolve when it is below, so that mixed mating is unstable [21–27].

Much work has since built on this seminal insight to explain the widespread occurrence of mixed mating in plant populations [2]. Several authors explored the effects of additional mechanisms relevant to the dynamics of mating, notably limited pollen and seed dispersal [28], variable pollination conditions [29] and pollen discounting – the reduction in pollen export that can accompany increased selfing [30–34]; all of which were shown to maintain mixed mating in some cases [2]. Others considered more elaborate biological scenarios for the effects of inbreeding depression, allowing it to vary, e.g., between female and

male components of fitness [35], as a function of population density [36], or of time and space [37]. These models show that strong differences in inbreeding depression across contexts can also select for mixed mating. However, their conclusions rely on the assumption of fixed inbreeding depression and so ignore purging, a major force in mating-system evolution in the face of which wide within-population variation in the magnitude of inbreeding depression may not be readily maintained [38].

Most theory on mating-system evolution assumes that the selfing rate is under genetic control, so that all individuals in the population have the same selfing rate at evolutionary equilibrium (see [2, 13, 39] for reviews). Yet, individuals may vary substantially in their selfing rates [5–9]. This variation could arise as a result of stochastic effects in plant-pollinator interactions [14, 40, 41]. However, it could also rise through a form of plasticity in which individuals adjust their mating behaviour according to environmental or physiological cues. Plastic responses of various kinds are common in plants, including on mating-related traits such as herkogamy or the timing of autonomous selfing, which have been shown to vary with environmental conditions [41–44]. One form of plasticity leading to inter-individual differences in selfing that has received particular attention is delayed selfing, where individuals self-fertilise only when outcrossing fails [45–47]. This plastic response is favoured in uncertain pollination environments, where the benefits of selfing vary between individuals [29, 48]. Much less attention has been paid to the fact that the costs of selfing should also vary among individuals in a population, simply because individuals inevitably differ in the number of deleterious mutations that they carry. In this context, a form of plasticity where individuals adjust their mating behaviour to their individual condition – an individual's overall vitality given its genetic background and environment – could also be favoured.

The notion that mating-related traits are expressed plastically in response to individual condition is well-established in dioecious animals [49–52]. It relies on the idea that secondary sexual traits are costly to produce and maintain. Individuals in good condition can afford to express larger ornaments, stronger courtship displays or more competitive behaviours, whereas those in poor condition cannot. This makes such traits reliable indicators of genetic quality, which the other sex (often females) can use when choosing mates to obtain indirect genetic benefits, as their offspring inherit alleles associated with higher condition [49, 53, 54]. Condition dependence also plays a central role in models of plastic switches between sexual and asexual reproduction. In these models, selection favours modifier alleles that increase the rate of sex in low-fitness genotypes, because recombination then allows the modifier to escape such deleterious genetic backgrounds [55–57]. Even so, the idea that an individual's selfing rate might be a plastic response to its condition, particularly its genetic condition, appears not to have been considered.

In this paper, we investigate the evolution of condition-dependent selfing using a combination of mathematical modelling and individual-based simulations. As a baseline, we analyse a two-locus model in which one locus affects condition and the other controls genotype-specific selfing rates, to ask whether selection favours individuals in different genetic conditions to self-fertilise at different rates. Because inbreeding depression is thought to arise from deleterious mutations at many loci, we then consider a more realistic polygenic case in which condition depends on mutations at numerous loci, and the selfing rate of each individual is determined by a gene-regulatory network that can evolve to respond to condition [58–61]. This approach lets us examine how the reaction norm linking condition to selfing evolves, while placing minimal constraints on its shape.

In the last part of the paper, we examine how two additional factors might modify the evolution and stability of condition-dependent selfing. The first is the effect of the environment on condition. Individual condition not only reflects genetic differences but also environmental variation in factors such as resource availability, competition, and exposure to pests and diseases [62, 63]. When condition-dependent selfing relies on condition as a cue to genetic condition, environmentally induced variation can blur the association between condition and genotype at loci affecting condition, which raises the question of whether environmental effects on condition could weaken, modify or perhaps even destabilise condition-dependent differences in selfing rate within populations. The second factor is the effect of pollen discounting on the balance between selfing and outcrossing. Pollen discounting measures the extent to which self-fertilisation reduces an individual's success as a pollen donor [32]. This can occur when pollen that could have sired outcrossed progeny is instead deposited on the same plant, either within flowers or via geitonogamous transfer among flowers [64, 65], or when changes in floral morphology that promote selfing, for instance reductions in herkogamy, compromise pollen export [66]. Such effects are known to alter the optimal selfing rate and can favour mixed mating under some scenarios [33]. In a condition-dependent scenario, pollen discounting may affect how selfing benefits vary with condition, and could therefore influence the shape of the reaction norm.

2 Condition-dependent self-fertilisation is favoured as an escape strategy

2.1 Two-locus model

We consider a large population of diploid hermaphrodites characterised by their genotype at two loci (Fig. 1). The first locus affects condition with two alleles: a wild-type allele 'A' and a deleterious allele

'a'. The condition of individuals with genotype AA, Aa and aa at this locus, which we refer to as the 'condition locus' hereafter, is given by $\varphi_{\mathrm{AA}} = 1$, $\varphi_{\mathrm{Aa}} = 1 - sh$ and $\varphi_{\mathrm{aa}} = 1 - s$, respectively, where s is the deleterious effect of allele a on condition and h is its dominance coefficient. During meiosis, the wild-type allele A mutates into deleterious allele a with probability μ_A and the deleterious allele a mutates into wild-type allele A with probability μ_a, so that the locus remains polymorphic at a balance between mutation and selection, and individuals in the population vary in their condition. The second locus is a selfing modifier at which alleles are additive and pleiotropically encode three genotype-specific selfing rates, $\boldsymbol{\alpha} = (\alpha_{\mathrm{AA}}, \alpha_{\mathrm{Aa}}, \alpha_{\mathrm{aa}}) \in [0,1]^3$, which express conditionally on genotype at the condition locus (e.g. α_{AA} is the selfing rate expressed in a AA homozygote). In this model, condition-dependent selfing therefore occurs whenever genotype-specific selfing rates differ. These rates each evolve via the input of rare and independent mutations of small and unbiased phenotypic effects ("continuum-of-alleles" model; [67]).

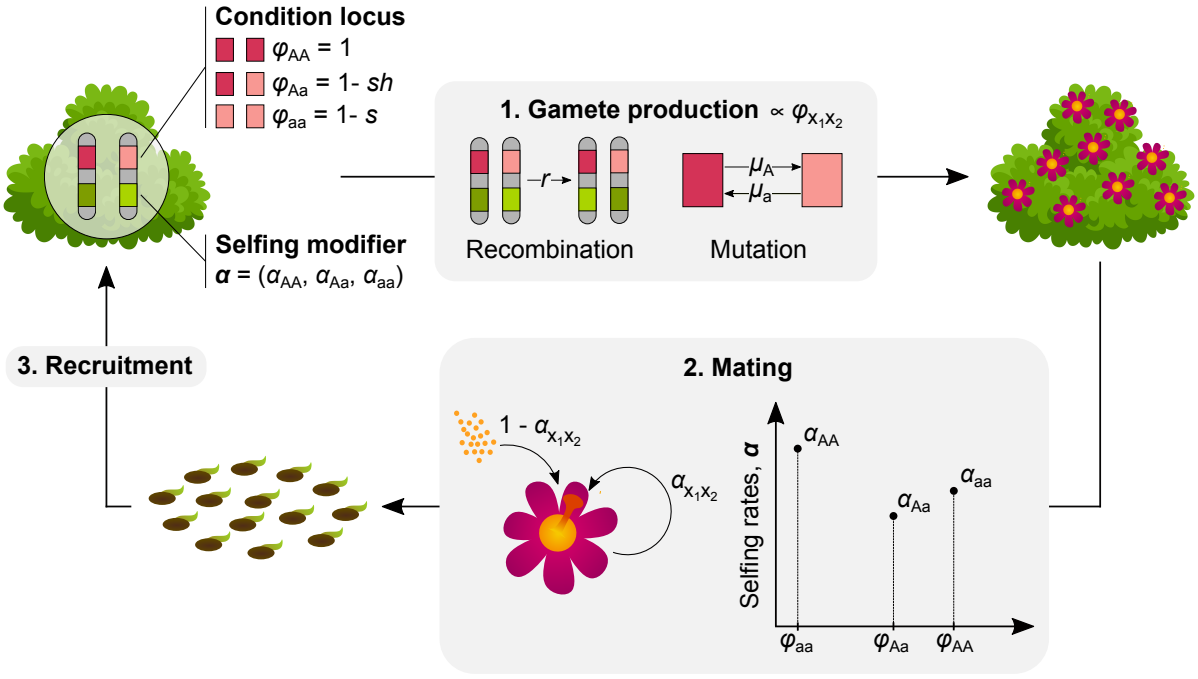

Figure 1: Life cycle and genetic bases of condition and selfing.

Each generation, individuals pass through the following life cycle events. (1) *Gamete production:* They first produce a large number of female and male gametes proportionally to their condition $\varphi_{x_1x_2}$, where $x_1, x_2 \in \{\mathrm{A}, \mathrm{a}\}$ denote the two alleles carried by the individual at the condition locus. The two loci recombine at rate $r \in [0, 1/2]$ and mutation occurs at the condition locus at a rate μ_x, $x \in \{\mathrm{A}, \mathrm{a}\}$, per allele during gametogenesis. (2) *Mating:* Individuals then self-fertilise a fraction $\alpha_{x_1x_2}$ of their ovules, which depends on their genotype at the modifier and on their condition. The remaining fraction of ovules $1 - \alpha_{x_1x_2}$ is fertilised via random mating. We assume that there is enough pollen exchanged for all

ovules to be fertilised (i.e., no pollen limitation), and that self-fertilising does not reduce an individual's contribution to the outcross pollen pool (i.e., no pollen discounting – we later relax this assumption). (3) *Recruitment:* Once all ovules have been fertilised, seeds mature, adults die and the next generation is sampled from the produced seeds, so that the population remains of large and constant size.

2.2 Effect of condition-dependent selfing on the condition locus

We start by fixing the relationship between selfing and condition to investigate how condition dependence influences the equilibrium frequency of the deleterious allele p^* and resulting mean condition $\overline{\varphi}^*$ in the population.

Linear condition dependence. In order to gain analytical traction, let us assume a linear relationship between condition and selfing, with genotype-specific selfing rates given by

$$\boldsymbol{\alpha} = (\alpha_{\mathrm{AA}},\, \alpha_{\mathrm{Aa}},\, \alpha_{\mathrm{aa}}) = \Big(\alpha_0,\quad \alpha_0 - d_\alpha h,\quad \alpha_0 - d_\alpha\Big)\,, \tag{1}$$

where $\alpha_0 \in [0,1]$ is the selfing rate of wild-type homozygotes, and $d_\alpha \in [-\alpha_0, 1-\alpha_0]$ gives the strength of condition dependence (where the dominance coefficient h of the deleterious allele features in the selfing rate of heterozygotes to ensure that the selfing rate varies linearly with condition, see Fig. 2A). Selfing rates are independent of condition when $d_\alpha = 0$, whereas the population experiences positive condition dependence for the selfing rate when $d_\alpha > 0$ and negative condition dependence when $d_\alpha < 0$ (Fig. 2A). Under this assumption, we show in Appendix A.1.2 that the equilibrium frequency of allele a can be expressed as

$$p^* = \begin{cases} \dfrac{\mu_A}{\big(s + d_\alpha/2\big)\big[h\,(1-F) + F\big]} + \mathcal{O}\left(s^2\right) & \text{when} \quad d_\alpha > -2s \\[2ex] 1 - \dfrac{\mu_a}{\big[-(s + d_\alpha/2)\big]\big[1 - h(1-F)\big]} + \mathcal{O}\left(s^2\right) & \text{when} \quad d_\alpha < -2s \end{cases} \tag{2}$$

to first order in s (i.e., under weak variation in fitness), where

$$F = \frac{\alpha_0}{2 - \alpha_0} \tag{3}$$

is the expected inbreeding coefficient at a neutral diallelic locus under partial selfing and without condition dependence (see, e.g., pp. 92–94 in [68]). This first-order approximation closely matches the equilibrium

frequency obtained when solving exact recursions numerically (Fig. 2B; Appendix A.1.2 for details).

The equilibrium frequency given in eq. (2) reflects a balance between mutation at the numerator and selection at the denominator, reducing to the classical expression for a deleterious allele at mutation-selection equilibrium in a partially selfing population in the absence of condition dependence ($d_\alpha = 0$; eq. 6b in [21]). Condition dependence appears at the denominator, where it modulates the intensity of selection against allele a. Positive condition dependence ($d_\alpha > 0$) decreases the equilibrium frequency of allele a relative to the condition independent case, whereas negative condition dependence ($d_\alpha < 0$) increases its frequency. Strongly negative condition dependence ($d_\alpha < -2s$, second line in eq. 2) can even bring the deleterious allele close to fixation (selection on allele a becomes positive as $s + d_\alpha/2$ becomes negative), where it is then maintained at a balance between selection and mutation reintroducing wild-type alleles into the population (Fig. 2B). Here, condition dependence affects selection at the condition locus because it leads alleles A and a to be associated with different average selfing rates: the allele associated with the higher rate enjoys a transmission advantage over the other, as selfing parents contribute more gene copies per offspring on average [17], which causes this allele to increase in frequency.

The effect of condition dependence on the equilibrium frequency of the deleterious allele is reflected in the mean condition of the population, which increases as this allele becomes less frequent under positive condition dependence, and conversely decreases under negative condition dependence (white triangles in Fig. 2B).

Arbitrary relationship between condition and selfing. We next investigate how the mechanism identified in the linear case applies more generally, by computing the equilibrium frequency of allele a for arbitrary genotype-specific selfing rates using a numerical approach. Consistent with our analytical results, we find that deleterious allele a can rise to a high frequency once the selfing rate of deleterious homozygotes (α_{aa}) is sufficiently high relative to that of wild-type homozygotes (α_{AA}), owing to the transmission advantage that it then enjoys (Figs. 2C-E). In addition, we find that whereas polymorphism was always maintained at a balance between mutation and selection in the linear case (and so would collapse in the absence of recurrent mutation), both alleles can persist as a protected polymorphism without recurrent mutation when heterozygotes show a higher selfing rate than both homozygotes. This is because the allele that is rarest in the population is more likely to be found in heterozygous state, and so has a higher average selfing rate than the frequent allele when heterozygotes self-fertilise more than homozygotes, leading to a form of overdominance and the maintenance of polymorphism (we show this analytically in Appendix A.1.3).

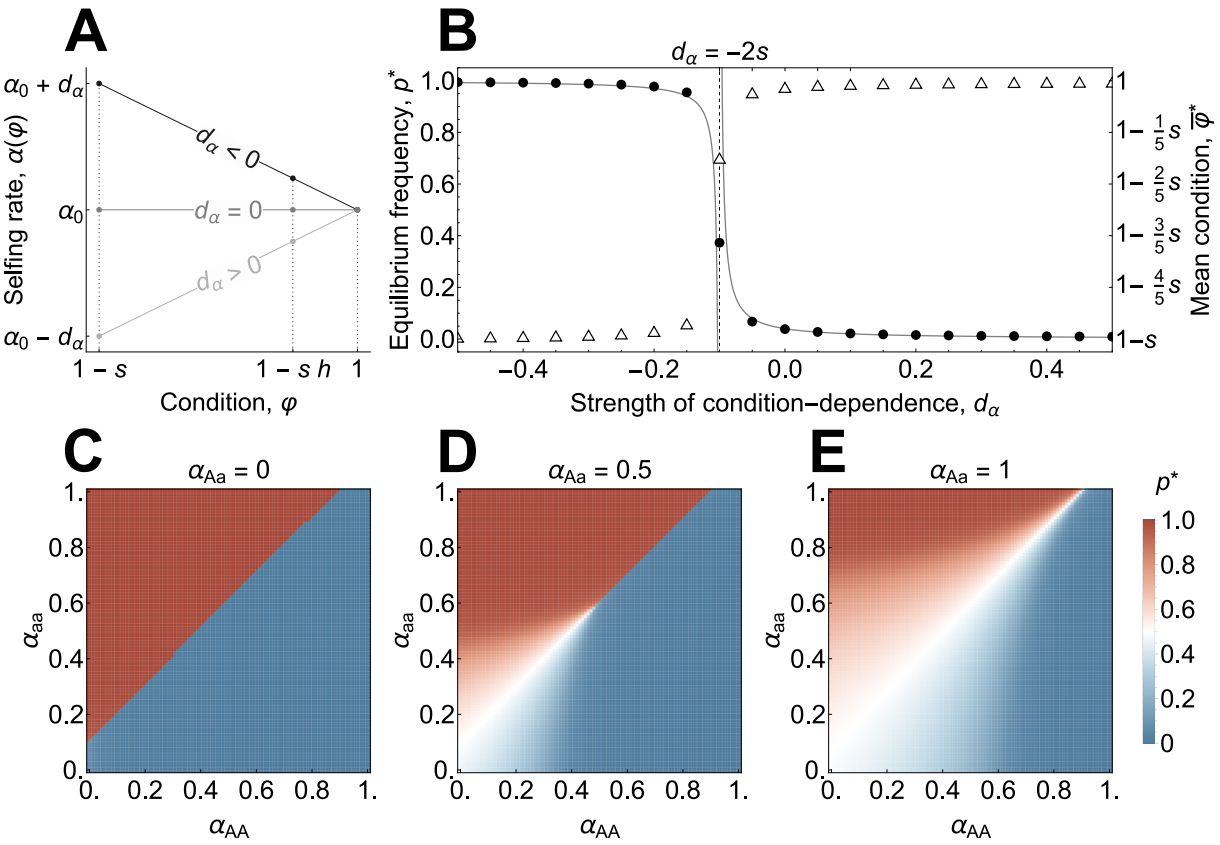

Figure 2: Effect of condition-dependent selfing on evolution at the condition locus. **A** Linear relationship between condition and the selfing rate, as assumed to compute eq. (2). $d_\alpha < 0$ leads to negative condition dependence and $d_\alpha > 0$ leads to positive condition dependence. **B** Equilibrium frequency of the deleterious allele a, p^*, and mean condition at this equilibrium, $\overline{\varphi}^*$, as a function of the strength of condition dependence, d_α. Dots and triangles respectively indicate the equilibrium frequency and mean condition computed numerically without approximation. Lines indicate the analytical approximations for p^* given in eqs. (2). Parameters specific to this plot: $\alpha_0 = 0.5$. **C-D-E** Equilibrium frequency p^* as a function of the selfing rates of wild-type homozygotes (x-axis) and deleterious homozygotes (y-axis) at the condition locus in the general case, for three selfing rates of heterozygotes ($\alpha_{\mathrm{Aa}} = 0,\ 0.5,\ 1$ from left to right). Parameters used in all plots: $s = 0.05$, $h = 0.25$, $\mu_A = \mu_a = 10^{-3}$.

2.3 Evolution of condition-dependent selfing

We now consider the evolution of condition-dependent selfing. To characterise selection on genotype-specific selfing rates $\boldsymbol{\alpha} = (\alpha_{\mathrm{AA}}, \alpha_{\mathrm{Aa}}, \alpha_{\mathrm{aa}})$, we employ an invasion analysis approach to compute the selection gradients on each of these rates, $s_{\mathrm{AA}}(\boldsymbol{\alpha})$, $s_{\mathrm{Aa}}(\boldsymbol{\alpha})$, and $s_{\mathrm{aa}}(\boldsymbol{\alpha})$, which we collect in vector

$$\boldsymbol{s}(\boldsymbol{\alpha}) = \left(s_{\mathrm{AA}}(\boldsymbol{\alpha}), \quad s_{\mathrm{Aa}}(\boldsymbol{\alpha}), \quad s_{\mathrm{aa}}(\boldsymbol{\alpha})\right). \tag{4}$$

Each of these gradients captures the strength and direction of selection on the corresponding genotype-specific selfing rate in a population expressing $\boldsymbol{\alpha}$ (Appendix A.2.1, [69]). A positive (resp. negative) selection gradient indicates that selection favours an increase (resp. decrease) in trait value, and the absolute value of the gradient indicates the strength of selection in this direction. Thus, condition dependence is favoured here whenever the sign of the gradient differs between genotype-specific selfing rates. We provide a detailed account of our analyses in Appendix A.2 and summarise our key results below.

Computing the selection gradients analytically for any $\boldsymbol{\alpha}$ is difficult. We therefore start by investigating special cases where analytical expressions can be obtained, beginning with the case where the population is completely outcrossing (i.e., $\boldsymbol{\alpha} = \mathbf{0}$). We show in Appendix A.2.2 that the selection gradients are then given by

$$\begin{aligned}\boldsymbol{s}(\mathbf{0}) &= \left(\frac{1}{4} + \mathcal{O}(s), \quad \frac{\mu_A}{2sh} + \mathcal{O}\left(s^2\right), \quad \left(\frac{\mu_A}{2sh}\right)^2 + \mathcal{O}\left(s^3\right)\right) \\ &= \left(\frac{q^*_{\mathrm{AA}}}{4} + \mathcal{O}(s), \quad \frac{q^*_{\mathrm{Aa}}}{4} + \mathcal{O}\left(s^2\right), \quad \frac{q^*_{\mathrm{aa}}}{4} + \mathcal{O}\left(s^3\right)\right),\end{aligned} \tag{5}$$

where q^*_{AA}, q^*_{Aa} and q^*_{aa} are the frequencies of genotypes AA, Aa and aa in the outcrossing population, respectively. The three gradients in eq. (5) are proportional to these frequencies because the strength of selection on a trait is proportional to the frequency with which it is expressed. Further, they are all positive, meaning that selection favours self-fertilisation irrespective of condition in a fully outcrossing population. This is because, when the rest of the population is fully outcrossing, alleles coding for increased self-fertilisation benefit from a substantial transmission advantage regardless of condition.

We next compute selection gradients under complete selfing, that is, in a population fixed for

$\boldsymbol{\alpha} = \mathbf{1}_3 = (1,1,1)$. We show in Appendix A.2.3 that these are given by

$$\begin{aligned} \boldsymbol{s}(\mathbf{1}_3) &= \left(\frac{1}{2} + \mathcal{O}(s), \quad \frac{\mu_A}{1+2r} + \mathcal{O}\left(s^3\right), \quad -\frac{r}{1+2r}\frac{\mu_A}{s} + \mathcal{O}\left(s^2\right)\right) \\ &= \left(\frac{1}{2}q^*_{\mathrm{AA}} + \mathcal{O}(s), \quad \frac{1}{4(1+2r)}q^*_{\mathrm{Aa}} + \mathcal{O}\left(s^3\right), \quad -\frac{r}{1+2r}q^*_{\mathrm{aa}} + \mathcal{O}\left(s^2\right)\right), \end{aligned} \tag{6}$$

which indicates that in a completely selfing population, wild-type homozygotes and heterozygotes are selected to remain fully selfing ($s_{\mathrm{AA}}(\mathbf{1}_3) > 0$ and $s_{\mathrm{Aa}}(\mathbf{1}_3) > 0$), whereas deleterious homozygotes are selected to become more outcrossing ($s_{\mathrm{aa}}(\mathbf{1}_3) < 0$).

This can be understood as follows. In a completely selfing population, heterozygous individuals at the condition locus are rare (only produced by mutation and rapidly removed due to inbreeding) and homozygotes only produce offspring of the same genotype (unless mutation occurs, which is negligibly rare because $\mu_x \ll s$). As a result, wild-type and deleterious homozygotes effectively form distinct lineages that do not cross, but compete for breeding spots. In this setting, deleterious homozygote lineages leave no descendant in the long-term because they are always outcompeted by the wild-type, so that their class-reproductive value tends to zero (see Appendix A.2.3 for details). Now, consider the fate of a mutant allele arising at the selfing modifier in a deleterious homozygote individual. If such an allele encodes complete selfing in this genetic context, it is guaranteed to leave no long-term descendant because it is trapped in a lineage that is doomed to extinction. In contrast, if this allele encodes some outcrossing, some of the ovules produced by its bearer will be outcrossed by pollen carrying the wild-type allele at the condition locus, which will give the mutant allele an opportunity to recombine onto a wild-type haplotype. Thus, from the point-of-view of alleles at the selfing modifier, outcrossing constitutes a strategy of escape from certain doom and is favoured as such. In line with this interpretation, the strength of selection on α_{aa} is zero in the absence of recombination ($r = 0$) because there is then no way to escape the deleterious background through outcrossing, and increases with r (eq. 6).

Finally, we analysed the evolution of genotype-specific selfing rates in the general case using a numerical approach described in Appendices A.2.4 and A.2.5. This analysis reveals that while selection always favours an increase in the selfing rate of wild-type homozygotes and heterozygotes, the genetic escape mechanism described above selects for ever lower selfing rates in deleterious homozygotes once other genotypes are highly selfing, so that eventually the population converges to complete outcrossing in dele-

terious homozygotes and complete selfing in other genotypes, i.e.,

$$\boldsymbol{\alpha}^* = (1,\ 1,\ 0) \tag{7}$$

at evolutionary equilibrium, when recombination is sufficiently frequent ($r \gg 0$; Supp. Fig. S1). Intuitively, once other genotypes are fully selfing, it is always preferable for deleterious homozygotes to outcross more, as any selfing lowers the chances of modifier alleles to escape this poor background.

When the recombination rate is very low ($r \approx 0$), however, complete selfing evolves for all genotypes. This is because the advantage of outcrossing as a deleterious homozygote becomes weak in this case, as it provides poor chances of recombining onto a wild-type haplotype (i.e., to escape), so that the production of wild-type offspring through mutation and selfing becomes a better escape route. Accordingly, this effect vanishes and condition dependence is always favoured when the deleterious allele cannot mutate back into the wild-type ($\mu_a = 0$; Fig. S2 in Appendix A.2.5).

3 Polygenic condition and the evolution of condition-dependent selfing

Our two-locus model suggests that selection broadly favours positive condition dependence for the selfing rate. We now consider the likely more realistic case where condition is the result of expression of alleles at many loci. Such a polygenic case is relevant because numerous deleterious mutations typically segregate simultaneously in natural populations and contribute to inbreeding depression, the principal force opposing selfing evolution, which is almost absent from the two-locus model [20, 22, 70, 71]. Investigating the evolution of condition-dependent selfing in this setting becomes more challenging, as individuals may carry many different multilocus genotypes at condition loci, so that we can no longer rely on a modifier locus encoding genotype-specific selfing rates. Instead, we must now consider the evolution of the plastic response of selfing to condition as a function that takes individual condition as input and returns a mating strategy. To study this, we turn to individual-based simulations.

3.1 The model

We simulate a population of N diploid hermaphrodites that follow the same life cycle as in the two-locus model: each individual $i \in \{1, \ldots, N\}$ first produces male and female gametes proportionally to its condition φ_i and then self-fertilises a fraction α_i of its ovules, while the remaining fraction is fertilised

via random mating. Following mating, seeds mature, adults die and the next generation is recruited from the produced seeds.

Individual condition is affected by $L \geqslant 1$ unlinked loci. Each locus $\ell \in \{1, ..., L\}$ has two alleles, a wild-type allele A_ℓ and a deleterious allele a_ℓ which mutate during meiosis at a rate $\mu_A = \mu_a = \mu$ (i.e., mutation to and from the deleterious allele occur at the same per-allele rate). Allele a_ℓ decreases individual condition by a proportion s when homozygous, and expresses proportionally to its dominance coefficient h when heterozygous. Condition loci are assumed to act multiplicatively [71, 72], so that the condition φ_i of an individual i homozygous for the deleterious allele at $n_{\mathrm{hom}}^{(i)}$ loci and heterozygous at $n_{\mathrm{het}}^{(i)}$ loci is given by

$$\varphi_i = (1-s)^{n_{\mathrm{hom}}^{(i)}}(1-sh)^{n_{\mathrm{het}}^{(i)}}. \tag{8}$$

To model the evolution of condition-dependent self-fertilisation, that is of the function

$$\alpha_i = f(\varphi_i) \tag{9}$$

that takes the condition φ_i of individual i as input and returns its selfing strategy α_i, one approach would be to assume that $f(\varphi_i)$ has a specific shape (e.g., a linear function of condition [73]) and consider the evolution of its parameters (e.g., its slope and intercept in the linear case). This approach simplifies the analysis, but introduces constraints that might interfere with the evolution of condition dependence. Instead, we assume that the selfing rate expressed by an individual is determined by a gene regulatory network that may evolve to respond to condition (Fig. 3A). Gene regulatory networks have been used in other contexts to model the evolution of a plastic responses to abiotic or social cues (e.g., [59–61]). They have been shown to be able to produce a wide range of functions from a limited number of genes, therefore allowing us to study the evolution of condition-dependent selfing with fewer constraints.

The architecture of the network is inspired from the Wagner model [58] and closely resembles the one used by previous authors [59–61]. A detailed explanation of the network model can be found in Appendix B.1. Briefly, the network involves a fixed number of loci, each of which contains a protein-coding gene that is expressed during individual development from seed to adult, and contributes to determining its selfing rate at the adult stage. The level of expression of these genes throughout the development of an individual is influenced by individual condition and by loci involved in the network (including by themselves), which may up- or down-regulate gene expression through cis-regulatory interactions. The selfing rate expressed by the individual is obtained as a weighted sum of the steady-state expression levels reached by network

loci at the end of development (Fig. 3A). The attributes of network loci that control their sensitivity to condition and regulatory interactions as well as their final contribution to phenotype evolve under a 'continuum-of-alleles' model [67]. Alleles at each network locus are additive, so that the attributes of a given locus in a diploid individual are given by the average of the two alleles, and network loci are assumed to recombine freely during meiosis. Further details on the model can be found in Appendix B.1.

3.2 Condition-dependent selfing evolves from gene-regulatory interactions and reduces the mutation load

We ran simulations for dominance coefficients ranging from $h = 0.10$ to $h = 0.45$ while keeping all other parameters fixed (see figure caption for parameter values, and Appendix B.1 for details on the simulation procedure). For each parameter set, we ran ten replicates of the model and additionally ran ten "control" runs where the network received a random value sampled from a uniform distribution as input instead of condition. These controls allowed us to check that the relationship between condition and selfing that evolves in our model is due to selection for condition dependence and not an artefact of network structure. For each simulation, the population was initialised as fixed for wild-type alleles at all condition loci and monomorphic for network loci attributes sampled in a normal distribution with mean zero and standard deviation $2\sigma_{\mathrm{g}}$, except for output weights which were fixed at zero to ensure that the population was initially fully outcrossing. Mutation was switched off at network loci for the first 5×10^3 generations to allow the population to reach mutation-selection balance at condition loci. Mutation was then allowed at network loci, and simulations were left to run for a total of 5×10^5 generations.

When inbreeding depression was weak enough to allow the initial emergence of self-fertilisation from initially complete outcrossing, simulations of our complete model then always showed the gradual emergence of condition dependence (Fig. 3B) and the establishment of a step-wise relationship between condition and selfing, with individuals above a condition threshold being purely selfing and lower condition individuals being purely outcrossing (Fig. 3C). In contrast, control runs remained close to complete outcrossing for high levels of inbreeding depression ($\delta > 1/2$, [21]) and evolved near complete selfing otherwise, with little variance in selfing rate among individuals in both cases (grey triangles in Fig. 3D), as expected in the absence of information on individual condition. The step-wise relationship that evolves in our simulations is consistent with the notion that positive condition dependence evolves as an escape strategy from deleterious backgrounds. Indeed, from the point of view of a selfing modifier, the cost-benefit balance of selfing (staying) versus outcrossing (escaping) in a particular genetic background is

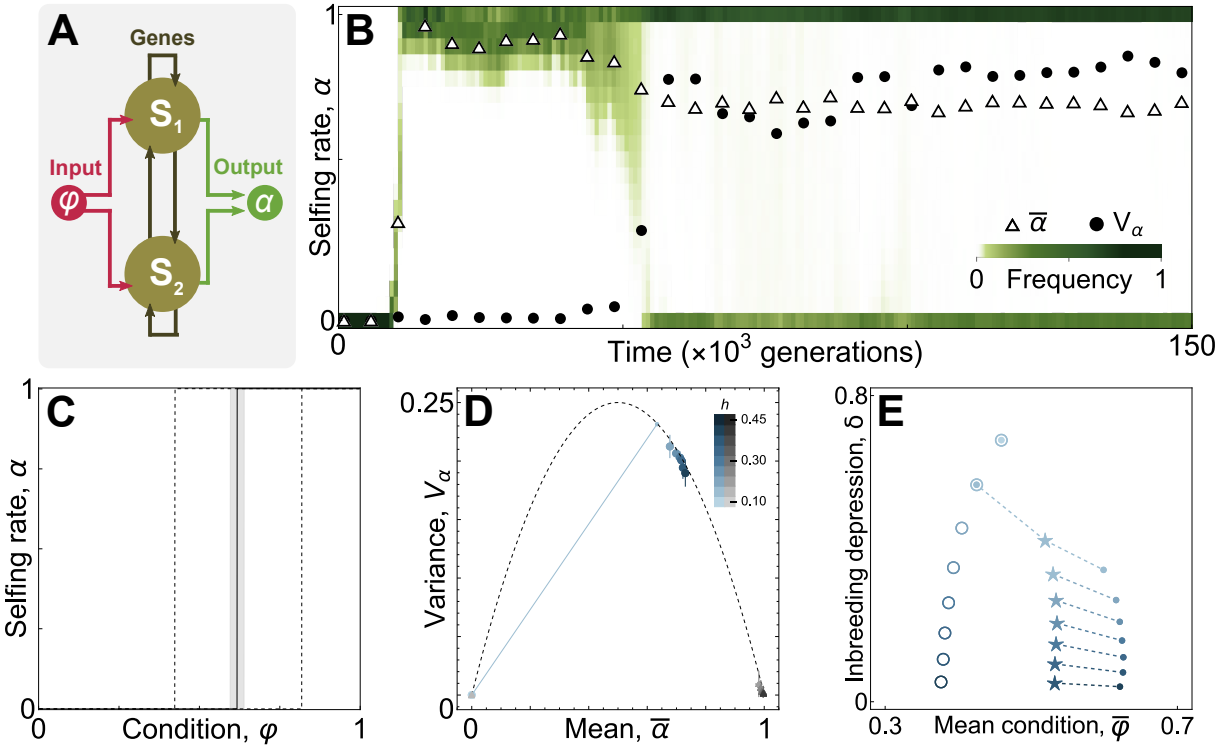

Figure 3: Evolution of condition-dependent selfing and its effect on the mutation load. **A** A gene regulatory network with $n_g = 2$ loci. Gene expression is affected by condition in proportion to input weights and by regulatory interactions among loci, which are given by the regulatory matrix. Once loci reach a steady state expression level, their equilibrium expression level is combined proportionally to output weights to obtain the individual's mating strategy. See Appendix B.1 for details. **B** Distribution of selfing rates in the population as a function of time in a sample simulation with $L = 10^3$ loci affecting condition. Shades of green indicate the proportion of individuals with a selfing rate in the corresponding interval at a given time step. The darker the colour, the more individuals. Triangles indicate the mean selfing rate and black points indicate variance scaled by the highest possible variance (variance of a binomial distribution with success probability $1/2$, which corresponds to a case where exactly half of the population has a selfing rate $\alpha = 0$ and the other half has $\alpha = 1$). The population rapidly evolves complete selfing once mutation is triggered at network loci, and then experiences the gradual establishment of condition dependence. Parameters specific to this simulation: $h = 0.25$. **C** Distribution of evolved condition-dependent selfing strategies for a hundred individuals every 50 generations over the last 10^5 generations. The solid black line indicates the median, grey shading gives the first and third quartiles and dashed lines indicate the minimal and maximal values, respectively, for each condition value. All individuals express a step-wise relationship between condition and selfing, varying only in the position of their step. **D** Mean and variance in the selfing rate averaged over the last 10^5 generations and between replicates. Blue points indicate runs of the complete model and grey triangles indicate control runs, darker colours indicate higher dominance coefficients (see legend on top right corner). The dashed line indicates the maximum achievable variance, which is reached when the population evolves condition-dependent selfing. The solid blue line connects replicates of the complete model for $h = 0.15$, some of which evolved condition-dependent selfing (4 out of ten), while the rest remained fully outcrossing. **E** Mean condition and inbreeding depression at evolutionary equilibrium as a function of the dominance coefficient of deleterious mutations. Open circles indicate where initial populations stood under complete outcrossing. Full circles indicate simulations where condition dependence evolved, and stars show the outcome of simulations with the same mean selfing rate, but no condition dependence. Parameters used in all simulations: $N = 5 \times 10^3$, $L = 10^3$, $s = 0.05$, $\mu = 5 \times 10^{-4}$, $\mu_g = 5 \times 10^{-3}$, $\sigma_g = 5 \times 10^{-2}$.

independent of the selfing rate expressed by its bearer. Either the load carried by the bearer is sufficiently low for selfing to be beneficial, or the load is high enough to make outcrossing preferable.

We also quantified the effect of condition dependence on the mutation load maintained at mutation-selection balance. To do this, we simulated populations with a fixed selfing rate that we took to be the average selfing rate observed over the last 5×10^4 generations in simulations where condition-dependent selfing evolved. We then compared the equilibrium mean condition and inbreeding depression attained in these fixed selfing simulations with the corresponding simulation runs where condition dependence had evolved (Fig. 3E). We found that positive condition dependence increases mean condition substantially and decreases inbreeding depression relative to the fixed selfing case. This is because positive condition dependence grants a transmission advantage to wild-type alleles, as they tend to be found in individuals in better condition who self-fertilise at a higher rate, which leads to more efficient purging.

Overall, simulation results indicate that the mechanisms described in our two-locus model also apply when condition is affected by many loci. Positive condition dependence for the selfing rate is favoured by natural selection, as it offers modifiers an escape strategy from more deleterious backgrounds, and reduces the mutation load in the population. Under the scenario considered here, selection favours an extreme form of condition dependence whereby low-condition individuals are fully outcrossing and high-condition ones are fully self-fertilising. We next extend our simulation model to investigate how two additional ecological mechanisms, namely environmental fluctuations (Section 3.3) and pollen discounting (Section 3.4), might influence the evolution of condition-dependent selfing.

3.3 Environmental fluctuations destabilise condition dependence

So far, variation in condition between individuals was only determined by their genotype at condition loci. However, variation in condition can also result from environmental differences between individuals [62, 63], for example if some individuals germinate on better quality soil or in less disturbed areas than others. Environmental effects might be especially relevant to the evolution of condition-dependent selfing, because they may obscure the relationship between individual condition and genotype at condition loci, which could in turn affect the evolution of condition dependence.

To study these effects, we simulate a population that follows the same life cycle as before (Section 3.1), except that it now evolves in a heterogeneous environment composed of many patches that host one adult plant each. Seeds produced by these plants are all dispersed away from their natal patch. Each patch

is characterised by an environmental variable, ϵ_i, which changes every generation and follows a normal distribution, i.e.,

$$\epsilon_i \sim \mathcal{N}(0, 1). \tag{10}$$

This variable could represent any relevant ecological factor, such as exposure to sunlight or water availability. A patch with $\epsilon_i = 0$ is optimal for plant development, and any deviation from this optimum reduces individual condition. More precisely, the condition of individual i, carrying $n_{\text{het}}^{(i)}$ and $n_{\text{hom}}^{(i)}$ heterozygous and homozygous deleterious mutations and developing in an environment ϵ_i is given by

$$\varphi_i = \exp\left(-\Delta_{\text{E}}\frac{{\epsilon_i}^2}{2}\right)(1-s)^{n_{\text{hom}}^{(i)}}(1-sh)^{n_{\text{het}}^{(i)}}, \tag{11}$$

where the first term captures the effect of the environment on condition, and the second and third term give the effect of mutations in homozygous and heterozygous state on condition, as before. The intensity of environmental effects increases with parameter $\Delta_{\text{E}} \geqslant 0$, and a stable environment is recovered when $\Delta_{\text{E}} = 0$.

We ran simulations where we varied the intensity of environmental effects ($\Delta_{\text{E}} = \{0.05,\ 0.25,\ 0.5,\ 1\}$), keeping all other parameters fixed for values that allowed the emergence of condition dependence in a stable environment. We find that environmental fluctuations have little impact on the evolution of condition-dependent selfing when their effect on condition is moderate ($\Delta_{\text{E}} = 0.05$ and $\Delta_{\text{E}} = 0.25$): a step-wise relationship between condition and selfing eventually evolves and is stable once established in most replicates, resulting in a high variance in selfing rate (Fig. 4A). Under strong environmental effects ($\Delta_{\text{E}} \geqslant 0.5$), meanwhile, evolutionary trajectories vary widely between replicates. Some rapidly evolve a step-wise relationship, whereas others take much longer to do so, sometimes remaining at a low level of condition dependence for the entire simulation, with a low variance in selfing rate. These differences among replicates are likely due to the fact that environmental fluctuations make condition a poorer indicator of individuals' genetic background and therefore weaken selection for condition dependence: because network loci are initialised with random attributes at the beginning of each simulation, some populations have an easier time evolving condition dependence than others from their initial state, and while this is the case in a stable environment as well ($\Delta_{\text{E}} = 0$, see Fig. S3), differences between populations are likely exacerbated under weaker selection.

We also find that strong environmental effects can affect the stability of condition-dependent selfing once it has evolved, with some populations repeatedly losing and later re-evolving it (Fig. 4B; see Supp. Figs. S3-S7 in Appendix B.3 for more replicates). This repeated loss of condition dependence may be due to the

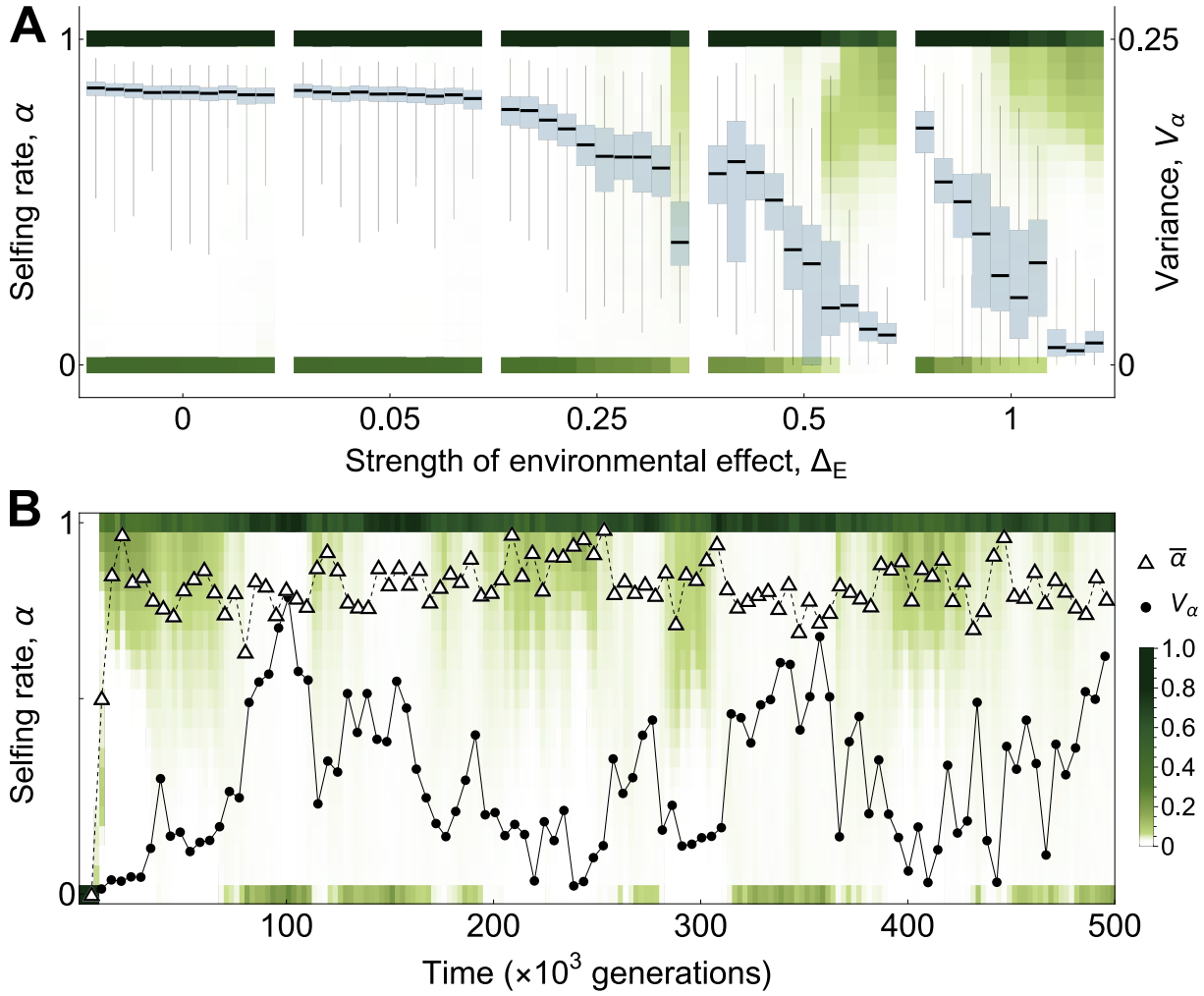

Figure 4: Effect of environmental fluctuations on the evolution of condition-dependent selfing. **A** Distribution of selfing rates in the population in the last 10^5 generations of the simulation for ten replicates and different strengths of environmental effects, increasing from left to right. Shades of green indicate the proportion of individuals expressing a selfing rate in the corresponding interval. The darker the colour, the more individuals in that interval (the colour scale is the same as below). Blue box plots show the distribution of the variance in selfing rate in the population over the last 10^5 generations. The distribution is bimodal with complete selfers and complete outcrossers, resulting in high variance when environmental effects are weak. Stronger environmental effects lead to more diverse distributions because they hinder the emergence of condition dependence and lead to its recurrent collapse and re-emergence once evolved. **B** Distribution of selfing rates in the population as a function of time in a sample simulation under strong environmental fluctuations ($\Delta_E = 1$). Shades of green indicate the proportion of individuals with a selfing rate in the corresponding interval at a given time step. The darker the colour, the more individuals. Triangles indicate the mean selfing rate and black points indicate variance. The population initially evolves condition dependence, and then repeatedly loses and re-evolves it. Parameters used in all simulations: $N = 5 \times 10^3$, $L = 10^3$, $s = 0.05$, $h = 0.25$, $\mu = 5 \times 10^{-4}$, $\mu_g = 5 \times 10^{-3}$, $\sigma_g = 5 \times 10^{-2}$.

fact that strong environmental effects often cause individuals with a good genetic background to be in poor condition, which leads them to outcross despite selfing being their optimal strategy. In this context, an allele making its bearer fully selfing irrespective of condition could increase in frequency if it finds itself in a good genetic background, and cause the collapse of condition dependence.

3.4 Pollen discounting leads to a continuum of mating strategies

Traits that promote selfing often interfere with pollen export, giving rise to a trade-off between selfing and male siring success through outcrossing known as pollen discounting [32], which can favour intermediate selfing rates in the absence of condition dependence [33]. As a final extension, we study the effect of pollen discounting on the evolution of condition-dependent selfing. We consider a population evolving in a stable, homogeneous environment (i.e., no environmental fluctuations). Individuals follow the same life cycle as before (Section 3.1), except that the amount of pollen exported by individual i, β_i, and so its contribution to the outcrossing pollen pool, now decreases with its selfing rate. Specifically, it is given by

$$\beta_i = \varphi_i \left(1 - \kappa {\alpha_i}^{\gamma}\right), \tag{12}$$

where $\kappa \in [0, 1]$ measures the intensity of pollen discounting, and $\gamma > 0$ is a parameter controlling the shape of the trade-off between selfing and pollen export (see Appendix B.2.2 for details).

Previous work demonstrates that linear or convex trade-off curves ($\gamma \leqslant 1$) do not allow the maintenance of intermediate selfing rates [27, 33], and so should not lead to qualitatively new results in our model. We therefore focused on concave relationships ($\gamma > 1$). We varied the intensity (κ) and concavity (γ) of the trade-off between selfing and pollen export, while keeping all other parameters fixed. Our simulations show that weak pollen discounting (small κ) leads to a step-wise relationship – similar to the baseline model – irrespective of the shape of the trade-off curve, presumably because pollen discounting only weakly affects the costs and benefits of selfing in this case. Stronger pollen discounting (large κ), in contrast, favours a more gradual increase in selfing rate with individual condition, leading to a continuum of selfing strategies (Fig. 5A,B). This is because the cost of selfing in terms of siring success increases sharply with the selfing rate under strong pollen discounting, causing the benefits of self-fertilisation to be overcome by the loss of outcrossing opportunities past a critical selfing rate that depends on condition. These results illustrate that including additional mechanisms relevant to the dynamics of mating can alter the relationship that evolves between condition and selfing, resulting in a diverse array of condition-dependent, mixed mating strategies.

We also quantified the effect of condition dependence on the load by comparing mean condition in the population at mutation-selection equilibrium with mean condition in a population where individuals have the same, fixed selfing rate given by the mean selfing rate observed in simulations where condition dependence evolved. We find that condition dependence again reduces the load relative to the condition independent case, though the effect is less pronounced for more linear trade-off curves (Fig. 5C). This is because more linear curves cause pollen discounting to increase more rapidly with selfing, which leads to lower selfing rates in highest-condition individuals. As a result, the difference in selfing rate between individuals with different genetic backgrounds is reduced, which decreases the transmission advantage enjoyed by wild-type alleles and so makes purging owing to condition dependence less efficient.

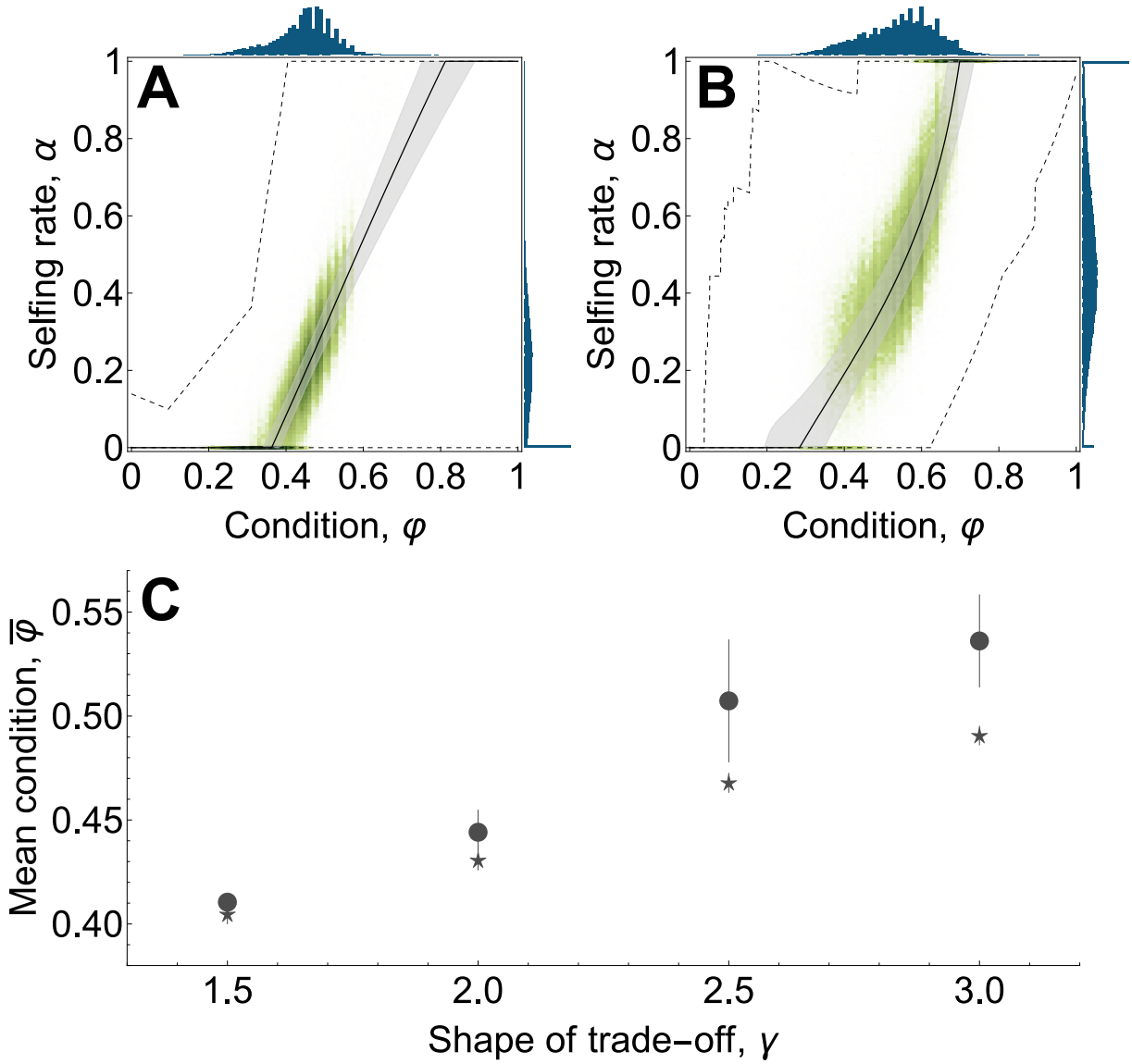

Figure 5: Effect of pollen discounting on the evolution of condition-dependent selfing and the mutation load. **A-B** Evolved condition-dependent selfing strategies in sample simulations under strong pollen discounting ($\kappa = 1$) for $\gamma = 2$ in panel **A** and $\gamma = 3$ in panel **B**. Shades of green represent the selfing rate and condition of a hundred individuals every 50 generations over the last 10^5 of a sample simulation. The lines give the quantiles of the distribution of selfing rates encoded by the gene regulatory networks carried by these same individuals as a function of condition. The solid line gives the median and the grey shading indicates the first and third quartiles. The dashed lines give the maximum and minimum selfing rates observed in the simulations. Note that the relationship between condition and selfing is only subject to selection over the range of condition values that actually occur, so that there are intervals on both ends of the relationship that behave as effectively neutral. The blue histograms give the distribution of condition (top) and selfing rate (right) in the population over the last 10^5 generations. **C** Effect of condition dependence on mean condition under strong pollen discounting. Points indicate mean condition over the last 10^5 generations of simulations where condition dependence evolved, and stars indicate mean condition in a simulation with a fixed selfing rate, taken to be the average rate observed in the corresponding simulation where condition dependence evolved. Parameters used in all simulations: $N = 5 \times 10^3$, $L = 10^3$, $s = 0.05$, $h = 0.25$, $\mu = 5 \times 10^{-4}$, $\mu_g = 5 \times 10^{-3}$, $\sigma_g = 5 \times 10^{-2}$.

4 Discussion

Most theory on the evolution of self-fertilisation considers genetically determined, non-plastic mating strategies [2, 39]. In this paper, we investigated how condition-dependent selfing might evolve, whereby individuals plastically adjust their mating strategy according to their biological condition. We found that positive condition dependence, whereby higher condition individuals self-fertilise at a higher rate, evolves whenever the mutation load is weak enough to allow the initial emergence of self-fertilisation from complete outcrossing. This positive relationship between selfing and condition is favoured as an escape strategy from deleterious genetic backgrounds, similar to the "abandon ship" mechanism, which has been shown to select for individuals in poorer condition to engage more in sexual reproduction [55, 56], recombine more often [57], and undergo mutation at a higher rate during meiosis [74]. The evolution of condition-dependent self-fertilisation therefore represents a novel manifestation of a more general mechanism, with specific biological implications that we discuss below.

We showed that selection favours a positive relationship between condition and the selfing rate, which we modelled as a single trait. In reality, however, the rate at which a plant self-fertilises is likely determined by the interaction of many aspects of its phenotype including, for example, the distance between anthers and pistils [75], the strength of self-incompatibility reactions in the style [76], the plant's allocation to pollen production [77, 78] or the overlap in the timing of sexual maturity of its female and male function [4, 79]. Our results imply that all these traits, rather than the selfing rate directly, should be under selection to evolve condition-dependent expression through their effect on selfing. The degree of condition dependence favoured for a given trait may however depend on several factors. A key factor that we highlighted is how much pollen discounting is caused by the trait when promoting selfing, as we showed that the shape and intensity of the relationship between selfing and pollen export is critical to the condition-dependent strategy favoured by selection. Traits that affect selfing are also likely to be under selection from other ecological and physiological sources, such as pollinator preferences or functional constraints (e.g., on floral morphology [65]), as well as life-history trade-offs, which could interact with selection for condition dependence in ways that have not been explored. In the future, understanding how this interaction between sources of selection shapes the evolution of traits affecting the selfing rate may provide useful insight into the diversity and phenotypic underpinnings of mating strategies in hermaphroditic species, and in particular into the mechanisms promoting the evolution of mixed mating, which remain elusive [2, 39].

Among the many traits that affect selfing, plant size has received special attention. At an intraspecific level, larger plants typically show elevated selfing rates, a pattern usually viewed as an inevitable consequence of the increase with size of pollen transfers among flowers of the same individual (geitonogamy; [64]), and interpreted as a cost to larger plants in terms of lost outcrossing opportunities [12, 64, 66]. Our results suggest that this increased selfing in larger plants may also be favoured by selection through two pathways. First, the size of a plant depends on its ability to extract resources from the environment and allocate them to growth, and is therefore inherently condition-dependent. If higher-condition plants tend to be larger, then condition-dependent selfing would cause larger individuals to self-fertilise more frequently even if size *per se* did not affect selfing. Second, since plant size is indeed thought to have an effect on its selfing rate, allocation to growth could be selected to become condition-dependent owing to this effect. Through this effect on growth, selection for condition-dependent selfing could therefore influence the evolution of traits that do not directly relate to mating as plant size plays a central role in many aspects of a plant's ecology, including its ability to competitively acquire resources or its attractiveness to animal pollinators, dispersers and predators.

Irrespective of the particular trait, the evolution of condition dependence relies on the ability of organisms to acquire information about their genetic background and adjust their strategy accordingly. We assumed that organisms are able to sense their condition directly by letting the selfing rate be determined by a gene regulatory network receiving individual condition as input. When individual condition is purely genetically determined, it acts as a reliable indicator of individual genotype and so condition dependence evolves readily from gene-regulatory interactions. Environment effects on condition hinder the evolution of condition dependence, because they obscure the relationship between condition and genotype, which makes it a less reliable indicator and so weakens selection for condition dependence. However, no amount of environmental fluctuations could entirely prevent condition-dependent selfing from evolving in our simulations, which suggests that the evolution of condition dependence may occur as long as individual condition has some genetic basis and organisms are able to sense their condition. In addition to environmental effects, the evolution of condition dependence could also be hindered if organisms do not sense their condition directly and instead rely on imperfect phenotypic proxies. Reliance on such proxies could also set up an evolutionary feedback between the evolution of the mating system and that of the trait(s) used as proxy, which could for example include individual growth rate or any other measure of metabolic activity.

Our findings point to a need for empirical studies relating plant traits to condition and mating strategy at the individual level. Such data is currently lacking, in part because selfing rates are often measured at the

level of the population and so can seldom be related to individual phenotype [5]. One exception to this comes from studies of herkogamy (the spatial separation of female and male organs), which often show that closer proximity between the two sexual functions leads to higher individual selfing rates (reviewed in [75]). One possible way of looking for condition-dependent selfing empirically could therefore be to relate the degree of herkogamy to condition at the individual level in species where it has been shown to affect the selfing rate. According to our model, lower herkogamy and accordingly higher selfing rates would be expected in higher condition individuals. Condition dependence for the selfing rate could also be revealed by an experimental design where plants with diverse genetic backgrounds are grown under controlled conditions in order to minimise environmental differences between individuals. One would quantify their condition through phenotypic proxies (e.g., plant biomass [80]) and leave them to exchange pollen. Individual selfing rates could then be estimated using the resulting seeds' genotypes, and related to proxies of condition. A positive relationship between these proxies and the selfing rate would then be expected. Alternatively, one could indirectly quantify the amount of deleterious variation carried by a plant, by measuring the performance of self-fertilised and outcrossed seeds produced via controlled crosses on said plant (or one with the same genotype), in order to quantify inbreeding depression within its progeny. In this setting, one would expect a negative relationship between the selfing rate of the parent and the magnitude of inbreeding depression measured among its offspring.

The genetic escape mechanism that we highlight should also select for condition dependence in traits that affect inbreeding in general – of which selfing is but an extreme case. Beyond hermaphroditic organisms, our results might therefore have implications for the evolution of condition dependence in organisms with separate sexes as well. In dioecious animals, this mechanism could for instance favour the evolution of condition-dependent dispersal – whereby lower condition individuals would tend to be more dispersive – or condition-dependent preference for mating with kin, in which case high condition individuals would be more prone to mate with individuals related to them. Behavioural preference and avoidance of inbreeding are both well-documented in animals [81], but the possibility that these preferences might vary between individuals as a function of their condition has not been considered, be it in theory or empirically.

In conclusion, our analyses demonstrate that selection broadly favours condition-dependent inbreeding, leading to a diverse array of mating strategies coexisting in populations. The consequences of this previously undescribed source of selection may be seen on many traits in partially selfing hermaphrodites as well as in dioecious organisms, though the emergence of condition dependence may be constrained by morphological and physiological trade-offs, and the strength of selection for condition dependence would be diminished by strong environmental effects or reliance on imperfect phenotypic proxies. The question

of how often condition-dependent inbreeding actually occurs in natural populations, and if so, through which phenotypic basis, is open for empirical investigation.

Acknowledgements. The authors would like to thank the Swiss National Science Foundation for funding (SNF grants 310030_215135 to JRP and PCEFP3181243 to CM).

Data availability. The code used for individual-based simulations, numerical analyses and to check analytical results is available at `10.5281/zenodo.18523420`.

Authors contributions. TL, JRP and CM conceived the study. TL carried out the analytical work and simulations, with input from CM. TL wrote the first draft. All authors contributed to revisions and approved the final manuscript. CM and JRP supervised the work and acquired the funding.

References

[1] S. C.H. Barrett and L.D. Harder. The comparative biology of pollination and mating in flowering plants. *Philosophical Transactions of the Royal Society of London B*, 351:1271–1280, 1996.

[2] C. Goodwillie, S. Kalisz, and C.G. Eckert. The evolutionary enigma of mixed mating systems in plants: Occurence, theoretical explanations, and empirical evidence. *Annual Review of Ecology, Evolution, and Systematics*, 36:47–79, 2005.

[3] P. Jarne and J.R. Auld. Animals mix it up too: the distribution of self-fertilization among hermaphroditic animals. *Evolution*, 60(9):1816–1824, 2006.

[4] S. C. Barrett and L. D. Harder. The ecology of mating and its evolutionary consequences in seed plants. *Annual Review of Ecology, Evolution, and Systematics*, 48:135–157, 2017.

[5] M.R. Whitehead, R. Lanfear, R.J. Mitchell, and J.D. Karron. Plant mating systems often vary widely among populations. *Frontiers in Ecology and Evolution*, 6:38, 2018.

[6] M. Ferriol, C. Pichot, and F. Lefèvre. Variation of selfing rate and inbreeding depression among individuals and across generations within an admixed Cedrus population. *Heredity*, 106(1):146–157, 2011.

[7] S. Nora, A. Aparicio, and R.G. Albaladejo. High correlated paternity leads to negative effects on progeny performance in two mediterranean shrub species. *PLOS ONE*, 11:e0166023, 2016.

[8] J. Brunet and C. G. Eckert. Effects of floral morphology and display on outcrossing in Blue Columbine, Aquilegia caerulea (Ranunculaceae). *Functional Ecology*, 12(4):596–606, 1998.

[9] J.D. Karron, R.T. Jackson, N.N. Thumser, and S.L. Schlicht. Outcrossing rates of individual Mimulus ringens genets are correlated with anther–stigma separation. *Heredity*, 79(4):365–370, 1997.

[10] C. Darwin. *The effects of cross and self fertilisation in the vegetable kingdom*. D. Appleton, 1877.

[11] D. Charlesworth and B. Charlesworth. The evolutionary genetics of sexual systems in flowering plants. *Proceedings of the Royal Society of London. Series B. Biological Sciences*, 205(1161):513–530, 1979.

[12] S.C.H. Barrett. Mating strategies in flowering plants: the outcrossing–selfing paradigm and beyond. *Philosophical Transactions of the Royal Society of London. Series B: Biological Sciences*, 358:991–1004, 2003.

[13] P. Jarne and D. Charlesworth. The evolution of the selfing rate in functionally hermaphrodite plants and animals. *Annual Review of Ecology and Systematics*, pages 441–466, 1993.

[14] S. Kalisz, D.W. Vogler, and K.M. Hanley. Context-dependent autonomous self-fertilization yields reproductive assurance and mixed mating. *Nature*, 430(7002):884–887, 2004.

[15] C.G. Eckert, K.E. Samis, and S. Dart. Reproductive assurance and the evolution of uniparental reproduction in flowering plants. In L.D. Harder and S.C.H. Barrett, editors, *Ecology and Evolution of Flowers*, pages 183–203. Oxford University Press, 2006.

[16] A. Sicard and M. Lenhard. The selfing syndrome: a model for studying the genetic and evolutionary basis of morphological adaptation in plants. *Annals of Botany*, 107:1433–1443, 2011.

[17] R.A. Fisher. Average excess and average effect of a gene substitution. *Annals of Human Genetics*, 11:53–63, 1941.

[18] D. Charlesworth and B. Charlesworth. Inbreeding depression and its evolutionary consequences. *Annual Review of Ecology and Systematics*, 18:237–268, 1987.

[19] B. Charlesworth and D. Charlesworth. The genetic basis of inbreeding depression. *Genetics Research*, 74(3):329–340, 1999.

[20] D. Charlesworth and J.H. Willis. The genetics of inbreeding depression. *Nature reviews genetics*, 10:783–796, 2009.

[21] R. Lande and D.W. Schemske. The evolution of self-fertilization and inbreeding depression in plants. I. genetic models. *Evolution*, 39:24–40, 1985.

[22] D. Charlesworth, M.T. Morgan, and B. Charlesworth. Inbreeding depression, genetic load, and the evolution of outcrossing rates in a multilocus system with no linkage. *Evolution*, 44:1469–1489, 1990.

[23] B. Charlesworth, M.T. Morgan, and D. Charlesworth. Multilocus models of inbreeding depression with synergistic selection and partial self-fertilization. *Genetics*, 57:177–194, 1991.

[24] R. Lande and E. Porcher. Maintenance of quantitative genetic variance under partial self-fertilization, with implications for evolution of selfing. *Genetics*, 200:891–906, 2015.

[25] D. Abu Awad and S. Billiard. The double edged sword: The demographic consequences of the evolution of self-fertilization. *Evolution*, 71:1178–1190, 2017.

[26] D. Abu Awad and D. Roze. Effects of partial selfing on the equilibrium genetic variance, mutation load and inbreeding depression under stabilizing selection. *Evolution*, 72:751–769, 2018.

[27] D. Abu Awad and D. Roze. Epistasis, inbreeding depression, and the evolution of self-fertilization. *Evolution*, 74(7):1301–1320, 2020.

[28] J. Ronfort and D. Couvet. A stochastic model of selection on selfing rates in structured populations. *Genetics Research*, 65:209–222, 1995.

[29] M.T. Morgan and W.G. Wilson. Self-fertilization and the escape from pollen limitation in variable pollination environments. *Evolution*, 59:1143–1148, 2005.

[30] K.E. Holsinger, M.W. Feldman, and F.B. Christiansen. The evolution of self-fertilization in plants: a population genetic model. *The American Naturalist*, 124(3):446–453, 1984.

[31] K.E. Holsinger. Mass-action models of plant mating systems: the evolutionary stability of mixed mating systems. *The American Naturalist*, 138:606–622, 1991.

[32] L.D. Harder and W.G. Wilson. A clarification of pollen discounting and its joint effects with inbreeding depression on mating system evolution. *The American Naturalist*, 152(5):684–695, 1998.

[33] M.O. Johnston. Evolution of intermediate selfing rates in plants: pollination ecology versus deleterious mutations. In *Mutation and Evolution*, pages 267–278. Springer, 1998.

[34] E. Porcher and R. Lande. The evolution of self-fertilization and inbreeding depression under pollen discounting and pollen limitation. *Journal of Evolutionary Biology*, 18:497–508, 2005.

[35] M.D. Rausher and S.-M. Chang. Stabilization of mixed-mating systems by differences in the magnitude of inbreeding depression for male and female fitness components. *The American Naturalist*, 154(2):242–248, 1999.

[36] P-O. Cheptou and U. Dieckmann. The evolution of self-fertilization in density-regulated populations. *Proceedings of the Royal Society of London. Series B: Biological Sciences*, 269:1177–1186, 2002.

[37] P.-O. Cheptou and A. Mathias. Can varying inbreeding depression select for intermediary selfing rates? *The American Naturalist*, 157:361–373, 2001.

[38] E. Porcher, J.K. Kelly, P.-O. Cheptou, C.G. Eckert, M.O. Johnston, and S. Kalisz. The genetic consequences of fluctuating inbreeding depression and the evolution of plant selfing rates. *Journal of Evolutionary Biology*, 22:708–717, 2009.

[39] J. Clo, D. Abu Awad, T. Bilde, G. Bocedi, C.R. Haag, J.R. Pannell, and M. Hartfield. Perspectives on mating–system evolution: comparing concepts in plants and animals. *Journal of evolutionary biology*, page voaf009, 2025.

[40] S.A. Richards, N.M. Williams, and L.D. Harder. Variation in pollination: causes and consequences for plant reproduction. *The American Naturalist*, 174(3):382–398, 2009.

[41] S.C.H. Barrett and L.D. Harder. The Ecology of Mating and Its Evolutionary Consequences in Seed Plants. *Annual Review of Ecology, Evolution, and Systematics*, 48:135–157, 2017.

[42] M. Vallejo-Marín and S.C.H. Barrett. Modification of flower architecture during early stages in the evolution of self-fertilization. *Annals of Botany*, 103(6):951–962, 2009.

[43] R.l Jorgensen and H.S. Arathi. Floral longevity and autonomous selfing are altered by pollination and water availability in collinsia heterophylla. *Annals of Botany*, 112(5):821–828, 2013.

[44] R.B. Spigler. Plasticity of floral longevity and floral display in the self-compatible biennial sabatia angularis (gentianaceae): untangling the role of multiple components of pollination. *Annals of botany*, 119(1):167–176, 2017.

[45] D.G. Lloyd. Some reproductive factors affecting the selection of self-fertilization in plants. *The American Naturalist*, 113:67–79, 1979.

[46] D.G. Lloyd. Self- and cross-fertilization in plants. II. the selection of self-fertilization. *International Journal of Plant Sciences*, 153:370–380, 1992.

[47] C. Goodwillie and J.J. Weber. The best of both worlds? a review of delayed selfing in flowering plants. *American Journal of Botany*, 105(4):641–655, 2018.

[48] A. Tsitrone, S. Duperron, and P. David. Delayed selfing as an optimal mating strategy in preferentially outcrossing species: theoretical analysis of the optimal age at first reproduction in relation to mate availability. *The American Naturalist*, 162(3):318–331, 2003.

[49] L. Rowe and D. Houle. The lek paradox and the capture of genetic variance by condition dependent traits. *Proceedings of the Royal Society of London. Series B: Biological Sciences*, 263(1375):1415–1421, 1996.

[50] M.D. Jennions, A.P. Møller, and M. Petrie. Sexually selected traits and adult survival: a meta-analysis. *The Quarterly Review of Biology*, 76(1):3–36, 2001.

[51] C. Fricke, J. Perry, and L. Chapman, T.and Rowe. The conditional economics of sexual conflict. *Biology Letters*, 5(5):671–674, 2009.

[52] E.O. Flintham, V. Savolainen, and C. Mullon. Male harm offsets the demographic benefits of good genes. *Proceedings of the National Academy of Sciences*, 120(10):e2211668120, 2023.

[53] A. Pomiankowski and Y. Iwasa. *How does mate choice contribute to exaggeration and diversity in sexual characters?*, page 203–220. Cambridge University Press, 2001.

[54] G.S. Van Doorn and F.J. Weissing. Sexual conflict and the evolution of female preferences for indicators of male quality. *The American Naturalist*, 168(6):742–757, 2006.

[55] L. Hadany and S.P. Otto. The evolution of condition-dependent sex in the face of high costs. *Genetics*, 176(3):1713–1727, 2007.

[56] Sarah P Otto. The evolutionary enigma of sex. *the american naturalist*, 174(S1):S1–S14, 2009.

[57] A.F. Agrawal, L. Hadany, and S.P. Otto. The evolution of plastic recombination. *Genetics*, 171(2): 803–812, 2005.

[58] A. Wagner. Evolution of gene networks by gene duplications: a mathematical model and its implications on genome organization. *Proceedings of the National Academy of Sciences*, 91(10):4387–4391, 1994.

[59] H. Ezoe and Y. Iwasa. Evolution of condition-dependent dispersal: a genetic-algorithm search for the ess reaction norm. *Researches on population ecology*, 39:127–137, 1997.

[60] J.N. Deshpande and E.A. Fronhofer. Genetic architecture of dispersal and local adaptation drives accelerating range expansions. *Proceedings of the National Academy of Sciences*, 119(31): e2121858119, 2022.

[61] J.N. Deshpande and E.A. Fronhofer. A gene-regulatory network model for density-dependent and sex-biased dispersal evolution during range expansions. *Peer Community Journal*, 5, 2025.

[62] A.J. Wilson and D.H. Nussey. What is individual quality? an evolutionary perspective. *Trends in ecology & evolution*, 25(4):207–214, 2010.

[63] A.B. Forsythe, T. Day, and W.A. Nelson. Demystifying individual heterogeneity. *Ecology Letters*, 24(10):2282–2297, 2021.

[64] T.J. de Jong, N.M. Waser, and P.G.L. Klinkhamer. Geitonogamy: the neglected side of selfing. *Trends in Ecology & Evolution*, 8(9):321–325, 1993.

[65] S.C.H. Barrett. Sexual interference of the floral kind. *Heredity*, 88(2):154–159, 2002.

[66] L.D. Harder and S.C.H. Barrett. Mating cost of large floral displays in hermaphrodite plants. *Nature*, 373(6514):512–515, 1995.

[67] M. Kimura. A stochastic model concerning the maintenance of genetic variability in quantitative characters. *Proceedings of the National Academy of Sciences*, 54(3):731–736, 1965.

[68] J.F. Crow and M. Kimura. *An introduction to population genetics theory*. Black Burn Press, 1970.

[69] P. Avila and C. Mullon. Evolutionary game theory and the adaptive dynamics approach: adaptation where individuals interact. *Philosophical Transactions of the Royal Society B: Biological Sciences*, 378(1876):20210502, 2023.

[70] A.F. Agrawal and M.C. Whitlock. Mutation load: the fitness of individuals in populations where deleterious alleles are abundant. *Annual Review of Ecology, Evolution, and Systematics*, 43(1): 115–135, 2012.

[71] D. Roze. Effects of interference between selected loci on the mutation load, inbreeding depression, and heterosis. *Genetics*, 201:745–757, 2015.

[72] B. Charlesworth. Optimization models, quantitative genetics, and mutation. *Evolution*, 44:520–538, 1990.

[73] Y. Iwasa and A. Pomiankowski. The evolution of mate preferences for multiple sexual ornaments. *Evolution*, 48(3):853–867, 1994.

[74] Y. Ram, L. Altenberg, U. Liberman, and M.W. Feldman. Generation of variation and a modified mean fitness principle: necessity is the mother of genetic invention. *Theoretical Population Biology*, 123:1–8, 2018.

[75] Ø. Opedal. Herkogamy, a principal functional trait of plant reproductive biology. *International Journal of Plant Sciences*, 179(9):677–687, 2018.

[76] D.A. Levin. The evolutionary significance of pseudo-self-fertility. *The American Naturalist*, 148 (2):321–332, 1996.

[77] C. Damgaard and R.J. Abbott. Positive correlations between selfing rate and pollen-ovule ratio within plant populations. *Evolution*, pages 214–217, 1995.

[78] K.-H. Chen and J.R. Pannell. Dioecy in a wind-pollinated herb explained by disruptive selection on sex allocation via inbreeding avoidance. *New Phytologist*, 247(6):2733–2745, 2025.

[79] S. Kalisz, A. Randle, D. Chaiffetz, M. Faigeles, A. Butera, and C. Beight. Dichogamy correlates with outcrossing rate and defines the selfing syndrome in the mixed-mating genus collinsia. *Annals of botany*, 109(3):571–582, 2012.

[80] B.S. Younginger, D. Sirová, M.B. Cruzan, and D.J. Ballhorn. Is biomass a reliable estimate of plant fitness? *Applications in plant sciences*, 5(2):1600094, 2017.

[81] V.L. Pike, C.K. Cornwallis, and A.S. Griffin. Why don't all animals avoid inbreeding? *Proceedings of the Royal Society B*, 288(1956):20211045, 2021.

Appendices to

"The evolution of condition-dependent self-fertilisation"

Thomas Lesaffre*, John R. Pannell and Charles Mullon

Department of Ecology and Evolution, University of Lausanne, 1015 Lausanne, Switzerland

*Corresponding author: thomas.lesaffre@unil.ch

Table of contents

Appendix A

Analysis of the two-locus model

In this Appendix, we analyse the two-locus model described in Section 2 of the main text. We first study the effect of a fixed relationship between condition and selfing on the condition locus (Section A.1), and then consider the evolution of condition-dependent selfing (Section A.2).

A.1 Effect of condition-dependent selfing on the condition locus

A.1.1 General population genetic recursions

We consider a population fixed for an arbitrary selfing strategy $\boldsymbol{\alpha} = (\alpha_{\mathrm{AA}}, \alpha_{\mathrm{Aa}}, \alpha_{\mathrm{aa}})$. In this population, we denote the frequency of genotype x_1x_2 (with $x_1,\ x_2 \in \{\mathrm{A}, \mathrm{a}\}$) at some arbitrary time t as $q_{x_1x_2}(t)$, and by $M_x(\boldsymbol{\alpha}, t)$ the frequency of allele $x \in \{\mathrm{A}, \mathrm{a}\}$ in the outcross pollen pool. Accounting for mutation among the gametes produced by each genotype, frequencies in the outcross pollen pool are given by

$$\begin{aligned} M_{\mathrm{A}}(\boldsymbol{\alpha}, t) &= (1-\mu_A)\, q_{\mathrm{AA}}(t)\frac{\varphi_{\mathrm{AA}}}{\overline{\varphi}(t)} + q_{\mathrm{Aa}}(t)\frac{1-\mu_A+\mu_a}{2}\frac{\varphi_{\mathrm{Aa}}}{\overline{\varphi}(t)} + \mu_a\, q_{\mathrm{aa}}(t)\frac{\varphi_{\mathrm{aa}}}{\overline{\varphi}(t)}, \\ M_{\mathrm{a}}(\boldsymbol{\alpha}, t) &= \mu_A\, q_{\mathrm{AA}}(t)\frac{\varphi_{\mathrm{AA}}}{\overline{\varphi}(t)} + q_{\mathrm{Aa}}(t)\frac{1-\mu_a+\mu_A}{2}\frac{\varphi_{\mathrm{Aa}}}{\overline{\varphi}(t)} + (1-\mu_a)\, q_{\mathrm{aa}}(t)\frac{\varphi_{\mathrm{aa}}}{\overline{\varphi}(t)}, \end{aligned} \tag{A1}$$

for allele A and a, respectively, where

$$\overline{\varphi}(t) = \varphi_{\mathrm{AA}} q_{\mathrm{AA}}(t) + \varphi_{\mathrm{Aa}} q_{\mathrm{Aa}}(t) + \varphi_{\mathrm{aa}} q_{\mathrm{aa}}(t) \tag{A2}$$

is the mean condition in the population at time t. Using these notations, genotypic frequencies in the next generation are given by

$$\begin{aligned} q_{\mathrm{AA}}(t+1) = {} & q_{\mathrm{AA}}(t)\frac{\varphi_{\mathrm{AA}}}{\overline{\varphi}(t)}(1-\mu_{\mathrm{A}})\left[\alpha_{\mathrm{AA}}(1-\mu_A) + (1-\alpha_{\mathrm{AA}})M_{\mathrm{A}}(\boldsymbol{\alpha}, t)\right] \\ & + q_{\mathrm{Aa}}(t)\frac{\varphi_{\mathrm{Aa}}}{\overline{\varphi}(t)}\frac{1-\mu_A+\mu_a}{2}\left[\alpha_{\mathrm{Aa}}\frac{1-\mu_A+\mu_a}{2} + (1-\alpha_{\mathrm{Aa}})M_{\mathrm{A}}(\boldsymbol{\alpha}, t)\right] \\ & + q_{\mathrm{aa}}(t)\mu_{\mathrm{a}}\frac{\varphi_{\mathrm{aa}}}{\overline{\varphi}(t)}\left[\alpha_{\mathrm{aa}}\mu_a + (1-\alpha_{\mathrm{aa}})M_{\mathrm{A}}(\boldsymbol{\alpha}, t)\right], \end{aligned} \tag{A3a}$$

$$
\begin{aligned}
q_{\mathrm{Aa}}(t+1) = {} & q_{\mathrm{AA}}(t)\frac{\varphi_{\mathrm{AA}}}{\overline{\varphi}(t)}\left\{2\mu_A(1-\mu_A)\alpha_{\mathrm{AA}} + (1-\alpha_{\mathrm{AA}})\big[(1-\mu_A)M_{\mathrm{a}}(\boldsymbol{\alpha},t) + \mu_A M_{\mathrm{A}}(\boldsymbol{\alpha},t)\big]\right\} \\
& + 2q_{\mathrm{Aa}}(t)\frac{\varphi_{\mathrm{Aa}}}{\overline{\varphi}(t)}\frac{1-\mu_A+\mu_a}{2}\frac{1-\mu_a+\mu_A}{2} \\
& + q_{\mathrm{aa}}(t)\frac{\varphi_{\mathrm{aa}}}{\overline{\varphi}(t)}\left\{2\mu_a(1-\mu_a)\alpha_{\mathrm{aa}} + (1-\alpha_{\mathrm{aa}})\big[(1-\mu_a)M_{\mathrm{A}}(\boldsymbol{\alpha},t) + \mu_a M_{\mathrm{a}}(\boldsymbol{\alpha},t)\big]\right\},
\end{aligned}
\tag{A3b}
$$

and

$$
\begin{aligned}
q_{\mathrm{aa}}(t+1) = {} & q_{\mathrm{AA}}(t)\frac{\varphi_{\mathrm{AA}}}{\overline{\varphi}(t)}\mu_A\left[\alpha_{\mathrm{AA}}\mu_A + (1-\alpha_{\mathrm{AA}})M_{\mathrm{a}}(\boldsymbol{\alpha},t)\right] \\
& + q_{\mathrm{Aa}}(t)\frac{\varphi_{\mathrm{Aa}}}{\overline{\varphi}(t)}\frac{1-\mu_a+\mu_A}{2}\left[\alpha_{\mathrm{Aa}}\frac{1-\mu_a+\mu_A}{2} + (1-\alpha_{\mathrm{Aa}})M_{\mathrm{a}}(\boldsymbol{\alpha},t)\right] \\
& + q_{\mathrm{aa}}(t)\frac{\varphi_{\mathrm{aa}}}{\overline{\varphi}(t)}(1-\mu_a)\left[\alpha_{\mathrm{aa}}(1-\mu_a) + (1-\alpha_{\mathrm{aa}})M_{\mathrm{a}}(\boldsymbol{\alpha},t)\right].
\end{aligned}
\tag{A3c}
$$

In each of the three equations in (A3), the three lines give the frequency of successful offspring of the considered genotype produced by AA, Aa and aa mothers, respectively.

To understand how these were obtained, let us focus on eq. (A3c), which gives the frequency of wild-type homozygotes aa in the next time step. Wild-type homozygote mothers AA contribute a proportion $q_{\mathrm{AA}}(t)\times\varphi_{\mathrm{AA}}/\overline{\varphi}(t)$ of the ovules produced by the population, a fraction μ_{A} of which carry the deleterious allele a. A fraction α_{AA} of these ovules is then self-fertilised and give rise to aa seeds if they get fertilised by a-carrying pollen, which occurs with probability μ_{A}. The remaining fraction $1-\alpha_{\mathrm{AA}}$ is fertilised through outcrossing, in which case they are fertilised by a-carrying pollen with probability $M_{\mathrm{a}}(\boldsymbol{\alpha},t)$. Heterozygous mothers Aa contribute a proportion $q_{\mathrm{Aa}}(t)\times\varphi_{\mathrm{Aa}}/\overline{\varphi}(t)$ of ovules, a fraction $(1-\mu_{\mathrm{a}}+\mu_{\mathrm{A}})/2$ of which carry the deleterious allele a. These are self-fertilised in proportion α_{Aa}, in which case they receive a-carrying pollen and give rise to a aa seed with probability $(1-\mu_{\mathrm{a}}+\mu_{\mathrm{A}})/2$. Otherwise, they are fertilised by outcrossing, and receive a-carrying pollen with probability $M_{\mathrm{a}}(\boldsymbol{\alpha},t)$. Finally, deleterious homozygote mothers aa contribute a proportion $q_{\mathrm{aa}}(t)\times\varphi_{\mathrm{aa}}/\overline{\varphi}(t)$ of ovules, a fraction $1-\mu_{\mathrm{a}}$ of which carry the deleterious allele a. These get self-fertilised at rate α_{aa} and receive a-carrying pollen with probability $1-\mu_{\mathrm{a}}$, otherwise, they get cross-fertilised and receive a-carrying pollen with probability $M_{\mathrm{a}}(\boldsymbol{\alpha},t)$.

The equilibrium genotypic frequencies can be obtained from eq. (A3) by finding

$$
q^*_{\mathrm{AA}},\ q^*_{\mathrm{Aa}} \text{ and } q^*_{\mathrm{aa}} \quad \text{such that} \quad q_{x_1x_2}(t) = q_{x_1x_2}(t+1) = q^*_{x_1x_2} \text{ for all } x_1,\ x_2 \in \{\mathrm{A},\mathrm{a}\}. \tag{A4}
$$

A more practical description. The description of population genetic dynamics in terms of genotypic frequencies given above is the most natural to derive from a particular biological scenario, but is difficult to work with in practice, especially when incorporating assumptions on the relative magnitude of parameters, as we will come to below. A more practical description, which we will use from now on, can be obtained from expressing genotypic frequencies as

$$\begin{aligned} q_{\mathrm{AA}}(t) &= (1-p(t))^2 + C(t) \\ q_{\mathrm{Aa}}(t) &= 2\left[p(t)(1-p(t)) - C(t)\right] \\ q_{\mathrm{aa}}(t) &= p(t)^2 + C(t), \end{aligned} \tag{A5}$$

where

$$p(t) = q_{\mathrm{aa}}(t) + \frac{q_{\mathrm{Aa}}(t)}{2} \quad \text{and} \quad C(t) = q_{\mathrm{aa}}(t) - p(t)^2$$

denote the frequency of allele a and the excess in homozygotes relative to the Hardy-Weinberg expectation at the condition locus at time t, respectively, and

$$\Delta p = p(t+1) - p(t) \quad \text{and} \quad \Delta C = C(t+1) - C(t) \tag{A6}$$

denote the change in these quantities over one generation, which is be readily obtained by rearranging eq. (A3). With this description, an equilibrium is defined as

$$p^*, C^* \quad \text{such that} \quad \Delta p = \Delta C = 0. \tag{A7}$$

Weak variation in condition. Throughout our analyses, we will assume that the effect of the deleterious allele a on condition is weak, $s \sim \mathcal{O}(\epsilon)$, and mutation at the condition locus is rare in both directions, $\mu_x \sim \mathcal{O}\left(\epsilon^2\right)$, so that $\mu_x \ll s$. To incorporate this assumption, our approach will rely in Taylor-expanding the change in allelic frequency and excess homozygosity at the condition locus around $\epsilon = 0$. In general, this will take the form

$$\mathcal{K} = \mathcal{K}_{(0)} + \epsilon\, \mathcal{K}_{(1)} + \frac{\epsilon^2}{2}\mathcal{K}_{(1)} + ... + \frac{\epsilon^n}{n!}\mathcal{K}_{(n)} + \mathcal{O}\left(\epsilon^{n+1}\right), \tag{A8a}$$

where

$$\mathcal{K}_{(n)} = \left.\frac{\partial^n \mathcal{K}}{\partial \epsilon^n}\right|_{\epsilon=0} \tag{A8b}$$

is the n^{th} order perturbation of $\mathcal{K}$ with respect to ϵ, and $\mathcal{K}$ can be any differentiable quantity (e.g., Δp and ΔC here).

A.1.2 Linear relationship

The explicit solution to eq. (A7) cannot be obtained for an arbitrary selfing strategy $\boldsymbol{\alpha}$, as differences in selfing rates between genotypes greatly complicate the dynamics. To gain analytical traction, we assume that genotype-dependent selfing rates $\boldsymbol{\alpha} = (\alpha_{\text{AA}}, \alpha_{\text{Aa}}, \alpha_{\text{aa}})$ follow a linear relationship. Specifically, we assume that they are given by

$$\boldsymbol{\alpha} = (\alpha_{\text{AA}}, \alpha_{\text{Aa}}, \alpha_{\text{aa}}) = \Big(\alpha_0, \alpha_0 - h d_\alpha,\ \alpha_0 - d_\alpha\Big), \tag{A9}$$

where d_α determines the slope of the line on which α_{AA}, α_{Aa} and α_{aa} lie. The selfing rate increases with condition when $d_\alpha > 0$ (positive condition dependence) and decreases with condition occurs when $d_\alpha < 0$ (negative condition dependence). We assume that condition dependence is weak, $d_\alpha \sim \mathcal{O}(\epsilon)$, in order to obtain analytical results, but numerical analyses show that the obtained approximation predicts exact solutions under a broad parameter range (see Fig. 2B in the main text).

Our aim is to compute the equilibrium allelic frequency p^* and excess homozygosity C^* at the condition locus to first order in ϵ. To do so, we expand the allelic frequency $p(t)$ and excess in homozygotes $C(t)$ using eq. (A8) as

$$p(t) = p_{(0)} + \epsilon\, p_{(1)} + \frac{\epsilon^2}{2} p_{(2)} + ... + \frac{\epsilon^n}{n!} p_{(n)} + \mathcal{O}\left(\epsilon^{n+1}\right) \tag{A10a}$$

and

$$C(t) = C_{(0)} + \epsilon\, C_{(1)} + \frac{\epsilon^2}{2} C_{(2)} + ... + \frac{\epsilon^n}{n!} C_{(n)} + \mathcal{O}\left(\epsilon^{n+1}\right), \tag{A10b}$$

where we dropped time t from perturbation terms for brevity. Similarly, the change in these variables over one generation can be written as sums of perturbations to the n^{th} order in ϵ, i.e.,

$$\Delta p = \Delta p_{(0)} + \epsilon\, \Delta p_{(1)} + \frac{\epsilon^2}{2} \Delta p_{(2)} + ... + \frac{\epsilon^n}{n!} \Delta p_{(n)} + \mathcal{O}\left(\epsilon^{n+1}\right) \tag{A10c}$$

and

$$\Delta C = \Delta C_{(0)} + \epsilon\, \Delta C_{(1)} + \frac{\epsilon^2}{2} \Delta C_{(2)} + ... + \frac{\epsilon^n}{n!} \Delta C_{(n)} + \mathcal{O}\left(\epsilon^{n+1}\right). \tag{A10d}$$

It follows from eq. (A7) that for a population to be at an equilibrium, we must have

$$\Delta p_{(n)} = \Delta C_{(n)} = 0 \tag{A11}$$

to all orders $n \in \{0, 1, ..., n\}$ in ϵ. Below, we solve eq. (A11) to increasingly high orders to compute perturbations terms in eq. (A10).

Injecting eq. (A10) into eq. (A6) and expanding it to order zero in ϵ, we find that the change in frequency and excess homozygosity at the condition locus are

$$\Delta p_{(0)} = 0 \quad \text{and} \quad \Delta C_{(0)} = \frac{1}{2}\Big[\alpha_0 p_{(0)}(1 - p_{(0)}) - C_{(0)}(2 - \alpha_0)\Big] \tag{A12}$$

to order zero. The change in allelic frequency is zero because all the processes that affect it, namely mutation, fecundity selection and condition dependence are neglected to this order, and so allelic frequencies will not change from one generation to the next in the absence of drift. The change in mean homozygosity to order zero, meanwhile, yields

$$\Delta C_{(0)} = 0 \quad \Rightarrow \quad C^*_{(0)} = F p_{(0)}(1 - p_{(0)}) \tag{A13}$$

at equilibrium, with

$$F = \frac{\alpha_0}{2 - \alpha_0}. \tag{A14}$$

Eq. (A13) corresponds to the expected excess homozygosity at a diallelic neutral locus under partial selfing in the absence of condition dependence (which is neglected to order zero).

The first-order perturbation of the change in frequency at the condition locus is given by

$$\Delta p_{(1)} = -\left(s + \frac{d_\alpha}{2}\right)\left[F + (1 - F)\Big(p_{(0)} + h\left(1 - 2p_{(0)}\right)\Big)\right] p_{(0)}\left(1 - p_{(0)}\right). \tag{A15}$$

The term in square brackets is strictly positive for $0 \leqslant h \leqslant 1$, so that there is two possible equilibria that satisfy eq. (A11), either $p^*_{(0)} = 0$ or $p^*_{(0)} = 1$. Which of the two is attained is determined by the relative strength of selection against the deleterious allele and condition dependence for the selfing rate. Under positive condition dependence ($d_\alpha > 0$), eq. (A15) is always negative, leading to $p^*_{(0)} = 0$. This indicates that the deleterious allele always remains rare in this situation, as higher order terms will only produce small deviations close to $p^*_{(0)} = 0$. Under negative condition dependence ($d_\alpha < 0$), on the other hand, eq. (A15) can become positive and lead to $p^*_{(0)} = 1$, indicating that the deleterious allele attains a

frequency close to one at equilibrium. Specifically, we have

$$p^*_{(0)} = \begin{cases} 1 & \text{if} \quad d_\alpha < -2s \\ 0 & \text{otherwise.} \end{cases} \tag{A16}$$

This result can be understood as follows. Fecundity selection always disfavours the deleterious allele a, but condition dependence generates an association between selfing rate and genotype at the condition locus, so that alleles at this locus experience different selfing rates and so benefit differentially from the transmission advantage of self-fertilisation [4]. Under positive condition dependence ($d_\alpha > 0$), the wild-type allele A already favoured by fecundity selection enjoys an additional transmission advantage, which further acts against allele a (eq. A15 becomes more negative). Conversely, negative condition dependence ($d_\alpha < 0$) counteracts fecundity selection by granting a transmission advantage to the deleterious allele a and offsets it completely when $d_\alpha < -2s$, leading to the near fixation of allele a. We calculate subsequent terms separately for the $p^*_{(0)} = 0$ and $p^*_{(0)} = 1$ cases.

When $p^*_{(0)} = 0$, the first-order perturbation of the change in homozygosity, $\Delta C_{(1)}$, is given by

$$\Delta C_{(1)} = \frac{1}{1+F}\Big(F p_{(1)} - C_{(1)}\Big), \tag{A17}$$

so that at equilibrium

$$\Delta C_{(1)} = 0 \quad \Rightarrow \quad C^*_{(1)} = F p^*_{(1)}, \tag{A18}$$

which again corresponds to the expected excess in homozygotes at a diallelic locus under neutrality (with terms in ${p^*_{(1)}}^2$ neglected because they are of order ϵ^2). When $p^*_{(0)} = 1$, on the other hand, we have

$$\Delta C_{(1)} = -\frac{1}{1+F}\Big(F p_{(1)} + C_{(1)}\Big), \tag{A19}$$

which gives

$$C^*_{(1)} = -F p^*_{(1)}. \tag{A20}$$

The minus sign in eq. (A20) compensates for the fact that $p_{(0)} = 1$ in this case, so that the first-order perturbation of allelic frequency $p^*_{(1)}$ must be negative or null (see below).

The second-order perturbation of the change in frequency $\Delta p_{(2)}/2$ with $p^*_{(0)} = 0$ ($d_\alpha > -2s$) is given by

$$\frac{\Delta p_{(2)}}{2} = \mu_A - \left(s + \frac{d_\alpha}{2}\right)\Big[h\,(1-F) + F\Big] p_{(1)}, \tag{A21}$$

leading to

$$p^* = p^*_{(1)} = \frac{\mu_A}{\left(s + \frac{d_\alpha}{2}\right)\left[h\left(1-F\right)+F\right]} + \mathcal{O}\left(\epsilon^2\right) \quad \text{and} \quad C^* = Fp^* + \mathcal{O}\left(\epsilon^2\right) \tag{A22}$$

at equilibrium. With $p^*_{(0)} = 1$ ($d_\alpha < -2s$), we find

$$\frac{\Delta p_{(2)}}{2} = -\mu_a + \left(s + \frac{d_\alpha}{2}\right)\Big[1 - h(1-F)\Big]p_{(1)}, \tag{A23}$$

yielding

$$\frac{\Delta p_{(2)}}{2} = 0 \quad \Rightarrow \quad p^*_{(1)} = \frac{\mu_a}{\left(s + \frac{d_\alpha}{2}\right)\Big[1 - h(1-F)\Big]}, \tag{A24}$$

which is negative because $d_\alpha < -2s$, and so

$$p^* = 1 + \frac{\mu_a}{\left(s + \frac{d_\alpha}{2}\right)\Big[1 - h(1-F)\Big]} + \mathcal{O}\left(\epsilon^2\right) \quad \text{and} \quad C^* = F(1-p^*) + \mathcal{O}\left(\epsilon^2\right). \tag{A25}$$

Eqs. (A22) and (A25) correspond to eq. (2) in the main text.

A.1.3 Heterozygote advantage

Polymorphism is always maintained at a balance between mutation and selection in the linear case above, and so would collapse in the absence of recurrent mutation, but we find in numerical analyses that the two alleles at the condition locus can be maintained at an intermediate frequency in the absence of mutation for arbitrary selfing strategies where heterozygotes self-fertilise at a higher rate than homozygotes, i.e., when

$$\alpha_{\mathrm{Aa}} > \alpha_{\mathrm{AA}},\ \alpha_{\mathrm{aa}}. \tag{A26}$$

This is because such strategies generate a form of overdominance at the condition locus that leads to a protected polymorphism. To show this analytically, we now assume that genotype-dependent selfing rates $\boldsymbol{\alpha} = (\alpha_{\mathrm{AA}}, \alpha_{\mathrm{Aa}}, \alpha_{\mathrm{aa}})$ are given by

$$\boldsymbol{\alpha} = \Big(\alpha_0, \quad \alpha_0 + d_\alpha, \quad \alpha_0\Big), \tag{A27}$$

so that homozygotes share the same selfing rate α_0 and heterozygotes may deviate from this rate by an amount d_α. Heterozygotes have a higher selfing rate than homozygotes when $d_\alpha > 0$ and a lower selfing rate when $d_\alpha < 0$. We make no assumption on the magnitude of d_α here.

To order zero in ϵ, we find that the change in frequency and excess homozygosity at the condition locus are given by

$$\Delta p_{(0)} = -\frac{d_\alpha}{2}\left(1-2p_{(0)}\right)\left(C_{(0)} - p_{(0)}q_{(0)}\right), \tag{A28a}$$

and

$$\Delta C_{(0)} = \frac{\alpha_0}{2}p_{(0)}q_{(0)} - \left(1-\frac{\alpha}{2}\right)C_{(0)} + \left(\frac{1-2p_{(0)}}{2}\right)^2\left\{1-\left[1+d_\alpha\left(C_{(0)}-p_{(0)}q_{(0)}\right)\right]^2\right\} \tag{A28b}$$

where $q_{(0)} = 1 - p_{(0)}$. Solving for equilibrium (eq. A11), we find that this system has three equilibria, either one of the alleles goes to fixation, i.e.,

$$p^*_{(0)} = 0 \quad \text{or} \quad p^*_{(0)} = 1, \tag{A29}$$

in which case $C^*_{(0)} = 0$; or alleles are equally frequent,

$$p^*_{(0)} = \frac{1}{2} \quad \text{and} \quad C^*_{(0)} = \frac{F}{4} \tag{A30}$$

with $F = \alpha_0/(2-\alpha_0)$. To determine the stability of these equilibria, we compute the Jacobian matrix $\boldsymbol{J}^*_{(0)}$,

$$\boldsymbol{J}^*_{(0)} = \begin{pmatrix} \left.\dfrac{\partial p'_{(0)}}{\partial p_{(0)}}\right|_* & \left.\dfrac{\partial p'_{(0)}}{\partial C_{(0)}}\right|_* \\ \left.\dfrac{\partial C'_{(0)}}{\partial p_{(0)}}\right|_* & \left.\dfrac{\partial C'_{(0)}}{\partial C_{(0)}}\right|_* \end{pmatrix}, \tag{A31}$$

where $p'_{(0)} = p_{(0)} + \Delta p_{(0)}$ and $C'_{(0)} = C_{(0)} + \Delta C_{(0)}$ denote allelic frequency and excess homozygosity in the next time step, and the $|_*$ notation indicates that all derivatives are evaluated at an equilibrium of the system (as given by eq. A29 and A30). An equilibrium point is considered to be stable when the leading eigenvalue of $\boldsymbol{J}^*_{(0)}$, $\lambda_{\boldsymbol{J}^*_{(0)}}$, has a real part strictly smaller than one in absolute value, i.e.,

$$|\lambda_{\boldsymbol{J}^*_{(0)}}| < 1. \tag{A32}$$

Checking for Condition (A32) for each of the three equilibria above, we can distinguish two cases. When

heterozygotes self-fertilise at a higher rate than homozygotes ($d_\alpha > 0$), the equilibrium where both alleles are maintained at equal frequency is the only stable one (eq. A30), indicating that selection favours their coexistence. When $d_\alpha < 0$, on the other hand, this equilibrium is unstable and both $p^*_{(0)} = 0$ and $p^*_{(0)} = 1$ are stable, meaning that the population will either fix allele A or allele a depending on initial conditions. These results can be understood by realising that the average selfing rate associated with an allele becomes strongly frequency-dependent when the rate of heterozygotes differs from homozygotes, because the rarer allele is more likely to be found in heterozygous state. When $d_\alpha > 0$, the rarer allele enjoys a transmission advantage over the other, leading to negative frequency-dependence and the maintenance of polymorphism. Conversely, $d_\alpha < 0$ leads to heterozygote disadvantage and so positive frequency-dependence and the fixation of the most frequent allele. These results neglect the effect of mutation and fecundity selection against a, but since these are small, they are only going to produce small deviations around the equilibria identified here.

A.2 Evolution of condition-dependent selfing

We now investigate the evolution of condition-dependent selfing. To do this, we assume that mutations at the modifier locus are rare, occur independently for each of the three traits and have weak, unbiased phenotypic effects. Under these assumptions, evolution at the modifier proceeds gradually, and evolutionary dynamics can be inferred from an invasion analysis [2, 3, 5, 9]. We describe our general approach and introduce necessary notations in Section A.2.1. We then solve special cases explicitly in Sections A.2.2-A.2.4, and present complementary numerical analyses in Section A.2.5.

A.2.1 Analytical method

We consider the invasion of a rare mutant allele m encoding a strategy $\boldsymbol{\alpha}_\mathrm{m} = (\alpha^\mathrm{m}_\mathrm{AA}, \alpha^\mathrm{m}_\mathrm{Aa}, \alpha^\mathrm{m}_\mathrm{aa})$ in a population otherwise fixed with allele M, which encodes a strategy $\boldsymbol{\alpha} = (\alpha_\mathrm{AA}, \alpha_\mathrm{Aa}, \alpha_\mathrm{aa})$. The dynamics of the mutant sub-population can be modelled by the recursion

$$\boldsymbol{n}_{t+1} = \mathbf{W}(\boldsymbol{\alpha}_\mathrm{m}, \boldsymbol{\alpha}) \cdot \boldsymbol{n}_t, \tag{A33}$$

where $\boldsymbol{n}_t = (n_{i,t})_{1 \leqslant i \leqslant 8}$ is a vector that gives the number of mutant individuals in each of the eight possible genotypic classes in the sub-population at time t (Table 1), and $\mathbf{W}(\boldsymbol{\alpha}_\mathrm{m}, \boldsymbol{\alpha})$ is an 8×8 matrix of which element $w_{ij}(\boldsymbol{\alpha}_\mathrm{m}, \boldsymbol{\alpha})$ gives the expected number of successfully established mutant offspring of

class i produced by a focal mutant of class j. We hereafter refer to $\mathbf{W}(\boldsymbol{\alpha}_{\mathrm{m}}, \boldsymbol{\alpha})$ as the invasion matrix.

Class	Genotype
1	AM / Am
2	AM / am
3	aM / Am
4	aM / am
5	Am / Am
6	Am / am
7	am / Am
8	am / am

Table 1: Class number and genotype as used throughout the analysis. For each genotype, the maternally inherited haplotype is given first, followed by the paternal haplotype after the slash symbol.

To facilitate writing the elements of the invasion matrix $\mathbf{W}(\boldsymbol{\alpha}_{\mathrm{m}}, \boldsymbol{\alpha})$, let us first denote as $F_x^*(\boldsymbol{\alpha})$ and $M_x^*(\boldsymbol{\alpha})$ the relative number of female and male gametes available for outcrossing carrying allele $x \in \{\mathrm{A}, \mathrm{a}\}$, respectively, produced by the resident population at its genetic and ecological equilibrium. These variables are given by

$$\begin{aligned} F_{\mathrm{A}}^*(\boldsymbol{\alpha}) &= (1-\mu_A)\, q_{\mathrm{AA}}^* \frac{\varphi_{\mathrm{AA}}}{\overline{\varphi}^*}(1-\alpha_{\mathrm{AA}}) + q_{\mathrm{Aa}}^* \frac{1-\mu_A+\mu_a}{2}\frac{\varphi_{\mathrm{Aa}}}{\overline{\varphi}^*}(1-\alpha_{\mathrm{Aa}}) + \mu_a\, q_{\mathrm{aa}}^* \frac{\varphi_{\mathrm{aa}}}{\overline{\varphi}^*}(1-\alpha_{\mathrm{aa}}), \\ F_{\mathrm{a}}^*(\boldsymbol{\alpha}) &= \mu_A\, q_{\mathrm{AA}}^* \frac{\varphi_{\mathrm{AA}}}{\overline{\varphi}^*}(1-\alpha_{\mathrm{AA}}) + q_{\mathrm{Aa}}^* \frac{1-\mu_a+\mu_A}{2}\frac{\varphi_{\mathrm{Aa}}}{\overline{\varphi}^*}(1-\alpha_{\mathrm{Aa}}) + (1-\mu_a)\, q_{\mathrm{aa}}^* \frac{\varphi_{\mathrm{aa}}}{\overline{\varphi}^*}(1-\alpha_{\mathrm{aa}}) \end{aligned} \tag{A34a}$$

and

$$\begin{aligned} M_{\mathrm{A}}^*(\boldsymbol{\alpha}) &= (1-\mu_A)\, q_{\mathrm{AA}}^* \frac{\varphi_{\mathrm{AA}}}{\overline{\varphi}^*} + q_{\mathrm{Aa}}^* \frac{1-\mu_A+\mu_a}{2}\frac{\varphi_{\mathrm{Aa}}}{\overline{\varphi}^*} + \mu_a\, q_{\mathrm{aa}}^* \frac{\varphi_{\mathrm{aa}}}{\overline{\varphi}^*}, \\ M_{\mathrm{a}}^*(\boldsymbol{\alpha}) &= \mu_A\, q_{\mathrm{AA}}^* \frac{\varphi_{\mathrm{AA}}}{\overline{\varphi}^*} + q_{\mathrm{Aa}}^* \frac{1-\mu_a+\mu_A}{2}\frac{\varphi_{\mathrm{Aa}}}{\overline{\varphi}^*} + (1-\mu_a)\, q_{\mathrm{aa}}^* \frac{\varphi_{\mathrm{aa}}}{\overline{\varphi}^*} \end{aligned} \tag{A34b}$$

where $q_{x_1x_2}^*$ is the equilibrium frequency of genotype x_1x_2 (with $x_1,\ x_2 \in \{\mathrm{A}, \mathrm{a}\}$) in the resident population and

$$\overline{\varphi}^* = \varphi_{\mathrm{AA}} q_{\mathrm{AA}}^* + \varphi_{\mathrm{Aa}} q_{\mathrm{Aa}}^* + \varphi_{\mathrm{aa}} q_{\mathrm{aa}}^* \tag{A35}$$

is the mean condition in the resident population. Further, we denote as α_i the selfing rate and φ_i the condition of a mutant of class i, and by $G_{xy}^{(i)}$ (with $x \in \{\mathrm{A}, \mathrm{a}\}$ and $y \in \{\mathrm{M}, \mathrm{m}\}$) the proportion of gametes with haplotype xy among those produced by a mutant of class i. The expressions for $G_{xy}^{(i)}$ variables are given in Table 2 (see associated caption for explanation).

Invasion matrix. Using the above notations, the number of successful mutant offspring of class 1 to 8 produced by a focal mutant of class i are given by

$$\mathbf{w}_i(\boldsymbol{\alpha},\boldsymbol{\alpha}_{\mathrm{m}}) = \begin{pmatrix} \frac{\varphi_i}{\overline{\varphi}^*}\left[2\alpha_i G^{(i)}_{\mathrm{AM}}G^{(i)}_{\mathrm{Am}} + (1-\alpha_i)M^*_{\mathrm{A}}(\boldsymbol{\alpha})G^{(i)}_{\mathrm{Am}}\right] + F^*_{\mathrm{A}}(\boldsymbol{\alpha})\frac{\varphi_i}{\overline{\varphi}^*}G^{(i)}_{\mathrm{Am}} \\ \frac{\varphi_i}{\overline{\varphi}^*}\left[2\alpha_i G^{(i)}_{\mathrm{AM}}G^{(i)}_{\mathrm{am}} + (1-\alpha_i)M^*_{\mathrm{A}}(\boldsymbol{\alpha})G^{(i)}_{\mathrm{am}}\right] + F^*_{\mathrm{A}}(\boldsymbol{\alpha})\frac{\varphi_i}{\overline{\varphi}^*}G^{(i)}_{\mathrm{am}} \\ \frac{\varphi_i}{\overline{\varphi}^*}\left[2\alpha_i G^{(i)}_{\mathrm{Am}}G^{(i)}_{\mathrm{aM}} + (1-\alpha_i)M^*_{\mathrm{a}}(\boldsymbol{\alpha})G^{(i)}_{\mathrm{Am}}\right] + F^*_{\mathrm{a}}(\boldsymbol{\alpha})\frac{\varphi_i}{\overline{\varphi}^*}G^{(i)}_{\mathrm{Am}} \\ \frac{\varphi_i}{\overline{\varphi}^*}\left[2\alpha_i G^{(i)}_{\mathrm{am}}G^{(i)}_{\mathrm{aM}} + (1-\alpha_i)M^*_{\mathrm{a}}(\boldsymbol{\alpha})G^{(i)}_{\mathrm{am}}\right] + F^*_{\mathrm{a}}(\boldsymbol{\alpha})\frac{\varphi_i}{\overline{\varphi}^*}G^{(i)}_{\mathrm{am}} \\ \frac{\varphi_i}{\overline{\varphi}^*}\alpha_i G^{(i)}_{\mathrm{Am}}G^{(i)}_{\mathrm{Am}} \\ \frac{\varphi_i}{\overline{\varphi}^*}\alpha_i G^{(i)}_{\mathrm{Am}}G^{(i)}_{\mathrm{am}} \\ \frac{\varphi_i}{\overline{\varphi}^*}\alpha_i G^{(i)}_{\mathrm{Am}}G^{(i)}_{\mathrm{am}} \\ \frac{\varphi_i}{\overline{\varphi}^*}\alpha_i G^{(i)}_{\mathrm{am}}G^{(i)}_{\mathrm{am}} \end{pmatrix}, \tag{A36}$$

which corresponds to the i^{th} column of the invasion matrix $\mathbf{W}(\boldsymbol{\alpha}_{\mathrm{m}},\boldsymbol{\alpha})$, i.e.,

$$\mathbf{W}(\boldsymbol{\alpha}_{\mathrm{m}},\boldsymbol{\alpha}) = \Big(\mathbf{w}_i(\boldsymbol{\alpha},\boldsymbol{\alpha}_{\mathrm{m}})\Big)_{1\leqslant i\leqslant 8}. \tag{A37}$$

To understand how the elements in eq. (A36) were computed, let us focus on its first entry, which gives the number of successfully recruited AM/Am offspring produced by a mutant of class i and is composed of two terms. The first term gives the number of successful AM/Am offspring produced by the mutant through its female function. It is proportional to the relative contribution of the mutant to the seed pool through its female function, which is given by its relative condition $\varphi_i/\overline{\varphi}^*$. The mutant self-fertilises a fraction α_i of its ovules, producing a proportion $2G^{(i)}_{\mathrm{AM}}G^{(i)}_{\mathrm{Am}}$ of AM/Am zygotes. The remaining ovules $(1-\alpha_i)$ are fertilised by resident individuals, in which case an AM/Am zygote can only be produced if the focal mutant contributes a Am haplotype (which it does with probability $G^{(i)}_{\mathrm{Am}}$) and receives resident pollen carrying haplotype AM, which occurs with probability $M^*_{\mathrm{A}}(\boldsymbol{\alpha})$. The second term gives the number of successful AM/Am offspring produced by the mutant through its male function, i.e. through the fertilisation of resident ovules. Similar to female function, a mutant of class i can only produce AM/Am offspring through outcrossing if it fertilises resident ovules carrying haplotype AM. This term is there-

fore proportional to the contribution of AM ovules to the pool of resident ovules available for outcrossing, $F^*_{\mathrm{A}}(\boldsymbol{\alpha})$. The mutant fertilises part of these ovules in proportion to its relative condition $\varphi_i/\overline{\varphi}^*$ in which case AM/Am offspring are formed when the mutant transmits haplotype Am, which occurs with probability $G^{(i)}_{\mathrm{Am}}$.

Class i	$G^{(i)}_{\mathrm{AM}}$	$G^{(i)}_{\mathrm{Am}}$	$G^{(i)}_{\mathrm{aM}}$	$G^{(i)}_{\mathrm{am}}$
1	$\frac{1-\mu_A}{2}$	$\frac{1-\mu_A}{2}$	$\frac{\mu_A}{2}$	$\frac{\mu_A}{2}$
2	$\frac{(1-r)(1-\mu_A)+r\mu_a}{2}$	$\frac{r(1-\mu_A)+(1-r)\mu_a}{2}$	$\frac{r(1-\mu_a)+(1-r)\mu_A}{2}$	$\frac{(1-r)(1-\mu_a)+r\mu_A}{2}$
3	$\frac{r(1-\mu_A)+(1-r)\mu_a}{2}$	$\frac{(1-r)(1-\mu_A)+r\mu_a}{2}$	$\frac{(1-r)(1-\mu_A)+r\mu_a}{2}$	$\frac{r(1-\mu_a)+(1-r)\mu_A}{2}$
4	$\frac{\mu_a}{2}$	$\frac{\mu_a}{2}$	$\frac{1-\mu_a}{2}$	$\frac{1-\mu_a}{2}$
5	0	$1-\mu_A$	0	μ_A
6	0	$\frac{1-\mu_A+\mu_a}{2}$	0	$\frac{1-\mu_a+\mu_A}{2}$
7	0	$\frac{1-\mu_A+\mu_a}{2}$	0	$\frac{1-\mu_a+\mu_A}{2}$
8	0	μ_a	0	$1-\mu_a$

Table 2: Proportion of gametes carrying genotype xy, $x \in \{\mathrm{A},\mathrm{a}\}$, $y \in \{\mathrm{M},\mathrm{m}\}$ among the gametes produced by a mutant individual of class $i \in \{1,...,8\}$. These expressions assume that recombination occurs first, followed by mutation at the condition locus. To understand how they were obtained, consider the gametes produced by an individual of class 2, i.e., with genotype AM/am. Following recombination, such an individual will produce haplotype AM, Am, aM and am in proportions $(1-r)/2$, $r/2$, $r/2$ and $(1-r)/2$, respectively. Alleles at the condition locus then each mutate with probability μ_x, $x \in \{\mathrm{A},\mathrm{a}\}$, so that haplotype AM for instance is produced either from AM recombinant haplotypes that did not mutate, which occurs with probability $(1-r)(1-\mu_A)/2$; or from a aM that mutated, which occurs with probability $r\mu_a/2$. Repeating this reasoning for each haplotype gives the proportions in the table.

Selection gradient in a class-structured population. The invasion fitness $\rho(\boldsymbol{\alpha}_{\mathrm{m}}, \boldsymbol{\alpha})$ of a mutant $\boldsymbol{\alpha}_{\mathrm{m}}$ in a population fixed for $\boldsymbol{\alpha}$, from which the selection gradients on α_{AA}, α_{Aa} and α_{aa} can be computed, is given by the leading eigenvalue of the invasion matrix $\mathbf{W}(\boldsymbol{\alpha}_{\mathrm{m}}, \boldsymbol{\alpha})$ [2]. Unfortunately, this eigenvalue cannot be computed explicitly and so cannot directly be used to characterise the evolution of condition-dependent selfing. Under the assumption that mutations have weak phenotypic effects, however, the selection gradients $\boldsymbol{s}(\boldsymbol{\alpha}) = (s_{\mathrm{AA}}(\boldsymbol{\alpha}), s_{\mathrm{Aa}}(\boldsymbol{\alpha}), s_{\mathrm{aa}}(\boldsymbol{\alpha}))$ on condition-dependent selfing rates can be obtained as

$$s_{x_1x_2}(\boldsymbol{\alpha}) = \boldsymbol{v}^{\circ}(\boldsymbol{\alpha}) \cdot \mathbf{D}_{x_1x_2}(\boldsymbol{\alpha}) \cdot \boldsymbol{q}^{\circ}(\boldsymbol{\alpha}), \tag{A38}$$

where $\boldsymbol{q}^{\circ}(\boldsymbol{\alpha}) = \left(q_i^{\circ}(\boldsymbol{\alpha})\right)_{1\leqslant i\leqslant 8}$ is the right eigenvector of $\mathbf{W}^{\circ}(\boldsymbol{\alpha}) = \mathbf{W}(\boldsymbol{\alpha},\boldsymbol{\alpha})$, the invasion matrix under neutrality, normalised such that

$$\sum_{i=1}^{8} q_i^{\circ}(\boldsymbol{\alpha}) = 1,$$

which gives the asymptotic frequencies of classes in the population under neutrality; $\mathbf{D}_{x_1x_2}(\boldsymbol{\alpha})$ is an 8×8 matrix, the (i,j)-entry of which $d_{ij}^{x_1x_2}(\boldsymbol{\alpha})$ is given by the derivative of the corresponding entry of the invasion matrix $\mathbf{W}(\boldsymbol{\alpha}_{\mathrm{m}},\boldsymbol{\alpha})$ with respect to $\alpha_{x_1x_2}^{\mathrm{m}}$ evaluated at the resident strategy, i.e.,

$$d_{ij}^{x_1x_2}(\boldsymbol{\alpha}) = \left.\frac{\partial w_{ij}(\boldsymbol{\alpha}_{\mathrm{m}},\boldsymbol{\alpha})}{\partial \alpha_{x_1x_2}^{\mathrm{m}}}\right|_{\boldsymbol{\alpha}_{\mathrm{m}}=\boldsymbol{\alpha}}, \tag{A39}$$

which measures the effect of a change in trait $\alpha_{x_1x_2}$ on the number of successful offspring of class i produced by a focal mutant of class j; and $\boldsymbol{v}^{\circ}(\boldsymbol{\alpha}) = \left(v_i^{\circ}(\boldsymbol{\alpha})\right)_{1\leqslant i\leqslant 8}$ is the left eigenvector of $\mathbf{W}^{\circ}(\boldsymbol{\alpha}) = \mathbf{W}(\boldsymbol{\alpha},\boldsymbol{\alpha})$, normalised such that

$$\boldsymbol{v}^{\circ}(\boldsymbol{\alpha})\cdot\boldsymbol{q}^{\circ}(\boldsymbol{\alpha}) = 1,$$

which gives the reproductive value of an individual of class i under neutrality, that is its long-term contribution to population growth. Background for this decomposition can be found, e.g., in [11] or Chap. 11 in [10]. See also Section 3 in [2] for a review. In what follows, we use this decomposition to study the evolution of condition-dependent selfing.

Weak variation in condition. Similar to our calculations under fixed condition-dependent selfing (Section A.1), we assume that $s\sim\mathcal{O}(\epsilon)$ and $\mu_x\sim\mathcal{O}(\epsilon^2)$ in order to obtain analytical results. To incorporate these assumptions, our approach will again rely on Taylor-expanding relevant quantities using eq. (A8). Applying this method to the selection gradient on $\alpha_{x_1x_2}$, we find that it can be expressed as

$$\begin{aligned}
s_{x_1x_2}(\boldsymbol{\alpha}) = {} & \boldsymbol{v}_{(0)}^{\circ}\cdot\mathbf{D}_{(0)}^{x_1x_2}\cdot\boldsymbol{q}_{(0)}^{\circ} \\
& + \epsilon\left(\boldsymbol{v}_{(1)}^{\circ}\cdot\mathbf{D}_{(0)}^{x_1x_2}\cdot\boldsymbol{q}_{(0)}^{\circ} + \boldsymbol{v}_{(0)}^{\circ}\cdot\mathbf{D}_{(1)}^{x_1x_2}\cdot\boldsymbol{q}_{(0)}^{\circ} + \boldsymbol{v}_{(0)}^{\circ}\cdot\mathbf{D}_{(0)}^{x_1x_2}\cdot\boldsymbol{q}_{(1)}^{\circ}\right) \\
& + \frac{\epsilon^2}{2}\Bigg[\boldsymbol{v}_{(2)}^{\circ}\cdot\mathbf{D}_{(0)}^{x_1x_2}\cdot\boldsymbol{q}_{(0)}^{\circ} + \boldsymbol{v}_{(0)}^{\circ}\cdot\mathbf{D}_{(2)}^{x_1x_2}\cdot\boldsymbol{q}_{(0)}^{\circ} + \boldsymbol{v}_{(0)}^{\circ}\cdot\mathbf{D}_{(0)}^{x_1x_2}\cdot\boldsymbol{q}_{(2)}^{\circ} \\
& \qquad + 2\left(\boldsymbol{v}_{(1)}^{\circ}\cdot\mathbf{D}_{(1)}^{x_1x_2}\cdot\boldsymbol{q}_{(0)}^{\circ} + \boldsymbol{v}_{(1)}^{\circ}\cdot\mathbf{D}_{(0)}^{x_1x_2}\cdot\boldsymbol{q}_{(1)}^{\circ} + \boldsymbol{v}_{(0)}^{\circ}\cdot\mathbf{D}_{(1)}^{x_1x_2}\cdot\boldsymbol{q}_{(1)}^{\circ}\right)\Bigg] \\
& + \mathcal{O}\left(\epsilon^3\right)
\end{aligned} \tag{A40}$$

for $x_1,x_2\in\{\mathrm{A},\mathrm{a}\}$, where $\boldsymbol{v}_{(k)}^{\circ}$, $\mathbf{D}_{(k)}^{x_1x_2}$ and $\boldsymbol{q}_{(k)}^{\circ}$, $k\in\{0,1,...,n\}$ are k^{th} order perturbations of $\boldsymbol{v}^{\circ}$, the vector of individual reproductive values under neutrality; of $\mathbf{D}_{x_1x_2}(\boldsymbol{\alpha})$, the matrix of effects; and of $\boldsymbol{q}^{\circ}$,

the vector of asymptotic class frequencies under neutrality, respectively.

Our aim will be to compute the perturbation terms that appear in eq. (A40) to increasing order in ϵ, starting with order zero (first line) and stopping at the first non-zero term (the *leading* order).

A.2.2 Complete outcrossing

Computing the selection gradients on genotype-specific selfing rates for an arbitrary strategy $\boldsymbol{\alpha}$ is difficult. We therefore start by investigating special cases. Here, we compute a leading order approximation for the selection gradients on the selfing rates in a completely outcrossing population ($\alpha_{\mathrm{AA}} = \alpha_{\mathrm{Aa}} = \alpha_{\mathrm{aa}} = 0$). We first solve for the genetic equilibrium reached by an outcrossing resident population and then compute the selection gradients.

Resident equilibrium. To compute the genetic equilibrium in the resident population, we use the same method as in Appendix A.1.2, i.e., we assume that $s \sim \mathcal{O}(\epsilon)$ and $\mu_x \sim \mathcal{O}\left(\epsilon^2\right)$, and expand the allelic frequency $p(t)$ and excess in homozygotes $C(t)$, and their change between generations around ϵ with $\alpha_{\mathrm{AA}} = \alpha_{\mathrm{Aa}} = \alpha_{\mathrm{aa}} = 0$ (eqs. A10-A11).

We find that the change in allelic frequency and homozygosity are given by

$$\Delta p_{(0)} = 0 \quad \text{and} \quad \Delta C_{(0)} = -C_{(0)} \tag{A41}$$

to zero-th order in ϵ. This indicates that in the absence of selection or mutation, the change frequency of allele a is expected to be zero, so that the population will retain the same allelic frequency indefinitely in the absence of drift, meanwhile the excess in homozygotes is expected to be zero in a strictly outcrossing population at equilibrium, as we have

$$\Delta C_{(0)} = 0 \quad \Leftrightarrow \quad C^*_{(0)} = 0. \tag{A42}$$

To first order in ϵ, the changes in allelic frequency and excess in homozygotes are given by

$$\Delta p_{(1)} = -s\left[p_{(0)} + h\left(1 - 2p_{(0)}\right)\right] p_{(0)}\left(1 - p_{(0)}\right) \quad \text{and} \quad \Delta C_{(1)} = -C_{(1)}, \tag{A43}$$

which at equilibrium yields

$$p^*_{(0)} = 0 \quad \text{and} \quad C^*_{(1)} = 0. \tag{A44}$$

Eq. (A43) reveals that selection against allele a always lowers its frequency in the population and drives it to extinction in the absence of mutation – which does not feature in the change in allelic frequency to first order in ϵ because $\mu_x \sim \mathcal{O}\left(\epsilon^2\right)$ – so that the equilibrium frequency of allele a to leading order in ϵ is expected to be zero.

To second order in ϵ, we have

$$\Delta p_{(2)} = 2\left(\mu_A - shp_{(1)}\right) \quad \text{and} \quad \Delta C_{(2)} = -C_{(2)}, \tag{A45}$$

which gives

$$p^*_{(1)} = \frac{\mu_A}{sh} \quad \text{and} \quad C^*_{(2)} = 0 \tag{A46}$$

at equilibrium. This corresponds to the classical result of [6] for $\mu_A \ll s$. The deleterious allele a is maintained at a balance between mutation and selection and the population is at Hardy-Weinberg equilibrium among newborns owing to random mating.

Finally, to third order in ϵ,

$$\Delta p_{(3)} = -3\left(shp_{(2)} + 2(1-h)\frac{\mu_A^2}{sh^2}\right), \tag{A47}$$

which yields

$$p^*_{(2)} = 2\left(1 - \frac{1}{h}\right)\left(\frac{\mu_A}{sh}\right)^2. \tag{A48}$$

Thus, when selection is weak and mutation is rare,

$$p^* = \frac{\mu_A}{sh}\left[1 + \left(1 - \frac{1}{h}\right)\frac{\mu_A}{sh}\right] + \mathcal{O}\left(\epsilon^3\right) \quad \text{and} \quad C^* = 0 + \mathcal{O}\left(\epsilon^3\right) \tag{A49}$$

under complete outcrossing.

Selection gradients to order zero. The right and left eigenvectors of the invasion matrix under neutrality $\mathbf{W}^\circ(\boldsymbol{\alpha})$, $\boldsymbol{q}^\circ$ and $\boldsymbol{v}^\circ$, which give the asymptotic class frequencies and class-specific reproductive values in the mutant population under neutrality, are defined as the solutions of

$$\mathbf{W}^\circ(\boldsymbol{\alpha}) \cdot \boldsymbol{q}^\circ = \boldsymbol{q}^\circ \quad \text{and} \quad \boldsymbol{v}^\circ \cdot \mathbf{W}^\circ(\boldsymbol{\alpha}) = \boldsymbol{v}^\circ, \tag{A50}$$

which must hold to all orders in ϵ. Thus, their zero-th order perturbations $\boldsymbol{q}^{\circ}_{(0)}$ and $\boldsymbol{v}^{\circ}_{(0)}$ must satisfy

$$\mathbf{W}^{\circ}_{(0)} \cdot \boldsymbol{q}^{\circ}_{(0)} = \boldsymbol{q}^{\circ}_{(0)} \quad \text{and} \quad \boldsymbol{v}^{\circ}_{(0)} \cdot \mathbf{W}^{\circ}_{(0)} = \boldsymbol{v}^{\circ}_{(0)}, \tag{A51}$$

with constraints $\boldsymbol{q}^{\circ}_{(0)} \cdot \mathbf{1} = 1$ and $\boldsymbol{v}^{\circ}_{(0)} \cdot \boldsymbol{q}^{\circ}_{(0)} = 1$, and where $\mathbf{W}^{\circ}_{(0)}$ is the zero-th order perturbation of $\mathbf{W}^{\circ}(\boldsymbol{\alpha})$. Solving eq. (A51) for $\boldsymbol{q}^{\circ}_{(0)}$ and $\boldsymbol{v}^{\circ}_{(0)}$, we obtain

$$\boldsymbol{q}^{\circ}_{(0)} = (1,\ 0,\ 0,\ 0,\ 0,\ 0,\ 0,\ 0) \quad \text{and} \quad \boldsymbol{v}^{\circ}_{(0)} = (1,\ 1,\ 1,\ 1,\ 2,\ 2,\ 2,\ 2). \tag{A52}$$

This indicates that to order zero in ϵ, the mutant population under neutrality is expected to be fixed for allele A at the condition locus ($q^{\circ}_{1(0)} = 1$, which stems from the fact that $p^{*}_{(0)} = 0$ and homozygotes for the mutant allele at the modifier cannot be produced under complete outcrossing), and the reproductive value of an individual homozygous for the mutant allele is exactly twice that of an heterozygous individual, because it carries twice as many mutant copies.

The matrices of fitness effects to order zero, meanwhile, are given by

$$\mathbf{D}^{\mathrm{AA}}_{(0)} = \begin{pmatrix} 0 & 0 & 0 & 0 & -1 & 0 & 0 & 0 \\ 0 & 0 & 0 & 0 & 0 & 0 & 0 & 0 \\ 0 & 0 & 0 & 0 & 0 & 0 & 0 & 0 \\ 0 & 0 & 0 & 0 & 0 & 0 & 0 & 0 \\ \frac{1}{8} & 0 & 0 & 0 & 1 & 0 & 0 & 0 \\ 0 & 0 & 0 & 0 & 0 & 0 & 0 & 0 \\ 0 & 0 & 0 & 0 & 0 & 0 & 0 & 0 \\ 0 & 0 & 0 & 0 & 0 & 0 & 0 & 0 \end{pmatrix}, \tag{A53a}$$

$$\mathbf{D}^{\mathrm{Aa}}_{(0)} = \begin{pmatrix} 0 & -\frac{r^2}{4} & -\frac{(1-r)^2}{4} & 0 & 0 & -\frac{1}{2} & -\frac{1}{2} & 0 \\ 0 & -\frac{r(1-r)}{4} & -\frac{r(1-r)}{4} & 0 & 0 & -\frac{1}{2} & -\frac{1}{2} & 0 \\ 0 & \frac{r^2}{4} & \frac{(1-r)^2}{4} & 0 & 0 & 0 & 0 & 0 \\ 0 & \frac{r(1-r)}{4} & \frac{r(1-r)}{4} & 0 & 0 & 0 & 0 & 0 \\ 0 & \frac{r^2}{8} & \frac{(1-r)^2}{8} & 0 & 0 & \frac{1}{4} & \frac{1}{4} & 0 \\ 0 & \frac{r(1-r)}{8} & \frac{r(1-r)}{8} & 0 & 0 & \frac{1}{4} & \frac{1}{4} & 0 \\ 0 & \frac{r(1-r)}{8} & \frac{r(1-r)}{8} & 0 & 0 & \frac{1}{4} & \frac{1}{4} & 0 \\ 0 & \frac{(1-r)^2}{8} & \frac{r^2}{8} & 0 & 0 & \frac{1}{4} & \frac{1}{4} & 0 \end{pmatrix}, \tag{A53b}$$

and

$$\mathbf{D}^{\mathrm{aa}}_{(0)} = \begin{pmatrix} 0 & 0 & 0 & 0 & 0 & 0 & 0 & 0 \\ 0 & 0 & 0 & -\frac{1}{4} & 0 & 0 & 0 & -1 \\ 0 & 0 & 0 & 0 & 0 & 0 & 0 & 0 \\ 0 & 0 & 0 & \frac{1}{4} & 0 & 0 & 0 & 0 \\ 0 & 0 & 0 & 0 & 0 & 0 & 0 & 0 \\ 0 & 0 & 0 & 0 & 0 & 0 & 0 & 0 \\ 0 & 0 & 0 & 0 & 0 & 0 & 0 & 0 \\ 0 & 0 & 0 & \frac{1}{8} & 0 & 0 & 0 & 1 \end{pmatrix}. \tag{A53c}$$

Inserting eqs. (A52) and (A53) into eq. (A40), we have

$$s_{\mathrm{AA}}(\mathbf{0}) = \frac{1}{4} + \mathcal{O}(\epsilon) \tag{A54}$$

Selection on α_{AA} therefore always favours an increase in the selfing rate of wild-type homozygotes in a completely outcrossing, and lower order terms need not be considered for this genotype. The gradients for heterozygotes and deleterious homozygotes, meanwhile, are given by

$$s_{\mathrm{Aa}}(\mathbf{0}) = s_{\mathrm{aa}}(\mathbf{0}) = 0 + \mathcal{O}(\epsilon), \tag{A55}$$

indicating that higher order terms must be computed.

Selection gradients to order ϵ. To first order in ϵ, eqs. (A50) become

$$\mathbf{W}^{\circ}_{(1)} \cdot \boldsymbol{q}^{\circ}_{(0)} + \mathbf{W}^{\circ}_{(0)} \cdot \boldsymbol{q}^{\circ}_{(1)} = \boldsymbol{q}^{\circ}_{(1)} \quad \text{and} \quad \boldsymbol{v}^{\circ}_{(0)} \cdot \mathbf{W}^{\circ}_{(1)} + \boldsymbol{v}^{\circ}_{(1)} \cdot \mathbf{W}^{\circ}_{(0)} = \boldsymbol{v}^{\circ}_{(1)}, \tag{A56}$$

and the renormalisation constraints imposed upon $\boldsymbol{q}^{\circ}$ and $\boldsymbol{v}^{\circ}$ give

$$\boldsymbol{q}^{\circ}_{(1)} \cdot \mathbf{1} = 0 \quad \text{and} \quad \boldsymbol{v}^{\circ}_{(1)} \cdot \boldsymbol{q}^{\circ}_{(0)} + \boldsymbol{v}^{\circ}_{(0)} \cdot \boldsymbol{q}^{\circ}_{(1)} = 0 \tag{A57}$$

for first order perturbations $\boldsymbol{q}^{\circ}_{(1)}$ and $\boldsymbol{v}^{\circ}_{(1)}$. Solving eqs. (A56) and (A57) for $\boldsymbol{q}^{\circ}_{(1)}$ and $\boldsymbol{v}^{\circ}_{(1)}$ yields

$$\boldsymbol{q}^{\circ}_{(1)} = \left(-2\frac{\mu_A}{sh},\ \frac{\mu_A}{sh},\ \frac{\mu_A}{sh},\ 0,\ 0,\ 0,\ 0,\ 0\right), \tag{A58a}$$

and

$$\boldsymbol{v}^{\circ}_{(1)} = \left(0,\ -\frac{sh}{r},\ -2sh,\ -s\left(1+\frac{h}{r}\right),\ 0,\ -sh\frac{1+2r}{r},\ -sh\frac{1+2r}{r}, -2s\left(1+\frac{h}{r}\right)\right). \tag{A58b}$$

Meanwhile, the first-order perturbations of matrices $\mathbf{D}_{\mathrm{Aa}}(\boldsymbol{\alpha})$ and $\mathbf{D}_{\mathrm{aa}}(\boldsymbol{\alpha})$, $\mathbf{D}^{\mathrm{Aa}}_{(1)}$ and $\mathbf{D}^{\mathrm{aa}}_{(1)}$, are given by

$$\mathbf{D}^{\mathrm{Aa}}_{(1)} = \begin{pmatrix}
0 & \frac{r\left[r(sh)^2+\mu_A\right]}{4sh} & \frac{(1-r)\left[(1-r)(sh)^2+\mu_A\right]}{4sh} & 0 & 0 & \frac{(sh)^2+\mu_A}{2sh} & \frac{(sh)^2+\mu_A}{2sh} & 0 \\
0 & \frac{(1-r)\left(r(sh)^2+\mu_A\right)}{4sh} & \frac{r\left[(1-r)(sh)^2+\mu_A\right]}{4sh} & 0 & 0 & \frac{(sh)^2+\mu_A}{2sh} & \frac{(sh)^2+\mu_A}{2sh} & 0 \\
0 & -\frac{r\left(r(sh)^2+\mu_A\right)}{4sh} & -\frac{(1-r)\left[(1-r)(sh)^2+\mu_A\right]}{4sh} & 0 & 0 & -\frac{\mu_A}{2sh} & -\frac{\mu_A}{2sh} & 0 \\
0 & -\frac{(1-r)\left(r(sh)^2+\mu_A\right)}{4sh} & -\frac{r\left[(1-r)(sh)^2+\mu_A\right]}{4sh} & 0 & 0 & -\frac{\mu_A}{2sh} & -\frac{\mu_A}{2sh} & 0 \\
0 & -\frac{shr^2}{8} & -\frac{sh(1-r)^2}{8} & 0 & 0 & -\frac{sh}{4} & -\frac{sh}{4} & 0 \\
0 & -\frac{shr(1-r)}{8} & -\frac{shr(1-r)}{8} & 0 & 0 & -\frac{sh}{4} & -\frac{sh}{4} & 0 \\
0 & -\frac{shr(1-r)}{8} & -\frac{shr(1-r)}{8} & 0 & 0 & -\frac{sh}{4} & -\frac{sh}{4} & 0 \\
0 & -\frac{sh(1-r)^2}{8} & -\frac{shr^2}{8} & 0 & 0 & -\frac{sh}{4} & -\frac{sh}{4} & 0
\end{pmatrix}, \tag{A59a}$$

and

$$\mathbf{D}^{\mathrm{aa}}_{(1)} = \begin{pmatrix}
0 & 0 & 0 & 0 & 0 & 0 & 0 & 0 \\
0 & 0 & 0 & \frac{1}{4}\left(s+\frac{\mu_A}{sh}\right) & 0 & 0 & 0 & s+\frac{\mu_A}{sh} \\
0 & 0 & 0 & 0 & 0 & 0 & 0 & 0 \\
0 & 0 & 0 & -\frac{1}{4}\left(s+\frac{\mu_A}{sh}\right) & 0 & 0 & 0 & -\frac{\mu_A}{sh} \\
0 & 0 & 0 & 0 & 0 & 0 & 0 & 0 \\
0 & 0 & 0 & 0 & 0 & 0 & 0 & 0 \\
0 & 0 & 0 & 0 & 0 & 0 & 0 & 0 \\
0 & 0 & 0 & -\frac{s}{8} & 0 & 0 & 0 & -s
\end{pmatrix}. \tag{A59b}$$

Using eqs. (A58) and (A59), the selection gradient on α_{Aa} becomes

$$s_{\mathrm{Aa}}(\mathbf{0}) = \frac{\mu_A}{2sh} + \mathcal{O}\left(\epsilon^2\right) \tag{A60}$$

to first order in ϵ, which shows that selection always favours an increase in the selfing rate of heterozygotes under complete outcrossing; whereas the selection gradient on α_{aa} becomes

$$s_{\mathrm{aa}}(\mathbf{0}) = 0 + \mathcal{O}\left(\epsilon^2\right), \tag{A61}$$

indicating that higher order terms must be computed.

Selection gradients to order ϵ^2. To compute the selection gradient on α_{aa} to second order in ϵ, we first remark that

$$\mathbf{D}^{\mathrm{aa}}_{(0)} \cdot \boldsymbol{q}^{\circ}_{(0)} = (0,\ 0,\ 0,\ 0,\ 0,\ 0,\ 0,\ 0), \tag{A62}$$

which implies that

$$\boldsymbol{v}^{\circ}_{(2)} \cdot \mathbf{D}^{\mathrm{aa}}_{(0)} \cdot \boldsymbol{q}^{\circ}_{(0)} = 0$$

irrespective of the elements of $\boldsymbol{v}^{\circ}_{(2)}$, so that we need not compute it. The second-order matrix of effects $\mathbf{D}^{\mathrm{aa}}_{(2)}$ is complicated, but can be found in the accompanying *Mathematica* notebook (available at `10.5281/zenodo.18523420`). Using this matrix, we have

$$\boldsymbol{v}^{\circ}_{(0)} \cdot \mathbf{D}^{\mathrm{aa}}_{(2)} \cdot \boldsymbol{q}^{\circ}_{(0)} = 0.$$

Using eqs. (A58- A59), we find that the selection gradient on α_{aa} reduces to

$$s_{\mathrm{aa}}(\mathbf{0}) = \frac{\boldsymbol{v}^{\circ}_{(0)} \cdot \mathbf{D}^{\mathrm{aa}}_{(0)} \cdot \boldsymbol{q}^{\circ}_{(2)}}{2} + \mathcal{O}\left(\epsilon^3\right). \tag{A63}$$

Thus, all that is left to do is to compute the second-order perturbation $\boldsymbol{q}^{\circ}_{(2)}$. From eq. (A50), $\boldsymbol{q}^{\circ}_{(2)}$ is the solution of

$$\mathbf{W}^{\circ}_{(2)} \cdot \boldsymbol{q}^{\circ}_{(0)} + \mathbf{W}^{\circ}_{(0)} \cdot \boldsymbol{q}^{\circ}_{(2)} + 2\mathbf{W}^{\circ}_{(1)} \cdot \boldsymbol{q}^{\circ}_{(1)} = \boldsymbol{q}^{\circ}_{(2)}, \tag{A64}$$

subject to the constraint

$$\boldsymbol{q}^{\circ}_{(2)} \cdot \mathbf{1} = 0. \tag{A65}$$

Solving eq. (A64) for $\boldsymbol{q}^{\circ}_{(2)}$ yields

$$\boldsymbol{q}^{\circ}_{(2)} = \left(-2\left(\frac{\mu_A}{sh}\right)^2 \left[1 - \frac{2}{h} + 2\left(1 - \frac{\mu_a}{\mu_A}\right)\right],\ -2\frac{h(\mu_a - \mu_A) + \mu_A}{\mu_A h}\left(\frac{\mu_A}{sh}\right)^2,\right.$$
$$\left. -2\frac{h(\mu_a - \mu_A) + \mu_A}{\mu_A h}\left(\frac{\mu_A}{sh}\right)^2,\ 2\left(\frac{\mu_A}{sh}\right)^2,\ 0,\ 0,\ 0,\ 0 \right), \tag{A66}$$

and the selection gradient on α_{aa} becomes

$$s_{\mathrm{aa}}(\mathbf{0}) = \frac{1}{4}\left(\frac{\mu_A}{sh}\right)^2 + \mathcal{O}\left(\epsilon^3\right). \tag{A67}$$

Summary. In this section, we have shown that selection gradients on genotype-specific selfing rates under complete outcrossing are given by

$$\boldsymbol{s}(\mathbf{0}) = \left(\frac{1}{4} \times 1 + \mathcal{O}(\epsilon),\ \ \frac{1}{4} \times 2\frac{\mu_A}{sh} + \mathcal{O}\left(\epsilon^2\right),\ \ \frac{1}{4} \times \left(\frac{\mu_A}{sh}\right)^2 + \mathcal{O}\left(\epsilon^3\right)\right) \tag{A68}$$

to leading order (eqs. A54, A60 and A67). These can be shown to be proportional to the equilibrium frequency of the corresponding genotype at the condition locus multiplied by a factor $1/4$, i.e.,

$$s_{x_1x_2}(\mathbf{0}) = \frac{q^*_{x_1x_2}}{4}, \tag{A69}$$

$\mathrm{x}_1, \mathrm{x}_2 \in \{\mathrm{A}, \mathrm{a}\}$ to leading order.

A.2.3 Complete selfing

Here, we compute a leading order approximation for the selection gradients on the selfing rates in a fully selfing population ($\alpha_{\mathrm{AA}} = \alpha_{\mathrm{Aa}} = \alpha_{\mathrm{aa}} = 1$). Similar to the previous section, we first solve for the genetic equilibrium reached by the resident population and then compute the selection gradients.

Resident equilibrium. Using the same decomposition as above (eq. A10), we find that the change in frequency and in excess homozygosity at the condition locus are given by

$$\Delta p_{(0)} = 0 \quad \text{and} \quad \Delta C_{(0)} = \frac{1}{2}\left[p_{(0)}\left(1 - p_{(0)}\right) - C_{(0)}\right] \tag{A70}$$

to order zero in ϵ. Similar to the complete outcrossing case, the change in frequency at the condition locus is null, because the effects of selection and mutation are both neglected to order zero. Meanwhile, we find that the equilibrium value of $C_{(0)}$ is simply given by

$$\Delta C_{(0)} = 0 \quad \Leftrightarrow \quad C^*_{(0)} = p^*_{(0)} \left(1 - p^*_{(0)}\right). \tag{A71}$$

To first order in ϵ, selection effects appear and we obtain

$$\Delta p_{(1)} = -s p_{(0)} \left(1 - p_{(0)}\right) \quad \text{and} \quad \Delta C_{(1)} = \frac{1}{2}\left(p_{(1)} - C_{(1)}\right), \tag{A72}$$

which yields

$$p^*_{(0)} = 0 \quad \Rightarrow \quad C^*_{(0)} = 0, \tag{A73}$$

and

$$C^*_{(1)} = p^*_{(1)} \tag{A74}$$

at equilibrium. Down to order ϵ^2, we then find that the change in frequency and excess homozygosity at the condition locus read

$$\Delta p_{(2)} = 2\left(\mu_A - s p_{(1)}\right) \quad \text{and} \quad \Delta C_{(2)} = \frac{1}{2}\left[p_{(2)} - C_{(2)} - 2\mu_A\left(2 + \frac{\mu_A}{s^2}\right)\right], \tag{A75}$$

so that at equilibrium

$$p^*_{(1)} = \frac{\mu_A}{s} \quad \Rightarrow \quad C^*_{(1)} = \frac{\mu_A}{s}, \quad \text{and} \quad C^*_{(2)} = p_{(2)} - 2\mu_A\left(2 + \frac{\mu_A}{s^2}\right). \tag{A76}$$

Finally, the third order perturbation of Δp is given by

$$\Delta p_{(3)} = -3 s p_{(2)} + 6\mu_A\left[2s(1-h) - \frac{\mu_a}{s}\right], \tag{A77}$$

giving

$$p^*_{(2)} = 2\mu_A\left[2(1-h) - \frac{\mu_a}{s^2}\right] \quad \text{and} \quad C^*_{(2)} = -2\mu_A\left(2h + \frac{\mu_A + \mu_a}{s^2}\right) \tag{A78}$$

at equilibrium. Thus, when selection is weak and mutations are rare,

$$p^* = \frac{\mu_A}{s}\left(1 - \frac{\mu_a}{s}\right) + 2(1-h)\mu_A + \mathcal{O}\left(\epsilon^3\right) \quad \text{and} \quad C^* = \frac{\mu_A}{s}\left(1 - \frac{\mu_A + \mu_a}{s}\right) - 2h\mu_A + \mathcal{O}\left(\epsilon^3\right) \tag{A79}$$

under complete selfing.

Class reproductive values and the basis to condition dependence. Before turning out attention to selection gradients to order zero, let us first compute the zero-th order perturbations of asymptotic class frequencies $\boldsymbol{q}^\circ$ and reproductive values $\boldsymbol{v}^\circ$ under neutrality, $\boldsymbol{v}^\circ_{(0)}$ and $\boldsymbol{q}^\circ_{(0)}$, which we do by solving eq. (A51) with $\alpha_{\mathrm{AA}} = \alpha_{\mathrm{Aa}} = \alpha_{\mathrm{aa}} = 1$. This yields

$$\boldsymbol{q}^\circ_{(0)} = \big(0,\ 0,\ 0,\ 0,\ 1,\ 0,\ 0,\ 0\big) \tag{A80a}$$

and

$$\boldsymbol{v}^\circ_{(0)} = \left(\frac{1}{2},\ \frac{r}{1+2r},\ \frac{1}{2(1+2r)},\ 0,\ 1,\ \frac{1}{2},\ \frac{1}{2},\ 0\right). \tag{A80b}$$

Eq. (A80a) shows that a fully selfing resident population would be fixed for allele A to leading order, and any neutral mutant appearing at the selfing modifier would be exclusively found in homozygous state within the mutant sub-population.

It is interesting to compare the expression for $\boldsymbol{v}^\circ_{(0)}$ obtained here (eq. A80b) with the one we found in the complete outcrossing case (eq. A52). Under complete outcrossing, we found that all genotypic classes had a positive reproductive value to zero-th order, with classes that are homozygous for the mutant allele at the modifier having a reproductive value exactly twice that of heterozygous classes, because they transmit twice as many mutant copies under complete outcrossing. In contrast, eq. (A80) reveals that the zero-th order reproductive values of deleterious homozygote classes (classes 4 and 8) is zero under complete selfing. This is because in the absence of outcrossing, heterozygotes at the condition locus are very rare at equilibrium (indeed they only occur due to recurrent mutation) and homozygotes only produce descendants with the same genotype as them at the condition locus, so that wild-type and deleterious homozygotes effectively form independent, competing lineages. In such a setup, the contribution of deleterious homozygotes to the long-term fate of the population will be zero to leading order, because they suffer from a fecundity disadvantage and so will always be outcompeted by wild-type homozygotes.

More broadly, this means that any mutant allele found in linkage with the deleterious allele will asymptotically be lost unless it can recombine onto a wild-type background before being "trapped" in a deleterious homozygote. This is illustrated by the reproductive values of classes heterozygous at the condition locus. Those classes that are heterozygous at the condition locus but homozygote for the mutant at the selfing modifier (classes 6 and 7) have a reproductive value exactly half that of a double homozygote carrying the wild-type (class 5), because half of their mutant copies will inevitably be associated with the deleterious allele and so make no asymptotic contribution to the future population. Meanwhile, the reproductive values of classes that are heterozygous at both loci (classes 2 and 3) depend on the recombination rate.

Class 2, which corresponds to genotype $\mathrm{AM/am}$, carries a mutant allele at the modifier in linkage with the deleterious allele. Its long-term contribution to the mutant population is thus zero unless recombination allows it to produce Am haplotypes. As a result, its reproductive value is zero when $r = 0$ and increases with r. Conversely, class 3 individuals, which carry genotype $\mathrm{Am/aM}$, see their reproductive value maximised for $r = 0$ and decrease with r because their mutant copy is already on the wild-type background. This deleterious background trap generates selection to escape it, which forms the basis to the evolution of condition-dependent self-fertilisation, as we will see below.

Selection gradients to order zero. We now compute selection gradients to order zero. The matrices of effects are identical to the complete outcrossing case to order zero, so using in eq. (A53), we find

$$s_{\mathrm{AA}}\left(\mathbf{1}_3\right) = \frac{1}{2} + \mathcal{O}\left(\epsilon\right), \tag{A81}$$

meaning that selection will always favour wild-type homozygotes to remain fully selfing when the rest of the population is fully selfing as well, and

$$s_{\mathrm{Aa}}\left(\mathbf{1}_3\right) = s_{\mathrm{aa}}\left(\mathbf{1}_3\right) = 0 + \mathcal{O}\left(\epsilon\right), \tag{A82}$$

so that higher order terms must be computed for other genotypes.

Selection gradients to order ϵ. First of all, we note that

$$\mathbf{D}^{\mathrm{aa}}_{(0)} \cdot \boldsymbol{q}^{\circ}_{(0)} = \mathbf{D}^{\mathrm{Aa}}_{(0)} \cdot \boldsymbol{q}^{\circ}_{(0)} = \mathbf{0}, \tag{A83}$$

which implies that we need not compute the first order perturbation of reproductive values $\boldsymbol{v}^{\circ}_{(1)}$ for now. To obtain the first order perturbation of class frequencies $\boldsymbol{q}^{\circ}_{(1)}$, we solve eqs. (A56-A57) with $\alpha_{\mathrm{AA}} = \alpha_{\mathrm{Aa}} = \alpha_{\mathrm{aa}} = 1$, which yields

$$\boldsymbol{q}^{\circ}_{(1)} = \left(0, \quad 0, \quad 0, \quad 0, \quad -\frac{\mu_A}{s}, \quad 0, \quad 0, \quad \frac{\mu_A}{s}\right). \tag{A84}$$

Meanwhile, the matrices of effects differ from the complete outcrossing case to first order in ϵ and are given by

$$\mathbf{D}^{\mathrm{Aa}}_{(1)} = \begin{pmatrix} 0 & \frac{r\left(rs^2h+\mu_A\right)}{4s} & \frac{(1-r)\left[(1-r)s^2h+\mu_A\right]}{4s} & 0 & 0 & \frac{s^2h+\mu_A}{2s} & \frac{s^2h+\mu_A}{2s} & 0 \\ 0 & \frac{(1-r)\left(rs^2h+\mu_A\right)}{4s} & \frac{r\left[(1-r)s^2h+\mu_A\right]}{4s} & 0 & 0 & \frac{s^2h+\mu_A}{2s} & \frac{s^2h+\mu_A}{2s} & 0 \\ 0 & -\frac{r\left(rs^2h+\mu_A\right)}{4s} & -\frac{(1-r)\left[(1-r)s^2h+\mu_A\right]}{4s} & 0 & 0 & -\frac{\mu_A}{2s} & -\frac{\mu_A}{2s} & 0 \\ 0 & -\frac{(1-r)\left(rs^2h+\mu_A\right)}{4s} & -\frac{r\left[(1-r)s^2h+\mu_A\right]}{4s} & 0 & 0 & -\frac{\mu_A}{2s} & -\frac{\mu_A}{2s} & 0 \\ 0 & -\frac{shr^2}{8} & -\frac{sh(1-r)^2}{8} & 0 & 0 & -\frac{sh}{4} & -\frac{sh}{4} & 0 \\ 0 & -\frac{shr(1-r)}{8} & -\frac{shr(1-r)}{8} & 0 & 0 & -\frac{sh}{4} & -\frac{sh}{4} & 0 \\ 0 & -\frac{shr(1-r)}{8} & -\frac{shr(1-r)}{8} & 0 & 0 & -\frac{sh}{4} & -\frac{sh}{4} & 0 \\ 0 & -\frac{sh(1-r)^2}{8} & -\frac{shr^2}{8} & 0 & 0 & -\frac{sh}{4} & -\frac{sh}{4} & 0 \end{pmatrix}, \tag{A85a}$$

and

$$\mathbf{D}^{\mathrm{aa}}_{(1)} = \begin{pmatrix} 0 & 0 & 0 & 0 & 0 & 0 & 0 & 0 \\ 0 & 0 & 0 & \frac{1}{4}\left(s+\frac{\mu_A}{s}\right) & 0 & 0 & 0 & s+\frac{\mu_A}{s} \\ 0 & 0 & 0 & 0 & 0 & 0 & 0 & 0 \\ 0 & 0 & 0 & -\frac{1}{4}\left(s+\frac{\mu_A}{s}\right) & 0 & 0 & 0 & -\frac{\mu_A}{s} \\ 0 & 0 & 0 & 0 & 0 & 0 & 0 & 0 \\ 0 & 0 & 0 & 0 & 0 & 0 & 0 & 0 \\ 0 & 0 & 0 & 0 & 0 & 0 & 0 & 0 \\ 0 & 0 & 0 & -\frac{s}{8} & 0 & 0 & 0 & -s \end{pmatrix}. \tag{A85b}$$

Using eqs. (A83-A85), the selection gradients on α_{Aa} and α_{aa} to first order in ϵ are therefore given by

$$s_{\mathrm{Aa}}(\mathbf{1}_3) = 0 + \mathcal{O}\left(\epsilon^2\right) \quad \text{and} \quad s_{\mathrm{aa}}(\mathbf{1}_3) = -\frac{r}{1+2r}\frac{\mu_A}{s} + \mathcal{O}\left(\epsilon^2\right) \tag{A86}$$

Eq. (A86) reveals that the selection gradient on α_{Aa} is zero to first order in ϵ, so that higher order terms must be computed. This is because the frequency of heterozygotes is of the order of the mutation rate under complete selfing, which is of order ϵ^2. As for the selection gradient on α_{aa}, eq. (A86) shows that it is negative to leading order, indicating that selection favours deleterious homozygotes to reduce their selfing rate when the rest of the population is fully selfing. To understand this result, one must think from the point of view of an allele at the selfing modifier, keeping in mind that alleles linked to the deleterious allele at the condition locus are asymptotically lost. For such an allele, complete selfing in deleterious homozygotes 'traps' it onto a deleterious background and so dooms it to extinction, whereas outcrossing gives it a chance at escaping the trap by mating with wild-type individuals and recombining. Accordingly, the gradient is zero when there is no recombination ($r = 0$) as outcrossing then no longer constitutes a viable escape route, and increases with r.

Selection gradients to order ϵ^2. To compute second order terms in ϵ (eq. A40), we first note that

$$\mathbf{D}^{\mathrm{Aa}}_{(0)} \cdot \boldsymbol{q}^{\circ}_{(0)} = \mathbf{D}^{\mathrm{Aa}}_{(1)} \cdot \boldsymbol{q}^{\circ}_{(0)} = \mathbf{D}^{\mathrm{Aa}}_{(2)} \cdot \boldsymbol{q}^{\circ}_{(0)} = \mathbf{0}, \tag{A87}$$

as we show in the accompanying *Mathematica* notebook, so that we need not compute first and second order perturbations of $\boldsymbol{v}^{\circ}$, $\boldsymbol{v}^{\circ}_{(1)}$ and $\boldsymbol{v}^{\circ}_{(2)}$. We next compute the second order perturbation of $\boldsymbol{q}^{\circ}$, $\boldsymbol{q}^{\circ}_{(2)}$ by solving eqs. (A64-A65), which yields

$$\boldsymbol{q}^{\circ}_{(2)} = \left(0, \quad 0, \quad 0, \quad 0, \quad 2\mu_A\left(\frac{\mu_A}{s^2} - 2(2-h)\right), \quad 4\mu_A, \quad 4\mu_A, \quad -2\mu_A\left(\frac{\mu_A}{s^2} + 2h\right)\right) \tag{A88}$$

so that the selection gradient on α_{Aa} is given by

$$s_{\mathrm{Aa}}(\mathbf{1}_3) = \frac{\mu_A}{1+2r} + \mathcal{O}\left(\epsilon^3\right) \tag{A89}$$

to leading order, demonstrating that selection favours complete selfing in heterozygotes.

A.2.4 Pre-existing positive condition dependence ($\alpha_{\mathrm{aa}} < \alpha_{\mathrm{Aa}} < \alpha_{\mathrm{AA}}$)

Section A.2.3 shows that selection favours a decrease in the selfing rate in deleterious homozygotes as an escape from the trap that constitutes linkage to the deleterious allele under complete selfing. But how much should the selfing rate of these homozygotes be reduced, and does this reduction eventually drive a change in the direction of selection on the selfing rate of other genotypes?

In this section, we consider the evolution of condition-dependent selfing under the looser assumption that $\alpha_{\mathrm{aa}} < \alpha_{\mathrm{Aa}} < \alpha_{\mathrm{AA}}$, which is a situation likely to be observed. Indeed, section A.2.2 demonstrates that selection favours an increase in all three genotype-specific selfing rates from complete outcrossing, but the strength of selection is proportional to the frequency of the three genotypes at the condition locus, and so

$$s_{\mathrm{aa}}(\mathbf{0}) \ll s_{\mathrm{Aa}}(\mathbf{0}) \ll s_{\mathrm{AA}}(\mathbf{0}).$$

This indicates that alleles increasing α_{AA} are much more likely to fix than alleles increasing α_{Aa}, which are themselves much more likely to fix than alleles increasing α_{aa}. Assuming the mutational input is identical and independent for all three traits, it follows that the selfing rate of wild-type homozygotes should increase much faster – in expectation – than that of heterozygotes, which in turn should increase much faster than that of deleterious homozygotes. That is, in a large population with rare mutations of small effect, we are likely to see

$$\alpha_{\mathrm{aa}} < \alpha_{\mathrm{Aa}} < \alpha_{\mathrm{AA}}, \tag{A90}$$

at least initially.

Selection on the selfing rate of wild-type homozygotes, α_{AA}. To order zero in ϵ, the change in allelic frequency $\Delta p_{(0)}$ and in homozygosity $\Delta C_{(0)}$ at the condition locus depend on the $\boldsymbol{\alpha}$ in a complicated way, so we refrain from giving them here (but they are available in the *Mathematica* notebook accompanying this Appendix; `10.5281/zenodo.18523420`). Solving for equilibrium (eq. A7), we find that

$$p^*_{(0)} = C^*_{(0)} = 0, \tag{A91}$$

so long as eq. (A90) holds. This is because, even in the absence of mutation or fecundity selection, allele A enjoys a transmission advantage relative to allele a here, as it is found in genotypes self-fertilising at a higher rate on average, and so displaces allele a competitively. Using eq. (A91), we may compute the

zero-th order perturbation of $\boldsymbol{q}^{\circ}$ and $\boldsymbol{v}^{\circ}$, $\boldsymbol{q}^{\circ}_{(0)}$ and $\boldsymbol{v}^{\circ}_{(0)}$, as the solutions of

$$\mathbf{W}^{\circ}_{(0)} \cdot \boldsymbol{q}^{\circ}_{(0)} = \boldsymbol{q}^{\circ}_{(0)} \quad \text{and} \quad \boldsymbol{v}^{\circ}_{(0)} \cdot \mathbf{W}^{\circ}_{(0)} = \boldsymbol{v}^{\circ}_{(0)}, \tag{A92}$$

with constraints $\boldsymbol{q}^{\circ}_{(0)} \cdot \mathbf{1}_3 = 1$ and $\boldsymbol{v}^{\circ}_{(0)} \cdot \boldsymbol{q}^{\circ}_{(0)} = 1$. These solutions are given in the accompanying *Mathematica* notebook. Using the matrix of effects $\mathbf{D}^{\mathrm{AA}}_{(0)}$ (which is identical to eq. (A53a)), we find that the selection gradient on α_{AA} reduces to

$$s_{\mathrm{AA}}(\boldsymbol{\alpha}) = \frac{1}{2(2-\alpha_{\mathrm{AA}})}, \tag{A93}$$

which depends only on α_{AA} and is strictly positive. This shows that wild-type homozygotes will evolve a selfing rate $\alpha_{\mathrm{AA}} \to 1$ irrespective of the selfing rates at other genotypes (provided that eq. A90 holds). We next compute selection gradients on α_{Aa} and α_{aa} under the assumption that $\alpha_{\mathrm{AA}} = 1$.

Selection on the selfing rate of heterozygotes, α_{Aa}. Using the same approach as in sections A.2.2 and A.2.3 (eqs. A10-A49; see accompanying *Mathematica* notebook for the detailed approach), we find that the equilibrium allelic frequency and homozygosity in the resident population are given by

$$p^* = \frac{2\mu_A\left[2(1-\alpha_{\mathrm{aa}})+\alpha_{\mathrm{Aa}}\right]}{(2-\alpha_{\mathrm{Aa}})(1-\alpha_{\mathrm{aa}})} + \mathcal{O}\left(\epsilon^3\right) \quad \text{and} \quad C^* = \frac{2\mu_A\alpha_{\mathrm{Aa}}}{(2-\alpha_{\mathrm{Aa}})(1-\alpha_{\mathrm{aa}})} + \mathcal{O}\left(\epsilon^3\right) \tag{A94}$$

to second order in ϵ. These highlight the effect of the transmission advantage on genetic dynamics at the condition locus. The higher α_{aa} and α_{Aa}, the lower the transmission advantage enjoyed by allele A over allele a, and the equilibrium frequency of allele a increases. In the absence of selfing in heterozygotes ($\alpha_{\mathrm{Aa}} = 0$), there is no excess homozygosity in the population ($C^* = 0$) to leading order, because there is then no way for a deleterious allele a arising through mutation to be transmitted in homozygous state.

After computing perturbations of $\boldsymbol{q}^{\circ}$ and $\boldsymbol{v}^{\circ}$ using the same approach as in sections A.2.2 and A.2.3 (see *Mathematica* notebook), we find that the selection gradient on the selfing rate of heterozygotes α_{Aa} reduces to

$$s_{\mathrm{Aa}}(\boldsymbol{\alpha}) = \frac{\mu_A}{2(2-\alpha_{\mathrm{Aa}})^2}\left[3 + \frac{2r(1-r)\alpha_{\mathrm{Aa}}}{2-\alpha_{\mathrm{Aa}}\big(1-2r(1-r)\big)}\right] + \mathcal{O}\left(\epsilon^3\right), \tag{A95}$$

which is strictly positive and does not depend on α_{aa}. Thus, selection favours the evolution of complete selfing in heterozygotes ($\alpha_{\mathrm{Aa}} \to 1$), similar to wild-type homozygotes.

Selection on the selfing rate of deleterious homozygotes, α_{aa}. To obtain the selection gradient on α_{aa}, we may now assume that $\alpha_{\mathrm{Aa}} = 1$. Terms of order ϵ^3 must be computed, as all lower order terms are zero. However, we show in the accompanying *Mathematica* notebook that

$$\boldsymbol{v}^{\circ}_{(0)} \cdot \mathbf{D}^{\mathrm{aa}}_{(0)} = \mathbf{D}^{\mathrm{aa}}_{(0)} \cdot \boldsymbol{q}^{\circ}_{(0)} = \mathbf{D}^{\mathrm{aa}}_{(3)} \cdot \boldsymbol{q}^{\circ}_{(0)} = (0,\ 0,\ 0,\ 0,\ 0,\ 0,\ 0,\ 0), \tag{A96}$$

which implies that all terms involving third order perturbations will be zero. In fact, we find that the selection gradient on α_{aa} simplifies to

$$\begin{aligned} s_{\mathrm{aa}}(\boldsymbol{\alpha}) &= \frac{\boldsymbol{v}^{\circ}_{(1)} \cdot \mathbf{D}^{\mathrm{aa}}_{(0)} \cdot \boldsymbol{q}^{\circ}_{(2)}}{2} + \mathcal{O}\left(\epsilon^4\right) \\ &= -\mu_A \frac{s}{(1-\alpha_{\mathrm{aa}})^2} \frac{4r}{1+4r} \left[1 - \frac{r(1-r)(1-\alpha_{\mathrm{aa}})}{[1+2r(1-r)](2-\alpha_{\mathrm{aa}})}\right] + \mathcal{O}\left(\epsilon^4\right) \end{aligned} \tag{A97}$$

which is strictly negative. Thus, although selection initially favours an increase in the selfing rate for all genotypes, deleterious homozygotes will always be selected towards a selfing rate of zero ($\alpha_{\mathrm{aa}} \to 0$) once the selfing rate of other genotypes is sufficiently high. In other words, selection favours the evolution of condition-dependent selfing, where high-condition individuals are completely self-fertilising and low-condition individuals are fully outcrossing.

A.2.5 Numerical analyses

To complement our analytical results, we investigated the evolution of condition-dependent selfing for an arbitrary initial relationship between α_{AA}, α_{Aa} and α_{aa} with numerical analyses in *Mathematica*. We used two different approaches, which we describe below.

Iteration of evolutionary dynamics. In the first approach, we assume that the population is initially fixed for an arbitrary selfing strategy $\boldsymbol{\alpha}_0 = (\alpha^0_{\mathrm{AA}}, \alpha^0_{\mathrm{Aa}}, \alpha^0_{\mathrm{aa}})$ and study how evolutionary dynamics proceed from there as follows. At any time step n, we start by determining the genetic equilibrium reached by a resident population expressing strategy $\boldsymbol{\alpha}_n = (\alpha^n_{\mathrm{AA}}, \alpha^n_{\mathrm{Aa}}, \alpha^n_{\mathrm{aa}})$, which we do by iterating the dynamics of genotypic frequencies $\boldsymbol{q}_t = (q_{\mathrm{AA}}(t), q_{\mathrm{Aa}}(t), q_{\mathrm{aa}}(t))$ given by eq. A3 until an equilibrium is reached, i.e.,

$$\mathbf{1}_3 \cdot \left(\boldsymbol{q}_{t+1} - \boldsymbol{q}_t\right)^2 < \epsilon_{\mathrm{q}} \tag{A98}$$

where $\epsilon_{\mathrm{q}} > 0$ is a small tolerance threshold. We then compute the selection gradient on the three traits at this equilibrium, $\boldsymbol{s}(\boldsymbol{\alpha}_n) = \left(s_{\mathrm{AA}}\left(\boldsymbol{\alpha}_n\right), s_{\mathrm{Aa}}\left(\boldsymbol{\alpha}_n\right), s_{\mathrm{aa}}\left(\boldsymbol{\alpha}_n\right)\right)$ using eq. (A38). The trait values expressed

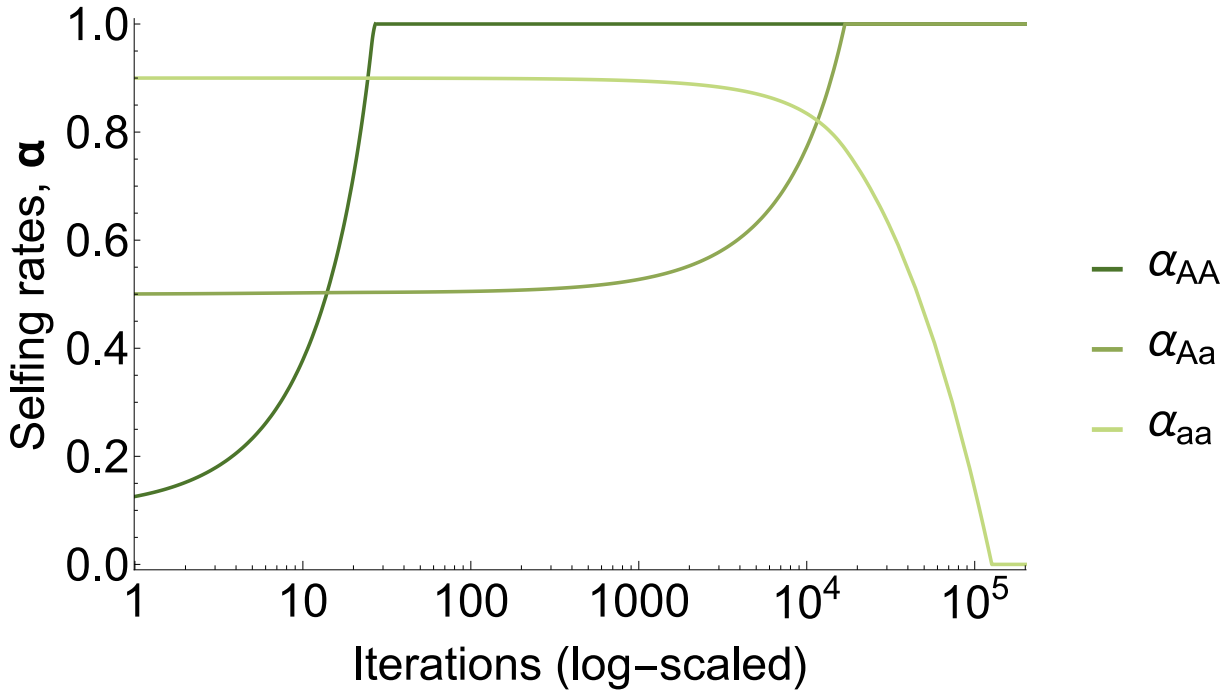

Figure S1: Evolution of condition-dependent selfing in the two locus model as a function of time (algorithm iterations) from initial negative condition dependence, $\boldsymbol{\alpha} = (0.1, 0.5, 0.9)$. Parameters used: $\mu_{\mathrm{A}} = \mu_{\mathrm{a}} = 10^{-3}$, $s = 0.05$, $h = 0.25$, $r = 0.5$.

in the population in the next time step are then given by

$$\boldsymbol{\alpha}_{n+1} = \boldsymbol{\alpha}_n + \Delta_\alpha \, \boldsymbol{s}(\boldsymbol{\alpha}_n), \tag{A99}$$

where $\Delta_\alpha > 0$ is a small phenotypic deviation and elements of $\boldsymbol{\alpha}_{n+1}$ are clipped to remain in the $[0, 1]$-interval. This algorithm is repeated until the change in trait between two time steps is sufficiently small, i.e.,

$$\mathbf{1}_3 \cdot (\boldsymbol{\alpha}_{n+1} - \boldsymbol{\alpha}_n)^2 < \epsilon_\alpha, \tag{A100}$$

where $\epsilon_\alpha > 0$ is a small tolerance threshold. Figure S1 illustrates the dynamics obtained using this approach.

Gradient interpolation. The approach given above can be greedy in computation time, as it is only valid for small phenotypic deviations and the selection gradients can be weak in some regions, leading to very small phenotypic changes from one iteration to the next. One way to circumvent this issue is to calculate the gradient for evenly spaced points in the $[0, 1]^3$ cube in which selfing strategies $\boldsymbol{\alpha} = (\alpha_{\mathrm{AA}}, \alpha_{\mathrm{Aa}}, \alpha_{\mathrm{aa}})$ are defined. For each point, we compute the equilibrium genotypic values in the resident population using eq. (A3) and then compute the selection gradient using eq. (A38), as above. The output

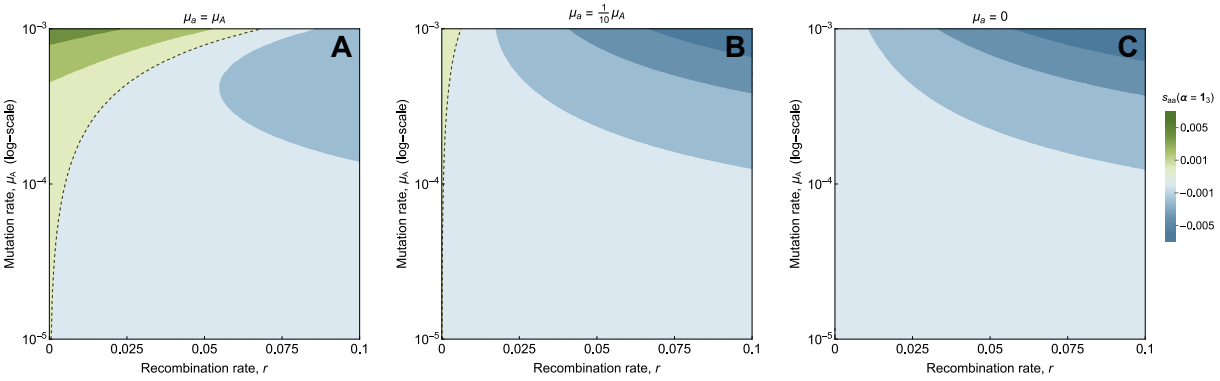

Figure S2: Effect of back-mutation on the evolution of condition-dependent selfing under low recombination rates. Plots give the value of the selection gradient on the selfing rate of deleterious homozygotes in a fully selfing population. Shades of blue indicate negative values, where condition dependence is favoured; shades of green indicate green values, where it is not. The dashed line indicates where the gradient changes sign. condition dependence is favoured for most of the parameter space, except when back-mutation is frequent and recombination very low. Parameters used: $s = 0.01$, $h = 0.25$.

of these calculations is stored to a file (see *Mathematica* notebook for technical details), and can be used to interpolate the selection gradient on $\boldsymbol{\alpha}$ in the entire phenotypic space. Given this interpolated gradient, we can then apply standard gradient descent methods to find the equilibrium strategy $\boldsymbol{\alpha}^* = (\alpha^*_{\mathrm{AA}}, \alpha^*_{\mathrm{Aa}}, \alpha^*_{\mathrm{aa}})$ favoured by selection.

Evolution of condition dependence and the effect of back-mutation. We used numerical analyses to investigate the evolution of condition-dependent selfing over a broad range of parameter values and found that a form of positive condition dependence where wild-type homozygotes and heterozygotes self-fertilise fully while deleterious homozygotes are purely outcrossing, i.e.,

$$\boldsymbol{\alpha}^* = (\alpha^*_{\mathrm{AA}}, \alpha^*_{\mathrm{Aa}}, \alpha^*_{\mathrm{aa}}) = (1,\ 1,\ 0) \tag{A101}$$

was favoured in almost all cases. However, we found that low recombination rates can sometimes prevent the evolution of condition dependence and lead to a pure selfing strategy instead ($\boldsymbol{\alpha}^* = \mathbf{1}_3$) because the benefits of outcrossing are low in this case, sufficiently so that the benefits reaped from self-fertilising when wild-type alleles are produced through back-mutation are larger. This is illustrated by the fact that selection favours the evolution of condition dependence for all $r \neq 0$ when there is no back-mutation ($\mu_a = 0$), as can be seen from Fig. S2.

Appendix B

Multilocus simulations

In this Appendix, we describe the simulation program and its extensions. The description given in this section focuses on the biological processes included in the simulation program. The program is coded in C++20 and available at `10.5281/zenodo.18523420`. We also provide additional results for parameter values not shown in the main.

B.1 The baseline program

The program simulates a population of N individuals, where each of them is characterised by its diploid genotype at L condition loci and at n_{g} network loci involved in a gene regulatory network that determines their selfing rate.

Condition. Condition loci are assumed to be diallelic, with a wild-type allele A_ℓ and a deleterious allele a_ℓ at each locus $l \in \{1, \ldots, L\}$. These loci are assumed to be unlinked meaning that they all recombine with probability $1/2$ during meiosis, and each allele mutates with probability $\mu_{A_\ell} = \mu_{a_\ell} = \mu$ during gametogenesis, in which case they change state (i.e., the wild-type becomes a deleterious allele or the deleterious allele becomes wild-type). The deleterious allele at each locus reduces its bearer's condition by a proportion s when homozygous and expresses proportionally to its dominance coefficient h in heterozygotes. Condition loci act multiplicatively, so that the condition of an individual i heterozygous at $n_{\mathrm{het}}^{(i)}$ loci and homozygous for the deleterious allele at $n_{\mathrm{hom}}^{(i)}$ loci is given by

$$\varphi_i = (1 - sh)^{n_{\mathrm{het}}^{(i)}} \times (1 - s)^{n_{\mathrm{hom}}^{(i)}}. \tag{B1}$$

Selfing rate. The gene regulatory network is composed of n_{g} loci and is inspired from the Wagner model [12]. Each locus $k \in \{1, ..., n_{\mathrm{g}}\}$ contains a protein-coding gene that is expressed as the individual develops into an adult and contributes to determining its selfing rate. The level of expression of each gene at developmental time step $t \in \{0, \ ... \ , T\}$ in individual i, which we denote as $S_k^{(i)}(t) \in \mathbb{R}$, is influenced by the combined action of individual condition φ_i, which acts as an external cue to the network,

and regulatory interactions within the network (including self-regulation). Specifically, we assume that each locus additionally carries n_{g} cis-regulatory sequences on which the gene products of the n_{g} genes involved in the network may bind to up- or down-regulate the gene expression at locus k. Each locus k is thus characterised by five attributes, an input weight $u_k^{(i)} \in \mathbb{R}$, which measures how much the expression of locus k is directly influenced by condition; a slope $a_k^{(i)} \in \mathbb{R}$ and a bias $b_k^{(i)} \in \mathbb{R}$, which determine the shape of the response of locus k to condition and regulation; a vector of regulatory weights $\boldsymbol{y}_k^{(i)} \in \mathbb{R}^{n_{\mathrm{g}}}$, the m^{th} element of which $y_{k,m}^{(i)}$ gives the regulatory effect of locus m on the expression of locus k; and an output weight $v_k^{(i)}$ which measures the final contribution of locus k to the phenotype. Alleles at each locus are additive, so that the attributes of locus k in a diploid individual carrying alleles k_1 and k_2 at this locus are given by the average of the two alleles, i.e.,

$$x_k^{(i)} = \frac{x_{k_1} + x_{k_2}}{2}$$

for $x \in \{u, a, b, \boldsymbol{y}, v\}$. Each allele mutates with probability μ_{g} during meiosis, in which case a normally distributed value with mean zero and standard deviation σ_{g} is added to each of its attributes.

At the beginning of development ($t = 0$), that is before any regulatory interaction, the level of expression of locus k is determined by its sensitivity to individual condition, i.e.,

$$S_k^{(i)}(0) = u_k^{(i)} \varphi_i. \tag{B2}$$

Then, given expression levels $\boldsymbol{S}_i(t) = \left(S_k^{(i)}(t) \right)_{1 \leqslant k \leqslant n_{\mathrm{g}}}$ at developmental time t, the expression level of locus k at $t+1$ is given by

$$S_k^{(i)}(t+1) = \frac{2}{1 + \exp\left[-a_k^{(i)} \left(\boldsymbol{S}_i(t) \cdot \boldsymbol{y}_k^{(i)} + u_k^{(i)} \varphi_i - b_k^{(i)} \right) \right]} - 1. \tag{B3}$$

The recursion given in eq. (B3) is iterated until expression levels reach a steady state $\boldsymbol{S}_i^* = \left(S_{k*}^{(i)} \right)_{1 \leqslant k \leqslant n_{\mathrm{g}}}$, defined as

$$\boldsymbol{S}_i^* = \boldsymbol{S}_i(t) = \boldsymbol{S}_i(t+1) \quad \text{such that} \quad \frac{1}{n_{\mathrm{g}}} \sum_{k=1}^{n_{\mathrm{g}}} \left(S_k^{(i)}(t+1) - S_k^{(i)}(t) \right)^2 < \epsilon_{\mathrm{g}}, \tag{B4}$$

where $0 < \epsilon_{\mathrm{g}} \ll 1$ is a small tolerance threshold, or the maximal development time T is reached. Those individuals that fail to converge to steady expression levels as defined by eq. (B4) within T iterations are assumed to be sterile owing to developmental instability [12]. Otherwise, the selfing rate expressed by

the individual is given by

$$\alpha_i = \begin{cases} 0 & \text{if} \quad \boldsymbol{v}_i \cdot \boldsymbol{S}_i^* < 0, \\ \boldsymbol{v}_i \cdot \boldsymbol{S}_i^* & \text{if} \quad 0 \leqslant \boldsymbol{v}_i \cdot \boldsymbol{S}_i^* \leqslant 1, \\ 1 & \text{if} \quad \boldsymbol{v}_i \cdot \boldsymbol{S}_i^* > 1, \end{cases} \tag{B5}$$

where $\boldsymbol{v}_i = \left(v_k^{(i)}\right)_{1 \leqslant k \leqslant n_\mathrm{g}}$ collects the output weights of the n_g loci involved in the network. Allowing the dot product $\boldsymbol{v}_i \cdot \boldsymbol{S}_i^*$ to vacate the $[0, 1]$-interval in which the selfing rate is defined prevents the occurrence of directional mutational bias due to boundary effects.

Initialisation. The population is initially fixed for the wild-type allele at all L condition loci and output weights v_0 at the n_g network loci. In this study, we set $v_0 = 0$ in all simulations to ensure that populations were initially purely outcrossing (see main text). To assess the sensitivity of our results to the initial state of the network, the input and regulatory weights, and the slope and bias of each trait locus were initialised by sampling values in Gaussian distributions with mean zero and standard deviation of $2\sigma_\mathrm{g}$. This led to initial networks with low sensitivity to condition and weak interactions among loci.

Detailed life-cycle. Each generation proceeds as follows. We first determine the condition φ_i of each individual $i \in \{1, \ldots, N\}$ using eq. (B1), and its selfing rate α_i by iterating its gene regulatory network as described above. If the network does not stabilise within T developmental time steps, the condition of the individual is flagged with a selfing rate $\alpha_\bullet = -1$, which serves to identify it as sterile. From these, we calculate the female and male fecundities of individual i, $f_{\female}(\varphi_i, \alpha_i)$ and $f_{\male}(\varphi_i, \alpha_i)$, as

$$f_{\female}(\varphi_i, \alpha_i) = f_{\male}(\varphi_i, \alpha_i) = \begin{cases} \varphi_i & \text{if} \quad \alpha_i \geqslant 0, \\ 0 & \text{otherwise.} \end{cases} \tag{B6}$$

Fecundities through both sex functions are equal here, but we distinguish between the two functions now in anticipation of extensions introduced in the next section.

To create the next generation, we generate N diploid offspring as follows. We first sample a maternal parent with replacement from the current generation. Each individual i has a probability of being sampled proportional to its female fecundity, $f_{\female}(\varphi_i, \alpha_i) / \sum_j f_{\female}(\varphi_j, \alpha_j)$. This maternal parent then self-fertilises with probability α_i, in which case the paternal parent is taken to be the same individual. Otherwise, a paternal parent $k \neq i$ is sampled from the current generation with a probability proportional to male

fecundity, i.e., individual $k \neq i$ has a probability $f_{\sigma}(\varphi_k, \alpha_k) / \sum_{j \neq i} f_{\sigma}(\varphi_j, \alpha_j)$ to be sampled.

Each parents transmit one haplotype to the offspring. Recombination occurs freely between all loci, meaning that alleles on the transmitted haplotype are equally likely to come from each of the two chromosomes of the parent, independently for each of the L condition loci and n_{g} network loci. Mutation occurs with probability μ for each allele at condition loci, in which case the allele switches state (i.e., mutating wild-type alleles become deleterious, and mutating deleterious alleles revert to wild-type). Meanwhile, mutation occurs with probability μ_{g} for each allele at regulatory loci, in which case a normally distributed value with mean zero and standard deviation σ_{g} is added to each of its attributes, i.e., network loci evolve under a continuum-of-alleles model [8].

Measurements and population back-up. We let simulations run for $t_{\max}$ generations. Every t_{mes} generations, we record the following information.

First of all, we save the condition φ_i, selfing rate α_i and the number of generations of selfing since the last outcrossing event along an individual's genealogy of randomly sampled n_{mes} individuals in the population. If enabled, we also record the GRN attributes of those individuals (this generates large output files and so should be used advisedly). In the extension that includes environmental fluctuations described in section B.2.1, we also record the environment they find themselves in.

Second, we record mean $\overline{\varphi}$ and variance σ_{φ}^2 in condition in the population, the magnitude of inbreeding depression δ, which we compute as

$$\delta = \frac{\overline{\varphi_{\mathrm{out}}} - \overline{\varphi_{\mathrm{self}}}}{\overline{\varphi_{\mathrm{out}}}}, \tag{B7}$$

where $\overline{\varphi_{\mathrm{self}}}$ and $\overline{\varphi_{\mathrm{out}}}$ are the mean condition of N selfed and N outcrossed individuals generated from randomly chosen parents, respectively; the mean $\overline{\alpha}$ and variance σ_{α}^2 in selfing rate in the population, the number of deleterious alleles per haploid genome at the condition loci n_{mut}, and the mean excess in homozygote F at condition loci relative to the Hardy-Weinberg expectation.

Third, we record the distribution of selfing rates and condition in the population with bins of size 0.01 and 0.001, respectively. Finally, every t_{save} generations, we back-up the entire population into a single file, which can then be used to relaunch simulations from the latest back-up (or indeed any back-up with the same number of individuals and loci).

B.2 Extensions

We extended our baseline simulation program to include two additional biological mechanisms, namely environmental fluctuations and pollen discounting. We describe these extensions in turn below.

B.2.1 Environmental fluctuations

To include environmental fluctuations, we assume that each patch is characterised by an environmental value, ε, which we take to be a normally distributed random variable

$$\varepsilon \sim \mathcal{N}(0, 1), \tag{B8}$$

that changes every generation. This value could represent any environmental variable relevant to plant development, such as exposure to sunlight or water availability. We assume that an environmental value $\varepsilon = 0$ is optimal and so maximises condition, while values deviating from zero result in lower condition. Specifically, the condition of an individual i heterozygous for $n_{\text{het}}^{(i)}$ deleterious alleles and homozygous for $n_{\text{hom}}^{(i)}$, developing in a patch with value ε_i, is given by

$$\varphi_i = \exp\left(-\Delta_{\text{E}}\frac{\varepsilon_i^2}{2}\right)\left(1-s\right)^{n_{\text{hom}}^{(i)}}\left(1-sh\right)^{n_{\text{het}}^{(i)}} \tag{B9}$$

Eq. (B9) is composed of three terms. The first term describes the effect that the environment has on individual condition. This environmental component is maximised for $\varepsilon_i = 0$, i.e., when the individual develops in optimal environmental conditions, and decreases as ε_i moves away from zero. Parameter Δ_{E} controls how fast condition decreases as the environment deviates from the optimum. The next two terms correspond to the effect of deleterious mutations in homozygous and heterozygous state on condition, as before.

B.2.2 Pollen discounting

To include pollen discounting in our model, that is, the reduction in pollen export that can accompany increased selfing, we modify our male fecundity function $f_{\male}(\varphi_i, \alpha_i)$, such that it is now given by

$$f_{\male}(\varphi_i, \alpha_i) = \begin{cases} \varphi_i \left(1 - \kappa {\alpha_i}^{\gamma}\right) & \text{if} \quad \alpha_i \geqslant 0, \\ 0 \quad \text{otherwise.} \end{cases} \tag{B10}$$

where $\kappa \in [0, 1]$ and $\gamma > 0$ respectively give the intensity and shape of the trade-off between selfing and pollen export. This functional shape is inspired from [7], who showed that non-linear pollen discounting effects can maintain mixed mating. A linear relationship is obtained with $\gamma = 1$, as commonly assumed in the mating system literature (e.g., [1]); and becomes non-linear as soon as $\gamma \neq 1$. The absence of pollen discounting is obtained for $\kappa = 0$, in which case we recover the baseline model.

B.3 Supplementary figures for environmental fluctuations

This section shows figures for all the simulations we ran for our environmental fluctuations extension.

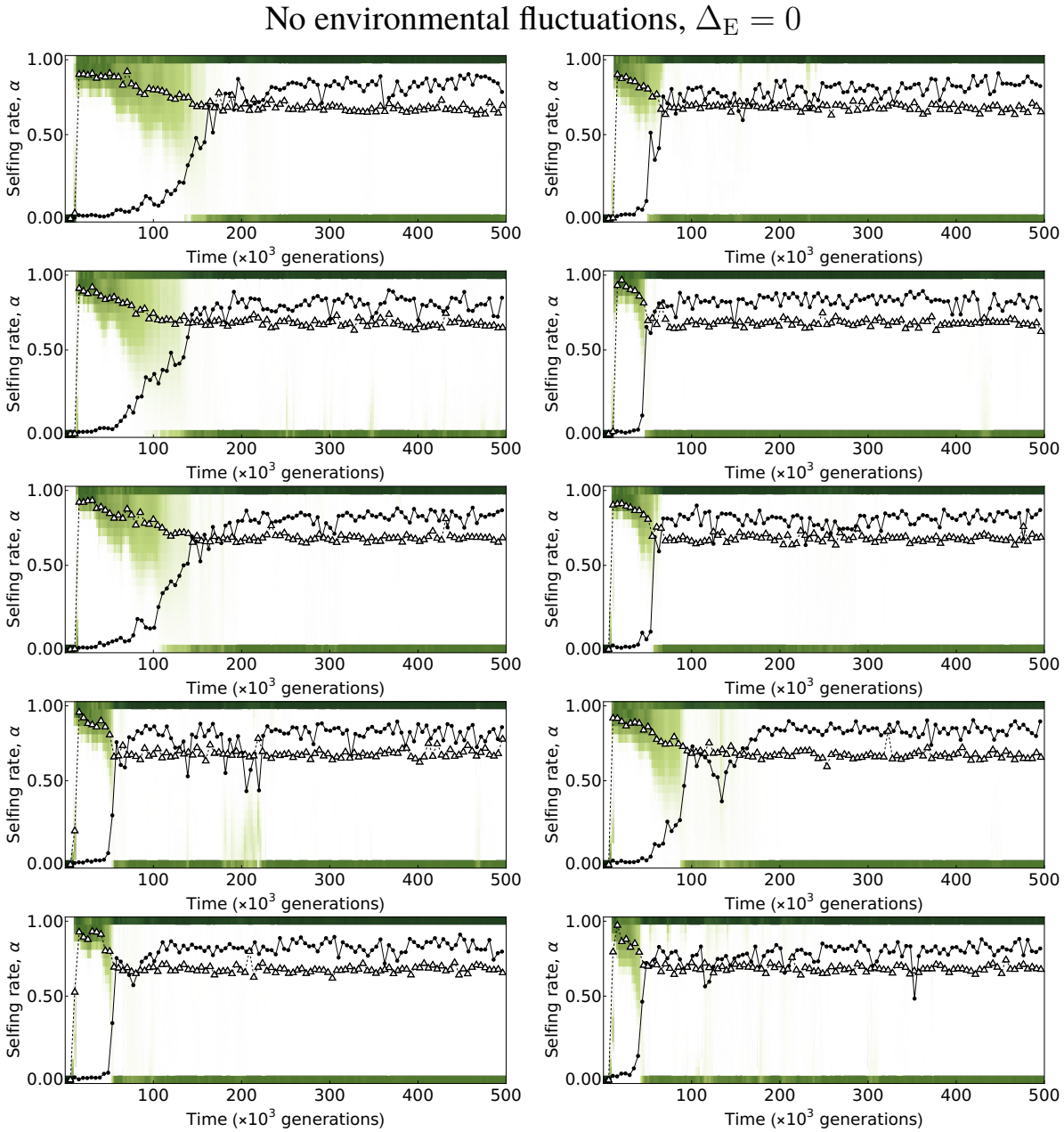

Figure S3: Simulation trajectories in the absence of environmental fluctuations ($\Delta_{\mathrm{E}} = 0$). As in the main text, green tiles indicate the proportion of individuals with a selfing rate in the corresponding range, and white triangles and black points respectively indicate mean and variance in the selfing rate. All simulations evolve condition-dependent selfing. Parameters used: $N = 5 \times 10^3$, $L = 10^3$, $\mu = 5 \times 10^{-4}$, $s = 0.05$, $h = 0.25$, $\mu_{\mathrm{g}} = 5 \times 10^{-3}$, $\sigma_{\mathrm{g}} = 0.05$.

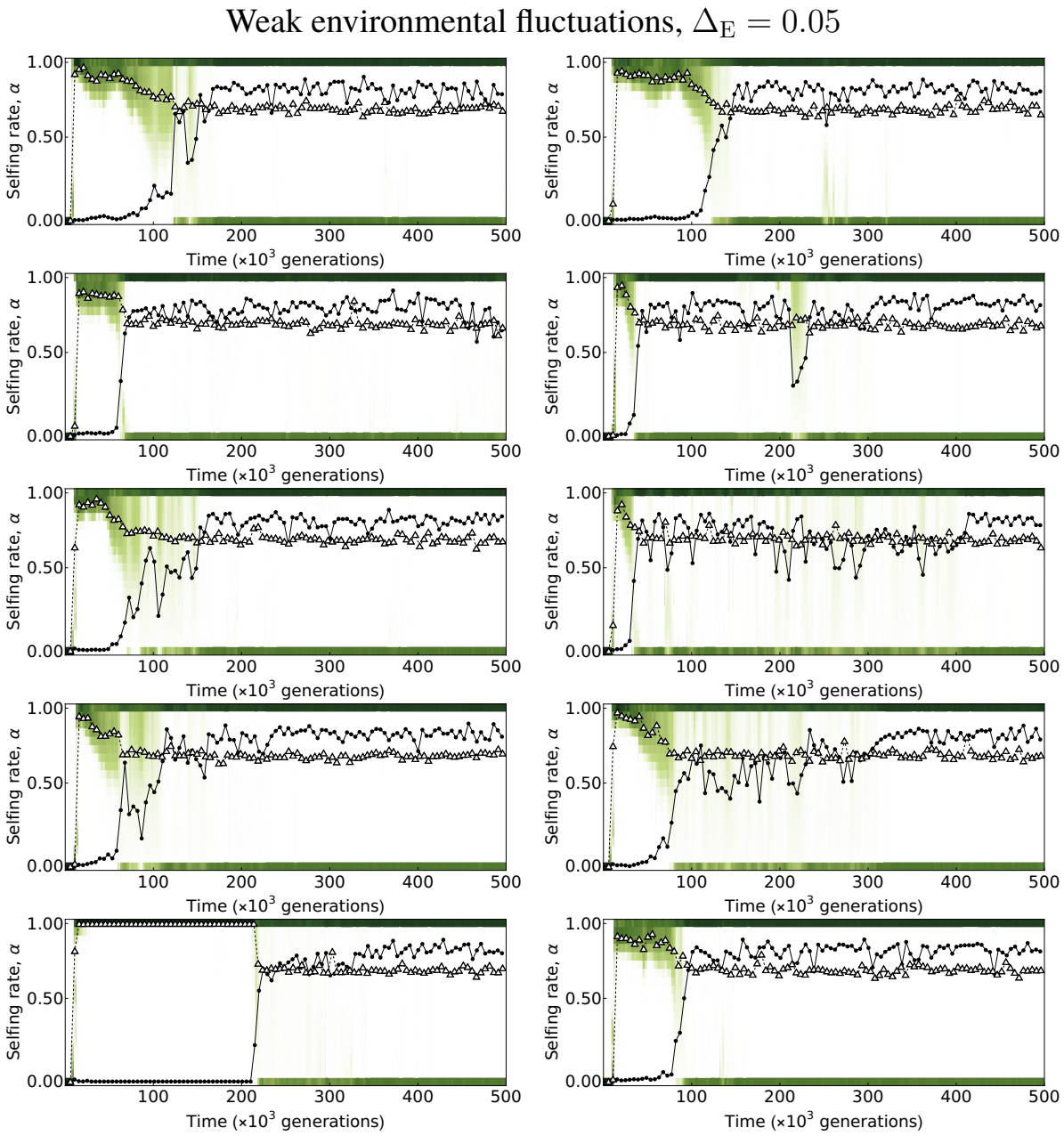

Figure S4: Simulation trajectories with weak environmental fluctuations ($\Delta_{\mathrm{E}} = 0.05$). As in the main text, green tiles indicate the proportion of individuals with a selfing rate in the corresponding range, and white triangles and black points respectively indicate mean and variance in the selfing rate. All simulations evolve condition-dependent selfing. Parameters used: $N = 5 \times 10^3$, $L = 10^3$, $\mu = 5 \times 10^{-4}$, $s = 0.05$, $h = 0.25$, $\mu_{\mathrm{g}} = 5 \times 10^{-3}$, $\sigma_{\mathrm{g}} = 0.05$.

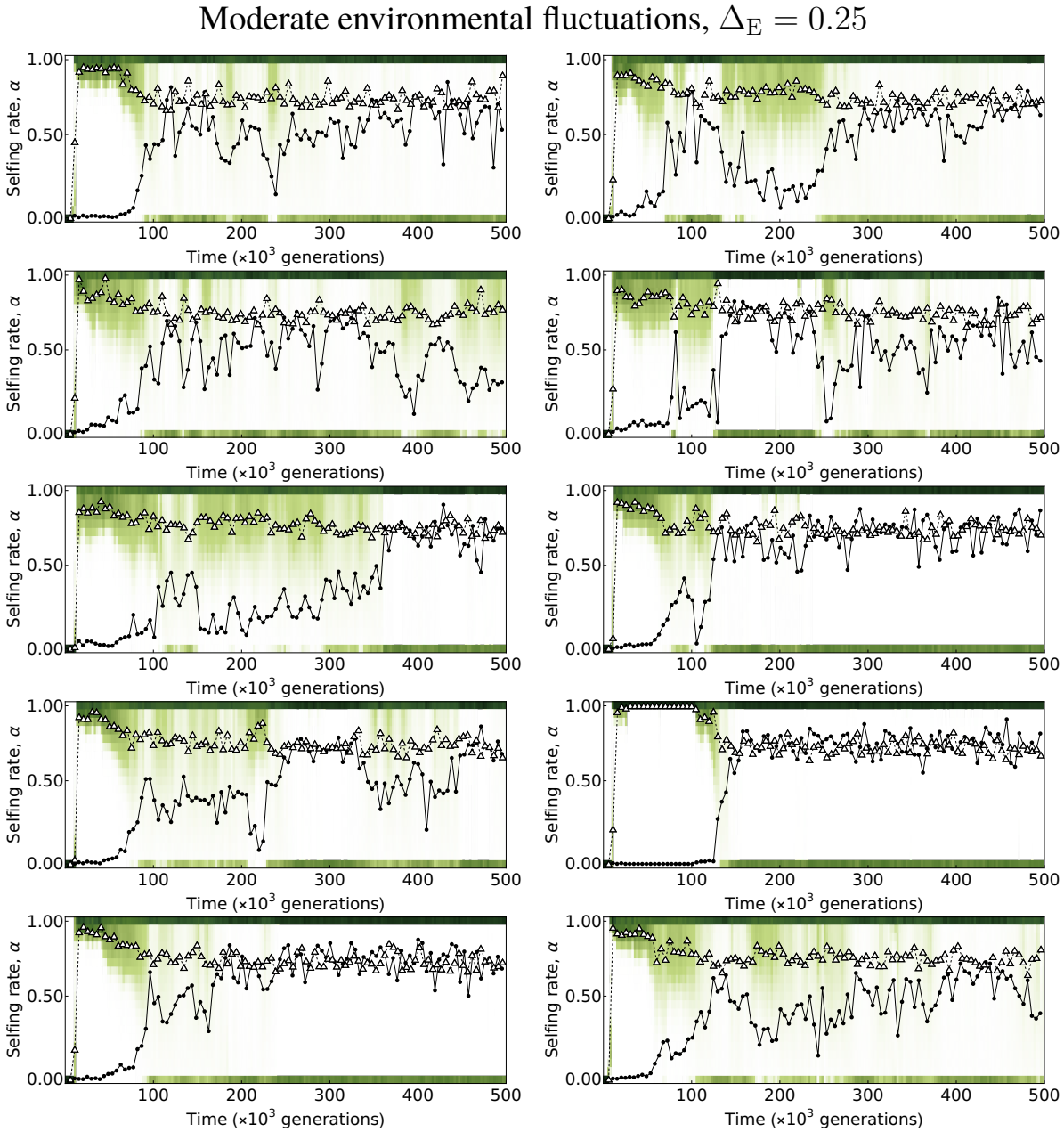

Figure S5: Simulation trajectories with moderate environmental fluctuations ($\Delta_{\mathrm{E}} = 0.25$). As in the main text, green tiles indicate the proportion of individuals with a selfing rate in the corresponding range, and white triangles and black points respectively indicate mean and variance in the selfing rate. All simulations evolve condition-dependent selfing. Parameters used: $N = 5 \times 10^3$, $L = 10^3$, $\mu = 5 \times 10^{-4}$, $s = 0.05$, $h = 0.25$, $\mu_{\mathrm{g}} = 5 \times 10^{-3}$, $\sigma_{\mathrm{g}} = 0.05$.

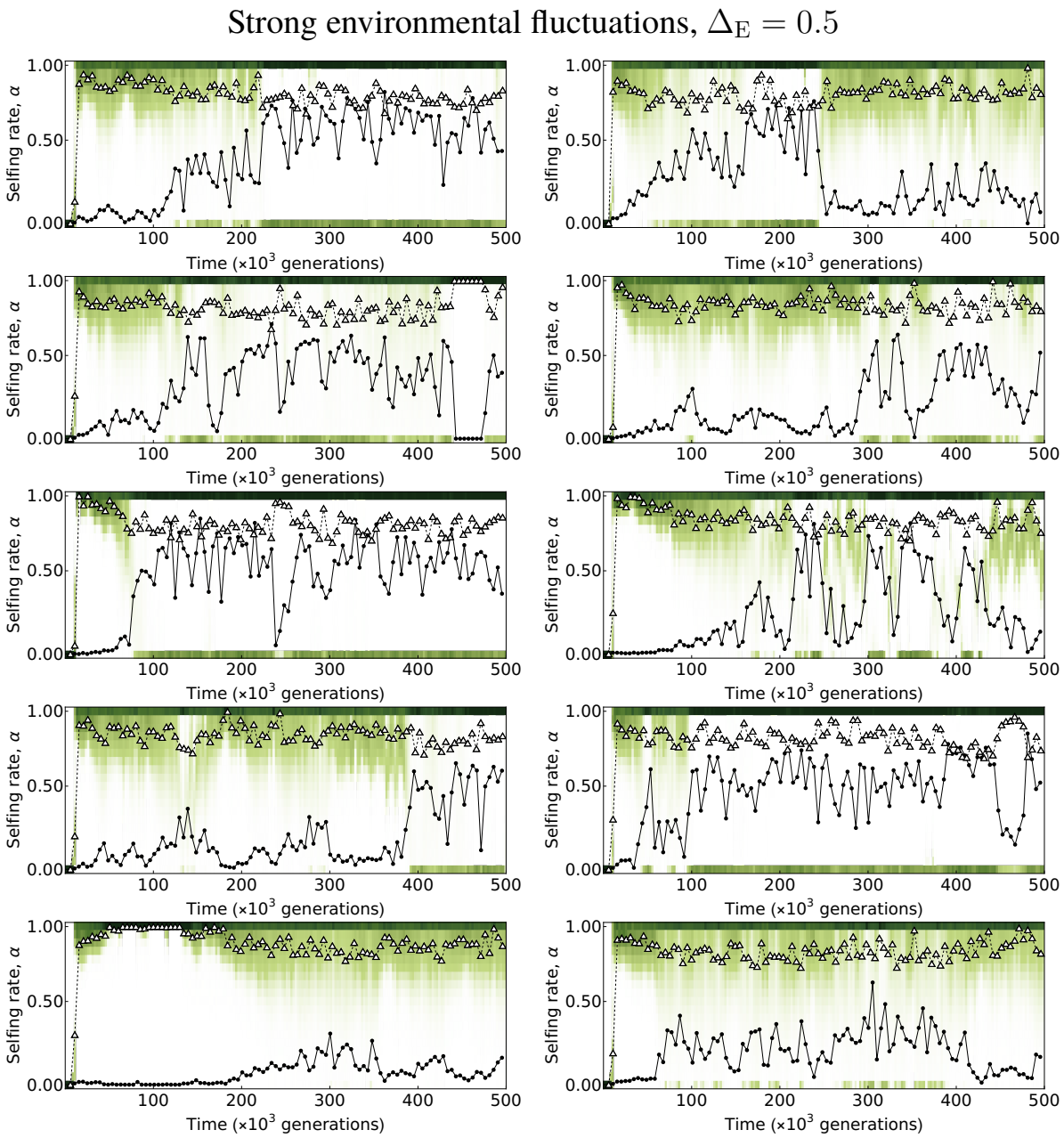

Figure S6: Simulation trajectories with strong environmental fluctuations ($\Delta_E = 0.5$). As in the main text, green tiles indicate the proportion of individuals with a selfing rate in the corresponding range, and white triangles and black points respectively indicate mean and variance in the selfing rate. All simulations evolve condition-dependent selfing. Parameters used: $N = 5 \times 10^3$, $L = 10^3$, $\mu = 5 \times 10^{-4}$, $s = 0.05$, $h = 0.25$, $\mu_g = 5 \times 10^{-3}$, $\sigma_g = 0.05$.

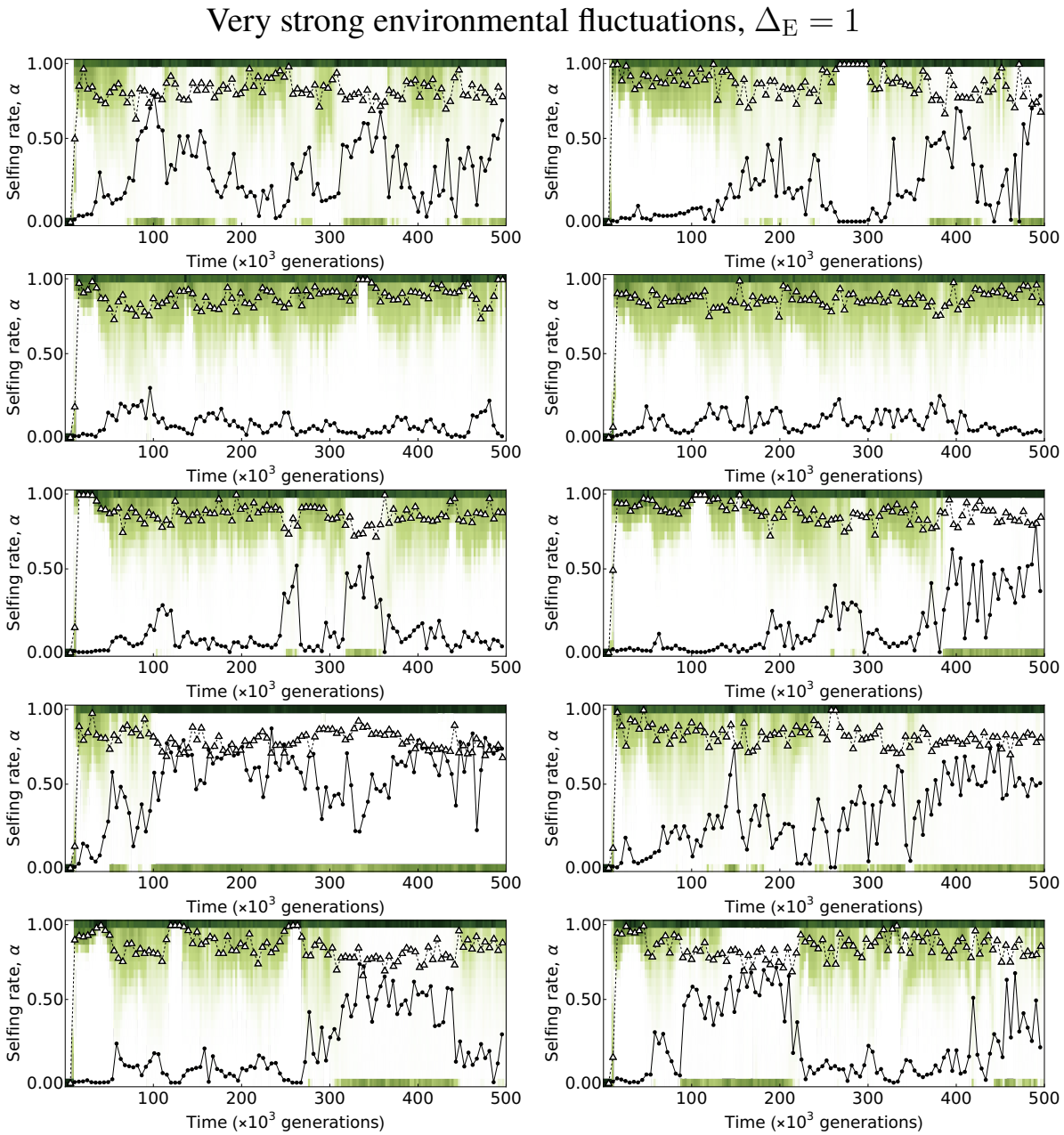

Figure S7: Simulation trajectories with very strong environmental fluctuations ($\Delta_{\mathrm{E}} = 1$). As in the main text, green tiles indicate the proportion of individuals with a selfing rate in the corresponding range, and white triangles and black points respectively indicate mean and variance in the selfing rate. All simulations evolve condition-dependent selfing. Parameters used: $N = 5 \times 10^3$, $L = 10^3$, $\mu = 5 \times 10^{-4}$, $s = 0.05$, $h = 0.25$, $\mu_{\mathrm{g}} = 5 \times 10^{-3}$, $\sigma_{\mathrm{g}} = 0.05$.

References

[1] D. Abu Awad and D. Roze. Epistasis, inbreeding depression, and the evolution of self-fertilization. *Evolution*, 74(7):1301–1320, 2020.

[2] P. Avila and C. Mullon. Evolutionary game theory and the adaptive dynamics approach: adaptation where individuals interact. *Philosophical Transactions of the Royal Society B: Biological Sciences*, 378(1876):20210502, 2023.

[3] F. Dercole and S. Rinaldi. Analysis of evolutionary processes. In *Analysis of Evolutionary Processes*. Princeton University Press, 2008.

[4] R.A. Fisher. Average excess and average effect of a gene substitution. *Annals of Human Genetics*, 11:53–63, 1941.

[5] S.A.H. Geritz, E. Kisdi, and J.A.J. Metz. Evolutionarily singular strategies and the adaptive growth and branching of the evolutionary tree. *Evolutionary Ecology*, 12(1):35–57, 1998.

[6] J.B.S. Haldane. The effect of variation of fitness. *The American Naturalist*, 71:337–349, 1937.

[7] M.O. Johnston. Evolution of intermediate selfing rates in plants: pollination ecology versus deleterious mutations. In *Mutation and Evolution*, pages 267–278. Springer, 1998.

[8] M. Kimura. A stochastic model concerning the maintenance of genetic variability in quantitative characters. *Proceedings of the National Academy of Sciences*, 54(3):731–736, 1965.

[9] J.A.J. Metz, S.D. Mylius, and O. Diekmann. When does evolution optimize? on the relation between types of density dependence and evolutionarily stable life history parameters. *IIASA Working Paper*, 1996.

[10] François Rousset. *Genetic structure and selection in subdivided populations*. Princeton University Press, 2004.

[11] P.D. Taylor. Allele-frequency change in a class-structured population. *The American Naturalist*, 135(1):95–106, 1990.

[12] A. Wagner. Evolution of gene networks by gene duplications: a mathematical model and its implications on genome organization. *Proceedings of the National Academy of Sciences*, 91(10):4387–4391, 1994.